Faculty of Science

Department of Biology

Institute of Zoology

Chair of Molecular Cell Physiology and Endocrinology

TECHNISCHE UNIVERSITÄT DRESDEN

dresden international phd program

Estrogen Receptor-Beta Dependent Activities of Dietary Compounds in a Genetically Modified Rat Raphe Nuclei-Derived Cell Line

DISSERTATION

For the Academic Degree of
Doctor rerum naturalium
(Dr. rer. nat.)

Submitted to

The Faculty of Science (Department of Biology)
at the Dresden University of Technology

Presented by

Dena Ahmed Mohamed Amer
Born on 24th January 1983 in Giza, Egypt

Submitted on 14th April 2011
Defended on 10th June 2011

Supervisors:

Prof. Dr. Günter Vollmer
(Professur für Molekulare Zellphysiologie und Endokrinologie, Institut für Zoologie, Technische Universität Dresden, Dresden)

Dr. Georg Kretzschmar
(Molekulare Zellphysiologie und Endokrinologie, Institut für Zoologie, Technische Universität Dresden, Dresden)

Prof. Dr. Dirk Lindemann
(Institut für Virologie, Medizinisch Theoretisches Zentrum, Technische Universität Dresden, Dresden)

Prof. Dr. Gerd Kempermann
(Center for Regenerative Therapies Dresden, Biotechnologisches Zentrum)

Reviewers:

Prof. Dr. Günter Vollmer
(Professur für Molekulare Zellphysiologie und Endokrinologie, Institut für Zoologie, Technische Universität Dresden, Dresden)

Prof. Dr. med. Gabriele M. Rune
(Zentrum für Experimentelle Medizin, Institut für Anatomie, Zelluläre Neurobiologie, Universitätsklinikum Hamburg-Eppendorf Hamburg)

Committee Members:

Prof. Dr. Michael Göttfert
(Professur für Molekulargenetik, Institut für Genetik, Technische Universität Dresden, Dresden)

Prof. Dr. Günter Vollmer
(Professur für Molekulare Zellphysiologie und Endokrinologie, Institut für Zoologie, Technische Universität Dresden, Dresden)

Prof. Dr. Gerd Kempermann
(Center for Regenerative Therapies Dresden, Biotechnologisches Zentrum)

Prof. Dr. Dirk Lindemann
(Institut für Virologie, Medizinisch Theoretisches Zentrum, Technische Universität Dresden, Dresden)

Prof. Dr. Rolf Entzeroth
(Professur für Spezielle Zoologie, Institut für Zoologie, Technische Universität Dresden, Dresden)

Erklärung entsprechend §5.5 der Promotionsordnung

Hiermit versichere ich, dass ich die vorliegende Arbeit ohne unzulässige Hilfe Dritter und ohne Benutzung anderer als der angegebenen Hilfsmittel angefertigt habe; die aus fremden Quellen direkt oder indirekt übernommenen Gedanken sind als solche kenntlich gemacht. Die Arbeit wurde bisher weder im Inland noch im Ausland in gleicher oder ähnlicher Form einer anderen Prüfungsbehörde vorgelegt.

Die Dissertation wurde im Zeitraum vom **1. November 2007** bis **14. April 2011** angefertigt und durch ***Prof. Dr. Günter Vollmer, Professur für Molekulare Zellphysiologie und Endokrinologie, Institut für Zoologie, Technische Universität Dresden*** betreut.

Meine Person betreffend erkläre ich hiermit, dass keine früheren erfolglosen Promotionsverfahren stattgefunden haben. Ich erkenne die Promotionsordnung der ***Fakultät für Mathematik und Naturwissenschaften (Fachrichtung Biologie), Technische Universität Dresden*** an.

Declaration according to §5.5 of the doctorate regulations

I herewith declare that I have produced this work without the prohibited assistance of third parties and without making use of aids other than those specified; notions taken over directly or indirectly from other sources have been identified as such. This work has not been previously presented in identical or similar form to any other German or foreign examination board.

The thesis work was conducted from **1st November 2007** upto **14th April 2011** under the supervision of ***Prof. Dr. Günter Vollmer at the Department of Molecular Cell Physiology and Endocrinology, Institute of Zoology, Dresden University of Technology.***

I declare that I have not undertaken any previous unsuccessful doctorate proceedings. I declare that I recognize the doctorate regulations of the ***Fakultät für Mathematik und Naturwissenschaften (Fachrichtung Biologie) of the Technische Universität Dresden.***

..... **.....**

(Place, Date) **(Signature)**

(In the name of God, Most Gracious, Most Merciful)

For Baba, Mama, Mohammed and Khalid

“Optimism is the faith that leads to achievement. Nothing can be done without hope and confidence”

Helen Keller

ACKNOWLEDGEMENTS

At this point of my PhD journey, it is with gratitude that I acknowledge those who offered their help and support and who made my life in Germany so precious and unforgettable.

It is only fitting to begin by expressing my deep appreciation to my thesis supervisor Prof. Dr. Günter Vollmer, who has given me the opportunity to join his lab and start my PhD studies based on his trust, confidence, full support and guidance. I hope I have lived up to his expectations. I sincerely present this thesis to him as a token for my appreciation. Thank you so much…

A very special thank you goes to my mentor, Dr. Georg Kretzschmar. I thank him for his continuous help, advice, guidance and countless hours of attention and contribution he devoted throughout the course of this work. Thanks for your priceless scientific input Georg; I have certainly learned alot from you. I have always enjoyed our moments of scientific heat discussions, which I will certainly miss.

I am also thankful to my first thesis advisory committee member, Prof. Dr. Dirk Lindemann, for his advice and guidance in every stage of the virology-related experiments conducted in his lab at the Medizinisch Theoretisches Zentrum in Dresden. In this context, I am deeply grateful to all his lab members for their warm and humble welcome. My very special thank you particularly goes to Nicole “Nikita” Stanke for her invaluable cheerfulness and constant caring, support, motivation, encouragement, optimism, patience and all the lovely moments we have spent together during my stay in Dresden.

I would also like to extend my gratitude to Dr. Oliver Zierau and his dear wife Christina Avdi. They were one of the special people who made my stay in Dresden a pleasant one. My cheerful moments with them resembled moments at home, which I found invaluable. Thank you so much Zivdis…

I am also thankful to my second thesis advisory committee member, Prof. Dr. Gerd Kempermann, for his trust and helpful scientific input during my TAC meetings.

Another valued thank you goes to Dr. Jens Mittag for his confidence in me and for his critical reading and constructive suggestions for my thesis. I will always be grateful for his efforts and contributions.

I furthermore express my gratefulness to Dr. Jannette Wober, Dr. Frank Möller, Anja Bliedtner, Sylvi Wolf, Felicitas Rataj, Manuela Bader and Annekathrin Keiler for all the joyful moments I have spent with them during the last three years and a half. They were very welcoming and keen to spare me a space in their tiny cozy office. They were very friendly and of great support whenever I needed it. I thank them for all the laughters, all the scientific brainstormings, all the gossipings and all the gatherings that are indeed unforgettable and are surely engraved in my heart. You were all very special in your own ways. We had a lot in common, yet we had a lot of differences to share. It was my pleasure to be introduced to your families and be part of your happy and sad moments. I apologize for all my shortcomings, yet I cherish my times with all of you. I wish you all the very best of luck. I would also like to thank our secretary Katrin Richter as well as our two technical assistants, Antje Beyer and Susanne Kolba, for all the administrative and technical help they have instantly offered whenever it was needed. I truly appreciate your efforts and trials to communicate in English with me. The whole of AG Vollmer will truly be missed.

Most importantly, I wish to dedicate this piece of work as well as express my heartfelt gratitude to my parents for their endless support, encouragement and constant prayers. I owe alot of merit to Babito, Mamito, Mohammed and Khalid for their extra-mega patience, motivation, desire and enthusiasm for me to continue and finish my PhD degree successfully. I love you all very dearly.

I would like to extend my dedication and gratitude to Dr. Ammar Ali El-Khidir. I am absolutely speechless towards his endless support and help throughout my PhD years and during my tough times. I deeply thank him for his priceless patience, for his constant motivation and support, for his cheerful gifts, for our scientific brainstorming sessions and… the list is never ending. He has offered alot for me and I definitely owe him loads.

Last but not least, a very big thank you goes to all my friends whom I was privileged to know during my stay in Germany, in particular Mia “Bia” Louise Begasse, Marcus “Mari” Jahnel, Vanessa “Vanilinda” Carlos, Loic “Locito” Alain Royer and Dr. Ana “Banana” Santo for all the caring, super duper joyful/laughter moments, emotional and academic support, skiing experience and the endless lovely gatherings. Moreover, my thank you extends to Soulafa Mamluk, Amani Said and Zeina Nicola for all our lovely Arabic gatherings/spirit/sense of humor. All of you truly made my life in Dresden very rich and unforgettable. I wish you all the very best of luck and thank you so much once again…

…and to all my dear friends in Egypt and U.A.E (You all know yourselves): Thank you for your supportive phone calls, for your prayers and for all the cheerful times I have spent with you whenever I visited.

I also acknowledge support from the Dresden International Graduate School for Biomedicine and Bioengineering (DIGS-BB). In particular, I would like to sincerely thank Frau Carolyn Fritzsche from the MPI-CBG International Office for her immediate assistance with all my paperwork required for moving in/out of Germany.

…and to finally acknowledge my stay in Germany and my German speaking abilities:

“…Es war ein freude zu leben und studiert im Deutschland, Dresden. Ich habe gelernt zu viel und Ich habe treffern zu viel wunderbar leute in diesen schöner Stadt. Ich habe genossen meinen Aufenthalt. Danke Danke Danke liebe leute…“

Dena Amer ^___^

TABLE OF CONTENTS

LIST OF ABBREVIATIONS

Abbreviation	Full Name
6-DMAN	6-(1,1-Dimethylallyl)naringenin
7-O-PN	7-(O-prenyl)naringenin-4'-acetate
8-PN	8-Prenylnaringenin
AF-1/AF-2	Activation Function-1/Activation Function-2
AMP	Adenosine Monophosphate
APS	Ammonium Persulfate
ATP	Adenosine Triphosphate
BCA	Bicinchoninic Acid
bp	base pair
BSA Fraction V	Bovine Serum Albumin Fraction V
CBP	CREB Binding Protein
cDNA	complementary Deoxyribonucleic Acid
CIAP	Calf Intestinal Alkaline Phosphatase
Cml-5	Gene encoding rat camello-like 5
C_T-value	Cycle Threshold value
CYPs	Cytochrome P450 Enzymes
DAI	Daidzein
DAPI	4', 6-diamidino-2-phenylindole
DCC-FCS	Fetal Calf Serum pre-treated with Dextran-Coated Charcoal
DEPC-treated water	Diethylpyrocarbonate-treated water
DMEM/F12	Dulbecco's Modified Eagle Medium/Nutrient Mixture F12
DMSO	Dimethyl Sulfoxide
DNA	Deoxyribonucleic Acid
dNTP	Deoxyribonucleotide Triphosphate
DOTAP	1, 2-Dioleoyl-3-Trimethylammonium-Propane
DPN	Diarylpropionitrile (Estrogen Receptor-beta agonist)
D-RNDA	RNDA cells grown under differentiating conditions
dsDNA	double-stranded Deoxyribonucleic Acid
E. coli	*Escherichia coli*

Abbreviation	**Full Name**
E1	Estrone
E2	17β-Estradiol
E3	Estriol
EC_{50}	Half maximal effective concentration
EDTA	Ethylenediaminetetraacetic Acid
EGFP	Enhanced Green Fluorescent Protein
EQ	Equol
ERE	Estrogen Responsive Element
ERα	Estrogen Receptor-alpha
ERβ	Estrogen Receptor-beta
ESR-1	Gene encoding human estrogen receptor-alpha
Esr-2	Gene encoding rat estrogen receptor-beta
ESR-2	Gene encoding human estrogen receptor-beta
F	Fulvestrant
FACS	Fluorescence-Activated Cell Sorting
FCS	Fetal Calf Serum
Fwd	Forward Primer
G418	Geneticin®
Gag/*Pol*/*Env*	Viral Structural Genes
GEN	Genistein
GPR30	G-protein coupled receptor 30
HPLC water	High Performance Liquid Chromatography water
HRPO	Horseradish Peroxidase
HRT	Hormone Replacement Therapy
HSDs	Hydroxysteroid Dehydrogenases
hsp	heat shock protein
ICC	Immunocytochemistry
IUPAC	International Union of Pure and Applied Chemistry
kb	kilobase
K_d	Dissociation Constant
kDa	kiloDalton

Abbreviation	**Full Name**
Krt-19	Gene encoding rat keratin, type I cytoskeletal 19
LB medium/agar	Lysogeny Broth medium/agar
LCoR	Ligand-dependent Co-repressor
MMLV-RT	Moloney Murine Leukemia Virus-Reverse Transcriptase
mRNA	messenger Ribonucleic Acid
NAR	Naringenin
NCoR	Nuclear Receptor Co-repressor
Nefm	Gene encoding rat neurofilament, Medium polypeptide
NF-H	Neurofilament-High
NF-L	Neurofilament-Low
NF-M	Neurofilament-Medium
NSE	Neuron Specific Enolase
PBS	Phosphate Buffered Saline
PBST	Phosphate Buffered Saline including Tween 20
PCR	Polymerase Chain Reaction
PEI Solution	Polyethyleneimine Solution
PPT	Propyl Pyrazole Triol (Estrogen Receptor-alpha agonist)
PSB-TCEP	Protein Solving Buffer containing reducing agent
PVDF	Polyvinylidene Fluoride
Rev	Reverse Primer
RIP140	Receptor Interacting Protein of 140 kDa
RNA	Ribonucleic Acid
Rps-18	Gene encoding rat ribosomal protein S18
SDS	Sodium Dodecyl Sulfate
SDS-PAGE	SDS-PolyAcrylamide Gel Electrophoresis
SERM	Selective Estrogen Receptor Modulator
SFDM	Serum-Free Defined Medium
SHBG	Sex Hormone Binding Globulin
Slc6a4	Gene encoding rat solute carrier family 6 member 4 (also known as serotonin re-uptake transporter)
SMRT	Silencing Mediator of Retinoid and Thyroid Receptors

Abbreviation	**Full Name**
Sox-18	Gene encoding rat sex determining region Y-box 18
SRC 1-3	Steroid Receptor Co-activator 1-3
StAR	Steroidogenic acute regulatory protein
SV40	Simian Virus 40
TAE Buffer	Tris-Acetate-EDTA Buffer
Taq DNA Polymerase	*Thermus aquaticus* DNA Polymerase
TE Buffer	Tris-EDTA Buffer
TEMED	Tetramethylethylenediamine
Tris	Tris(hydroxylmethyl)aminomethane
UD	Undiluted viral stock
Zdhhc-2	Gene encoding rat zinc finger, DHHC-type containing 2
ΔC_T / $\Delta\Delta C_T$	delta C_T-value / delta delta C_T-value

LIST OF FIGURES

LIST OF TABLES

ABSTRACT

Estrogens greatly affect the activity and connectivity of serotonergic neural cell populations, which extend from clusters of nuclei in the brainstem, termed the raphe nuclei, where estrogen receptor β is the most abundantly expressed estrogen receptor subtype. Estrogenic effects on the raphe nuclei are primarily important for influencing various neuropsychological behaviors, including depression, mood swings and anxiety behaviors. Because of this connection, phases of intense hormone fluctuations for instance during menopause are often associated with several mood disturbances that often reduce the quality of life of menopausal women. Accordingly, long-term use of hormone replacement therapy appeared to be the method of choice for many menopausal women to help alleviate vasomotor symptoms, which may include neuropsychological changes such as depression. However, given the limitations and number of serious health risks attributed to hormone replacement therapy, natural compounds such as phytoestrogens are receiving widespread awareness due to their occurrence in medicinal plant extracts and a wide variety of food items including dietary supplements with respective health claims. Flavonoids, particularly the isoflavones and the naringenin-type flavanones, belong to a group of polyphenolic plant-derived secondary metabolites known to possess estrogen-like bioactivities. Nevertheless, little is known about their transactivational activity and their potential to regulate endogenous gene expression of estrogen responsive genes in the raphe nuclei due to the lack of suitable cellular models expressing sufficient amounts of functional estrogen receptor β.

Hence, a raphe nuclei-derived cell line that expresses a functional estrogen receptor β was sought as a model to investigate effects of flavonoids *in vitro*. In this regard, RN46A-B14 cells derived from embryonic day 13 rat medullary raphe nuclei were primarily used in this study as the main cellular model. Nonetheless, expression of endogenous estrogen receptor β in these cells was not sufficient to pursue downstream investigations of estrogen-dependent activities. To overcome this deficit, a rat raphe nuclei-derived *in vitro* model that overexpresses a functional estrogen receptor β was initially established (herein termed RNDA cells) by stably transducing its parent cell line, RN46A-B14 cells, with a suitable lentiviral expression vector encoding a human estrogen

receptor β gene. The stable expression and the functional characterization of the transgenic receptor was confirmed by Western blot analysis and luciferase reporter gene assays, respectively. The same reporter gene assay was used to scrutinize the transactivational activity of the flavonoids in RNDA cells. Key results revealed that Genistein, Daidzein, Equol, Naringenin and 8-Prenylnaringenin demonstrated high transactivational activity in a concentration-dependent manner by stimulating luciferase expression from an estrogen responsive element-regulated reporter gene construct transiently transfected in RNDA cells. Low transactivational activity was observed in RNDA cells in response to increasing concentrations of 7-(O-prenyl)naringenin-4'-acetate. However, no transactivational activity was noticed in response to 6-(1,1-Dimethylallyl)naringenin in the studied cell model. All effects elicited by the flavonoids were antagonized by the pure estrogen receptor antagonist, Fulvestrant, indicating that all substances act by binding to and activating the transgenic ERβ. Additional effects were observed in RNDA cells in response to a co-treatment of 1 µM of either Genistein or Daidzein, but not Equol, with 10 nM 17β-Estradiol. Slight antagonistic effects were observed in the same studied cell line when either 8-Prenylnaringenin or 7-(O-prenyl)naringenin-4'-acetate, but not Naringenin or 6-(1,1-Dimethylallyl)naringenin, were co-added with 17β-Estradiol.

Results from the reporter gene assays were validated on the basis of regulation of mRNA expression of estrogen responsive genes following the global assessment of 17β-Estradiol-induced gene expression in this cell line using a DNA microarray technique. Out of 212 estrogen-regulated genes with at least two-fold change of expression, six were selected according to specific features of estrogenic regulation of expression. The expression of the six selected 17β-Estradiol-regulated genes was validated using quantitative real-time PCR analysis. The regulation of mRNA expression of the selected genes in response to the tested flavonoids was then investigated in RNDA cells. Additionally, because RNDA cells encode a temperature-sensitive mutant of the Simian Virus 40 large T-antigen, their neuronal differentiation is constitutive upon shifting them from conditions promoting proliferation (permissive temperature) to differentiation (non-permissive temperature). Hence, the regulation of mRNA expression of the selected

genes in response to the tested flavonoids was additionally investigated as RNDA cells differentiate.

In RNDA cells grown under proliferative conditions, 17β-Estradiol up-regulated mRNA expression of *camello-like 5*, *sex determining region Y-box 18* and *keratin type I cytoskeletal 19*. Similar effects were observed in response to 8-Prenylnaringenin, Genistein, Daidzein and Equol. In addition, 17β-Estradiol down-regulated mRNA expression of *neurofilament medium polypeptide* and *zinc finger DHHC-type containing 2*. Similar effects were observed in response to 8-Prenylnaringenin, Naringenin, Genistein, Daidzein and Equol. Yet, no effect was observed on the regulation of mRNA expression of *solute carrier family 6 member 4* in response to 17β-Estradiol or the flavonoids in RNDA cells grown under proliferative conditions. When RNDA cells were shifted to conditions promoting differentiation, changes in cell morphology, in mRNA expression levels and in responsiveness towards 17β-Estradiol or the flavonoids were observed. These expression studies additionally highlighted some of the genes as indicator genes for RNDA cellular differentiation.

The newly established RNDA cell line should prove useful to elucidate basic physiological properties of estrogen receptor β in the raphe nuclei. The present study should serve as the basis to help shed light on molecular and cellular mechanisms following the action of phytoestrogens, endocrine disruptors or other exogenous estrogen receptor ligands in neural cell populations, particularly the raphe nuclei, for further applications within the brain.

1. INTRODUCTION

The transition to menopause is a complex physiological process, often accompanied by the additional effects of social adjustment and ageing. Menopause is defined as the permanent termination of menstruation due to cessation of ovarian function (i.e. reduced secretion of ovarian hormones). Clinically speaking, natural menopause (not associated with a pathological cause) is diagnosed after 12 months of amenorrhea. Usually, women in their mid to late 40s begin their menopausal transition and this can last for 4 - 5 years. The final menstrual period generally happens when women are between 40 and 58 years old (Nelson, 2008). It has been estimated in the year 2010 that approximately 171 million women from the Western world were living their menopausal transition (Rampp *et al.*, 2008).

Obvious vasomotor symptoms have been associated with fluctuating hormone levels, including hot flushes as well as changes in neuropsychological functioning. Mood disorders, including depression, are some of the neuropsychological changes occurring during menopause, which are highly prevalent in the general population. They are associated with significant morbidity and functional impairment (Wells *et al.*, 1989; Wittchen and Hoyer, 2001). Epidemiological studies have consistently demonstrated higher rates of depressive illness in women than in men. In fact, rates of depression in women are approximately 21.3 % as opposed to 12.7 % for men (Kessler *et al.*, 1994). The gender difference in depression is not noticeable until puberty (Angold *et al.*, 1999), suggesting that ovarian hormones may contribute to depression.

Given the higher prevalence of depression in women, interest in studying and treating mood disorders across the women's reproductive life cycle, particularly during the menopausal transition, is on the rise (Douma *et al.*, 2005; Meltzer-Brody, 2010). It has been pointed out that estrogens have favorable effects on mood and cognition, mediated through serotonergic neural cell populations that extend from clusters of nuclei in the brainstem known as raphe nuclei, where estrogen receptor β is the most abundantly expressed estrogen receptor subtype (McEwen and Alves, 1999). Accordingly, menopausal women have been treated with hormone replacement therapy (HRT) for

more than 60 years, which was shown to alleviate depression and anxiety behavior (Klaiber *et al.*, 1979; Schmidt *et al.*, 2000; Rasgon *et al.*, 2002). In addition, HRT has been shown to reduce incidence of colon cancer (Chen, 2009) and promote increased bone mineral density in osteoporotic postmenopausal women (Tuppurainen *et al.*, 2010); resulting in a significant improvement in women's quality of life.

Despite the benefits of HRT, an increased incidence of breast and endometrial cancer was found to be highly associated with long-term use of HRT, where the cancers seem to be larger and more advanced amongst hormone-therapy users (Dupont and Page, 1991; Steinberg *et al.*, 1991; Beral *et al.*, 1999; Chlebowski *et al.*, 2003; Chlebowski *et al.*, 2009). Grodstein et al. (1997) reported lower rates of mortality amongst HRT users as compared to women who had never taken hormones. Nevertheless, the overall benefit of long-term use of HRT had to be questioned because of increased risk of mortality from development of breast cancer (Grodstein *et al.*, 1997).

As a result, a recurrence of consumer interest in phytoestrogens, i.e. plant-derived secondary metabolites possessing estrogen-like bioactivity, has been noticed due to their occurrence in medicinal plant extracts and a wide variety of food items including dietary supplements with respective health claims (Henderson *et al.*, 1994; Sullivan *et al.*, 1997; Torgerson and Bell-Syer, 2001). Flavonoids are considered one of the major classes of such plant-derived secondary metabolites with low toxicity and weak cytostatic properties. Hence, they are classified as suitable candidates for *in vitro* and *in vivo* studies (Gester *et al.*, 2001; Tokalov *et al.*, 2004) to help identify new alternative therapeutic options to possibly alleviate menopause-related mood disorders, without leading to additional health risks. Even though these substances are sold as medicinal plant remedies or as dietary supplements and have reached quite remarkable market shares, conclusive data on their effects in the raphe nuclei remain to be elusive due to the lack of suitable raphe nuclei-derived cellular models expressing sufficient amounts of functional estrogen receptor β. As a result, it is crucial to create and establish such raphe nuclei-derived cellular models to shed light on the estrogenic potencies as well as the molecular and cellular events in response to flavonoids and other phytoestrogens for further applications within the brain, particularly in the raphe nuclei.

2. THEORETICAL BACKGROUND

2.1. The Endocrine System

The endocrine system is a complex body signaling system consisting of ductless glands that produce and secrete chemical messengers called hormones. The term “endocrine” refers to the direct secretion of such hormones into the bloodstream in response to specific stimuli (Hiller-Sturmhofel and Bartke, 1998). Once in the blood, hormones are transported towards specific target cell(s) and ultimately trigger a cascade of biochemical reactions via their interaction with associated target cell membrane or intracellular receptor proteins. As a result, the development and the regulation of many body functions are homeostatically maintained (Kalra and Kalra, 2010). The regulation and the process of hormone release mainly relies on constant feedback mechanisms maintained via the hypothalamus-pituitary-gonadal axis (Vadakkadath Meethal and Atwood, 2005; Meethal *et al.*, 2009).

There exist three main chemical classes of hormones. The first class of hormones are the ones consisting of short polypeptide sequences and are primarily secreted from either the hypothalamus, pituitary gland or the pancreas (Hiller-Sturmhofel and Bartke, 1998). Those include oxytocin (Lee *et al.*, 2009) and insulin (Permutt *et al.*, 1981). More complex protein hormones possess oligosaccharide side-chains covalently attached to them. Those are often referred to as glycoprotein hormones, which include follicle-stimulating hormone and luteinizing hormone (Pierce and Parsons, 1981). The second class of hormones are the monoamine hormones which are derivatives of aromatic amino acids: phenylalanine, tryptophan or tyrosine; of which serotonin, epinephrine (adrenaline), norepinephrine and dopamine are characterized (Bortolato *et al.*, 2008; Enna, 2010).

The third class of hormones are steroid hormones, a group of chemical messengers derived from cholesterol (Lucki and Sewer, 2010). These hormones are either produced from the adrenal cortex such as glucocorticoids and mineralocorticoids, or the gonads such as androgens, progestogens and endogenous estrogens (Simons, 2008). Steroid hormones share a common structural arrangement. The steroid core is composed of 17 carbon atoms bonded together to take the form of four fused rings: three cyclohexane

rings (designated as rings A, B, and C) and one cyclopentane ring (designated as ring D) (**Figure 2-1**). They differ by the functional groups attached to these four rings as well as the oxidation state of the rings (Moss, 1989). From all five aforementioned steroid hormones, endogenous estrogens will be the main focus of the present study.

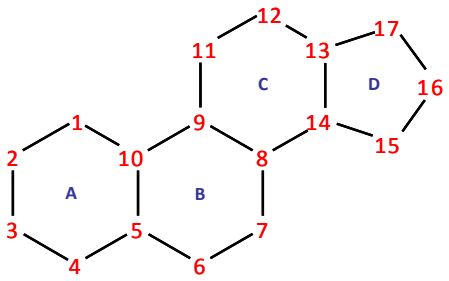

Figure 2-1: The basic skeleton of all steroids including steroid hormones. Carbon atom numbering is denoted in red and the IUPAC lettering of the rings is denoted in blue.

2.2. Biosynthesis of Endogenous Estrogens

Estrogen hormones were first discovered in the 1920s (George and Wilson, 1988). They are primarily responsible for the emergence of female secondary sex characteristics, such as breast development, typical body proportions, estrogen-dependent changes of the female genital tract as well as the distribution of subcutaneous adipose tissue. Typical target organs for the estrogens include the external genitalia, vagina, uterus, fallopian tubes and the ovaries. However, they could also act on non-reproductive target tissues, such as bones, the cardiovascular system, the liver and the central nervous system (Dötsch *et al.*, 2001).

The *de novo* synthesis of endogenous estrogens predominantly takes place in the ovaries, one of the main endocrine organs involved in the *de novo* production of steroid hormones. Synthesis takes place by the help of steroidogenic enzymes, such as several specific cytochrome P450 enzymes (CYPs) and hydroxysteroid dehydrogenases (HSDs) (Miller, 1988). The multienzyme process is stimulated when luteinizing hormone, produced from the anterior portion of the pituitary gland, binds to its cognate receptors expressed in the highly vascularized theca cells of the ovaries.

The precursor of steroid hormones is cholesterol (a 27 carbon molecule), which is transported into the mitochondria of theca cells, where steroidogenesis starts by

conversion of cholesterol to pregnenolone (a 21 carbon molecule) by means of the CYP11A (a cholesterol side-chain cleaving enzyme bound to the inner membrane of the mitochondrion) (Parker and Schimmer, 1995). This transfer of cholesterol across the mitochondrial membranes is considered the rate-limiting step of steroidogenesis and is mediated by the steroidogenic acute regulatory protein (StAR) (Sugawara *et al.*, 1996). The conversion of cholesterol to pregnenolone involves hydroxylation at the side-chain of cholesterol at carbon-20 and carbon-22 and ultimately cleavage of the side-chain takes place. Pregnenolone then gets converted to progesterone in two steps. The first step involves oxidation of the 3-hydroxyl group to a keto group. The second step involves the transfer of the double bond from carbon-5 to carbon-4. Both reactions are catalyzed by 3β-hydroxysteroid dehydrogenase (3β-HSD) and delta 4, 5-isomerase, respectively (Sanderson, 2006) (**Figure 2-2**). Progesterone is further converted to 17-hydroxyprogesterone by 17α-hydroxylase, where a hydroxyl group is added to carbon-17. The 17, 20 lyase enzyme then removes the side-chain from the steroid nucleus to form the weak androgen, namely androstenedione. Catalyzed by 17β-hydroxysteroid dehydrogenase (17β-HSD), testosterone (a 19 carbon molecule) is formed and both androgen molecules diffuse to the neighboring poorly vascularized granulosa cells where aromatization takes place (Chung *et al.*, 1987; Sanderson, 2006) (**Figure 2-2**).

Aromatization is the last step in the formation of endogenous estrogen (i.e. formation of the 18 carbon molecules) (**Figure 2-3**). This reaction is catalyzed by the P450 aromatase monooxygenase enzyme complex, which functions as a demethylase, hence removing the methyl group from carbon-10. In addition, the keto group on carbon-3 gets converted to a hydroxyl group (Ryan, 1982). The first and least abundant endogenous estrogen, Estrone (E1), is generally produced in ovaries as well as adipocytes from its androgen precursor androstenedione. The second and main physiological endogenous estrogen, 17β-Estradiol (E2), is produced in the ovaries from testosterone. E2 and E1 usually exist in metabolic equilibrium due to the action of 17β-HSD. Almost 98 % of circulating E2 is either bound to albumin or to sex hormone binding globulin (SHBG), a specific carrier protein that binds estrogens with high affinity. The third endogenous estrogen, Estriol (E3), is primarily produced during pregnancy from E1 and E2 (Dötsch *et al.*, 2001; Gruber *et al.*, 2002) (**Figure 2-3**).

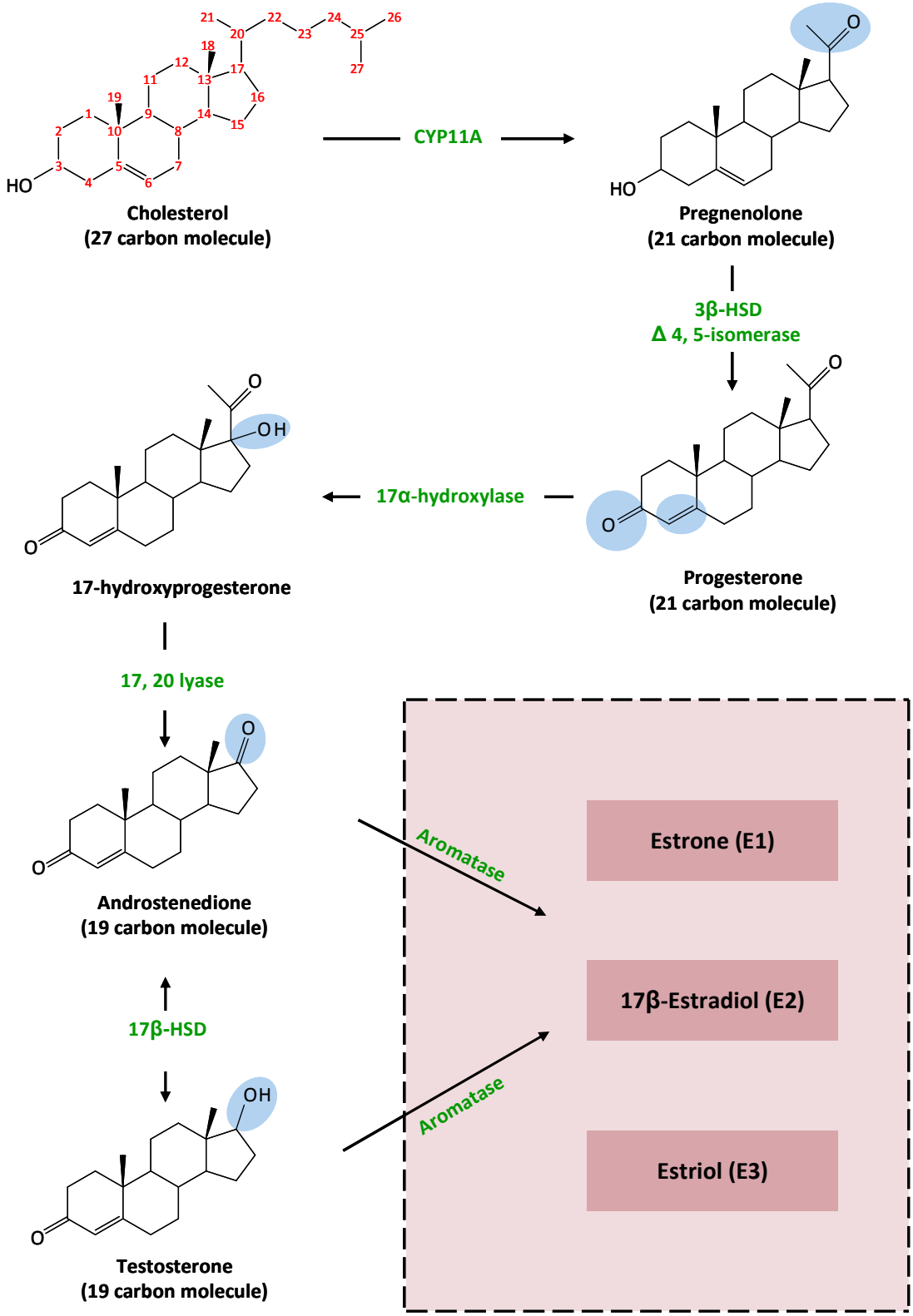

Figure 2-2: Biosynthesis of endogenous estrogens. Progesterone and the androgen molecules are primarily produced in theca cells (unshaded area) from the starting molecule cholesterol. The androgens then diffuse to granulosa cells (shaded area), where aromatization results in the synthesis of the three endogenous estrogens. Carbon atom numbering is shown in red, enzymes are shown in green and any change in biochemical structure is highlighted in light blue. **Abbreviations:** CYP11A, cytochrome P450 11A; 3β- and 17β-HSD, 3β- and 17β-hydroxysteroid dehydrogenase; Δ 4, 5 isomerase, delta-4, 5 isomerase.

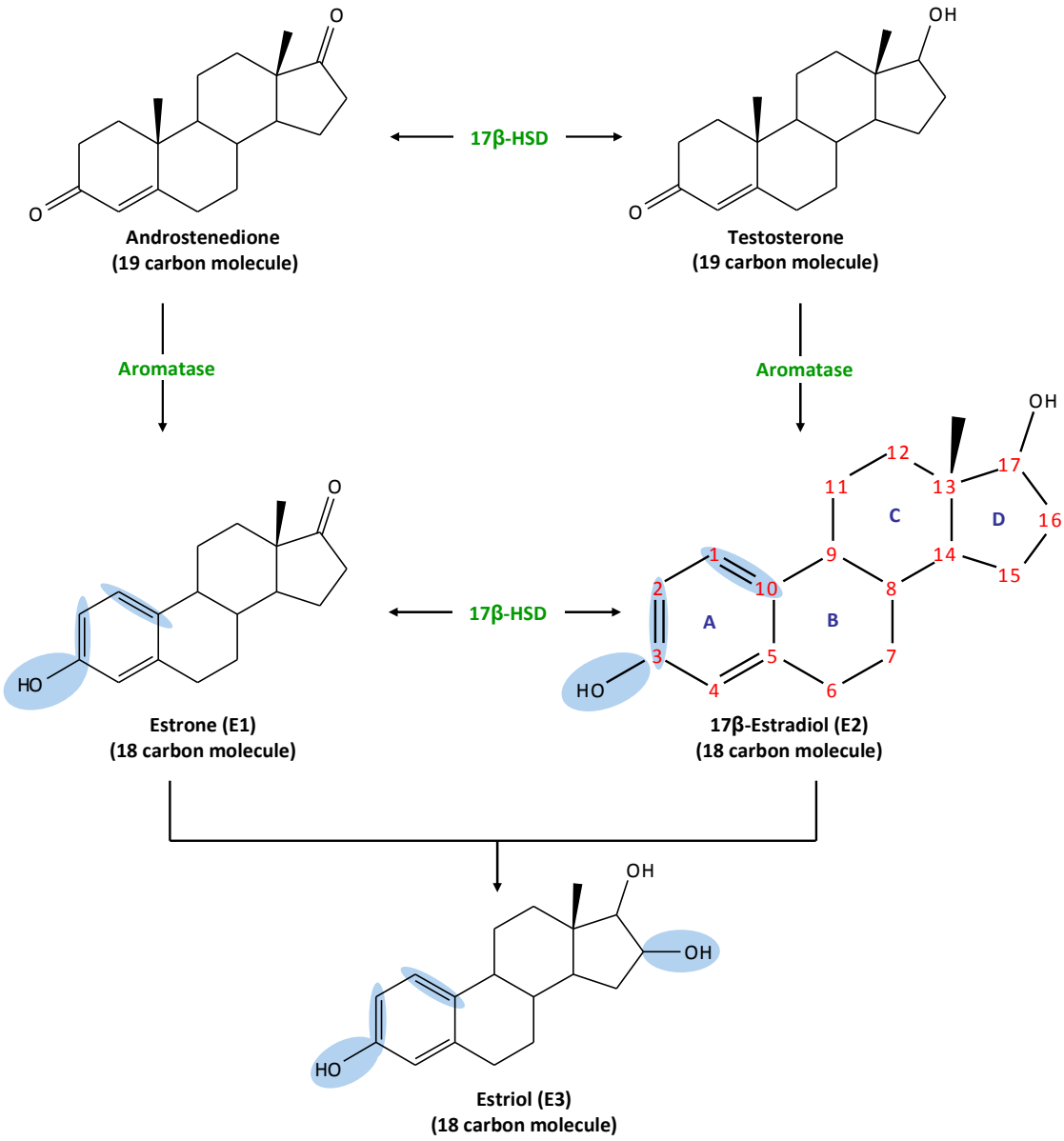

Figure 2-3: Aromatization of androgens in the granulosa cells of the ovaries. Out of all three endogenous estrogens, the main physiological estrogen is E2 (the zoomed-in molecule). Carbon atom numbering is denoted in red, enzymes are denoted in green, the IUPAC ring lettering is denoted in dark blue and any change in biochemical structure is highlighted in light blue. **Abbreviations:** 17β-HSD, 17β-hydroxysteroid dehydrogenase.

Besides the ovaries, Wehrenberg and colleagues (2001) revealed the existence of StAR mRNA and protein in rat and marmoset hippocampi using *in situ* hybridization and immunohistochemistry techniques (Wehrenberg *et al.*, 2001). The same group also indicated the co-expression of StAR and the aromatase enzyme in their studied hippocampi (Wehrenberg *et al.*, 2001). Although it was already known that hippocampal neurons express aromatase [Reviewed in (Beyer, 1999)], Wehrenberg and colleagues

(2001) strongly proposed, based on their results, that *de novo* synthesis of E2 may certainly occur in hippocampal neurons (Wehrenberg *et al.*, 2001), given that StAR-positive cells always contain side-chain cleavage enzyme as well as 3β-HSD (Furukawa *et al.*, 1998).

2.3. Estrogen Receptors: The Alpha and Beta

Endogenous estrogens are retained in target cells by an intranuclear binding protein, termed the estrogen receptor (ER). ERs are a subfamily of the nuclear receptor superfamily of ligand-activated transcription factors that are highly conserved evolutionary from invertebrates to higher organisms. Nuclear receptors also include thyroid receptor, progesterone receptor, Vitamin D receptor, mineralocorticoid receptors and several "orphan" receptors; whose ligands are not yet identified (Robinson-Rechavi *et al.*, 2003; Margolis and Christakos, 2010).

2.3.1. Research History of Estrogen Receptors

Based on the specific binding of tritium-labelled 17β-Estradiol in the uterus and vagina, Jensen and Jacobson (1962) came to the conclusion more than 40 years ago that the biological effects of estrogens had to be mediated by a specific receptor (Jensen and Jacobson, 1962). These studies were further extended by Noteboom and Gorski (1965), who reported that the receptor is stereo-specific and could be classified as a protein (Noteboom and Gorski, 1965). Following extensive studies on this protein, Green and co-workers (1986) published their landmark paper in 1986 regarding the cloned and sequenced complete complementary DNA (cDNA) of the ER from human breast cancer cell line MCF-7. The gene is encoded by 8 exons corresponding to a 595 amino acid residue polypeptide with a molecular weight of approximately 66 kilodaltons (kDa) that binds E2 with high affinity [dissociation constant (K_d) = 0.4 nM] (Green *et al.*, 1986; Kuiper *et al.*, 1998). Following this discovery, homologous receptors, showing significant sequence homology, were rapidly isolated from the rat (Koike *et al.*, 1987), mouse (White *et al.*, 1987) and chicken (Maxwell *et al.*, 1987).

Up until 1995, it was assumed that there was only one ER responsible for mediating the physiological and pharmacological effects of estrogens. However, the proposed existence of only a single ER gene failed to explain the complicated tissue selectivity of estrogens and antiestrogens *in vivo* as well as the differential effect of these substances in various cell lines (Katzenellenbogen *et al.*, 1996). This led to the cloning and identification of a second novel ER, named ER-beta (ERβ), at the end of 1995. This ERβ was cloned from a rat prostate cDNA library corresponding to a 485 amino acid residue polypeptide with a molecular weight of approximately 54 kDa which also binds E2 with high affinity (K_d = 0.6 nM) (Kuiper *et al.*, 1996; Kuiper *et al.*, 1998). The former cloned ER was then renamed ER-alpha (ERα) to distinguish it from the newly discovered estrogen receptor.

Following this breakthrough, the cDNAs encoding ERβ in humans (Mosselman *et al.*, 1996; Enmark *et al.*, 1997) and mice (Tremblay *et al.*, 1997) were all cloned and showed significant sequence homology with their respective ERα. Furthermore, human ERβ shows the most sequence identity in its translated region, approximately 89%, to the rat ERβ as compared to any other mammalian ERβ (Enmark and Gustafsson, 1999).

Both ERs are encoded by two independent genes. In humans, for example, ERα and ERβ are encoded by *ESR1* and *ESR2*, respectively. The human ERα and ERβ genes have been mapped to band q25.1 of chromosome 6 and q23.2 of chromosome 14, respectively (Enmark *et al.*, 1997) .

2.3.2. Structural and Functional Domains of Estrogen Receptors

ERs, like all other members of the nuclear receptor family, are composed of six independent yet interacting structural and functional domains denoted A to F, as shown in **Figure 2-4** (Beato, 1989; Mangelsdorf *et al.*, 1995). Biochemical and mutational analyses of the receptors have revealed two main domains (C and E) that are highly conserved between different species (Green and Chambon, 1986). Those two domains are mainly essential for the receptor to efficiently activate the transcription of target genes (Kumar *et al.*, 1987).

The central cysteine-rich C domain is a highly conserved domain of the ER alpha and beta subtypes and is responsible for their DNA-binding activity. It contains two type II zinc

finger clusters, which play an important role in receptor dimerization and in binding to specific DNA sequences termed estrogen responsive elements (ERE), located in the promoter and/or enhancer regions of target genes (Klinge, 2001).

EREs consist of short palindromic sequences that comprise inverted repeats of 5'-GGTCA-3' separated by three variable nucleotides, resulting in 5'-GGTCAnnnTGACC-3' (Walker *et al.*, 1984). The DNA binding domains of ERα and ERβ are highly homologous in their amino acid sequence (**Figure 2-4**) (Kumar *et al.*, 1987; Forman and Samuels, 1990). Particularly, there exists a sequence, the P-box, which is identical in the two receptors and critical for target-DNA recognition and specificity (Vanacker *et al.*, 1999). As a result, ERα and ERβ are expected to bind to a variety of EREs with similar affinity and specificity.

The second moderately conserved domain of the ER alpha and beta subtypes is the E domain and corresponds to the ligand-binding domain. This domain mediates ligand binding in addition to receptor dimerization, nuclear translocation and efficient transactivation of target gene expression (Evans, 1988; Giguere *et al.*, 1988). Crystallographic studies have established that the structure of E domain displays an α-helical sandwich topology typical for all nuclear receptor ligand-binding domains. It is composed of 12 helices (H1 - H12) arranged in three anti-parallel layers separated by β-sheets (Moras and Gronemeyer, 1998). As shown in **Figure 2-4**, the domain harbors a complex region, namely ligand-dependent activation function 2 (AF-2), whose structure and function are regulated by the binding of ligands (Danielian *et al.*, 1992; Darimont *et al.*, 1998). Even though the overall conformation of the ER ligand-binding domain is quite similar in the presence of different ligands, the carboxyl-terminal transactivation function (AF-2, H12) is highly sensitive to the nature of the bound compound. For example, when an agonist, such as 17β-Estradiol, is bound to the ligand-binding domain, H12 is moved over the ligand-binding pocket presenting a binding surface for recruitment of co-activators (Brzozowski *et al.*, 1997). In contrast, when an antagonist is bound, H12 is positioned away from the ligand-binding cavity and instead occupies the hydrophobic groove formed by H3, H4 and H5. In such a position, H12 sterically inhibits the co-activator interaction surfaces (Shiau *et al.*, 1998).

The remaining domains include the N-terminal A/B domain, which encodes a ligand-independent activation function 1 (AF-1) (**Figure 2-4**) (Berry *et al.*, 1990), a region regulated by growth factors acting through the mitogen-activated protein kinase pathway, where phosphorylation of the serine residue at position 118 is required for its full activity (Kato *et al.*, 1995). In addition, the AF-1 region is involved in the activation of target gene expression in a promoter- and cell- specific manner (Kobayashi *et al.*, 2000). As for the flexible hinge D domain, which joins the DNA- and ligand- binding domains, its function is incompletely understood, even though it has been suggested that it is probably required in maintaining the integrity of the functional structure of the nuclear receptors (Miyamoto *et al.*, 2001). Finally, the F domain is of uncertain function; nonetheless this region may affect ER dimerization (Yang *et al.*, 2008).

It is important to note that the greatest sequence diversity between ERα and ERβ is present in the A/B domain at the N-terminus (18 %), the hinge D domain (30 %) and in the F domain at the C-terminus (18 %) (**Figure 2-4**). As a result, preparations of specific ERβ cDNA probes, primers and antibodies are mostly targeted to those regions (Brandenberger *et al.*, 1997; Saunders *et al.*, 1997).

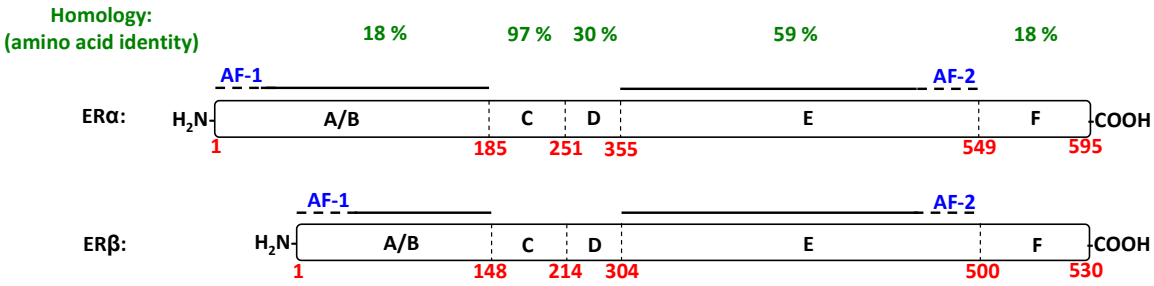

Figure 2-4: Schematic diagram representing the domain structure of the estrogen receptors. The different domains are denoted from A to F. Domain C (DNA-binding domain) is the highly conserved domain between ERα and ERβ, followed by domain E (Ligand-binding domain). Amino acid sequence numbers are shown in red and denote human ERs (Enmark and Gustafsson, 1999). Percentage of amino acid identities in all domains are based on (Shao and Brown, 2004). **Abbreviations:** ERα and ERβ, Estrogen Receptor alpha and beta; AF-1, Activation Function-1; AF-2, Activation Function-2.

2.3.3. Anatomical Distribution of Estrogen Receptors

From rat tissue extracts, messenger RNA (mRNA) encoding ERβ is highly expressed in the prostate and ovary (particularly in granulosa cells) (Byers *et al.*, 1997; Kuiper *et al.*, 1997).

Moderate ERβ expression was detected in testis, uterus, mammary gland, bladder and lung, whereas pituitary, epididymis, thymus and various regions of the central nervous system including the hypothalamus, cerebellum, substantia nigra, olfactory lobe as well as the spinal cord revealed low expression of ERβ mRNA. However, no mRNA encoding ERβ was detected in the spleen, heart, liver, stomach or kidney (Kuiper *et al.*, 1997). The ERα mRNA was highly expressed in the pituitary, testis, epididymis, kidney, liver, mammary gland, uterus and adrenal, which all showed moderate or no expression of ERβ mRNA. Besides the weak expression in hypothalamus, the olfactory lobe, substantia nigra, cerebellum and spinal cord were all negative for ERα (Kuiper *et al.*, 1997). It has also been shown that ERα mRNA is the dominant expressed ER in adipose tissue (Lundholm *et al.*, 2004) and pancreatic islets (Geisler *et al.*, 2002).

Additionally, very low expression of ERα has been detected in normal and cancerous colons (Waliszewski *et al.*, 1997; Campbell-Thompson *et al.*, 2001). Nevertheless, Foley and colleagues (2000) reported the expression of ERβ in normal colon tissues, but not in colon adenocarcinoma, using Western blotting (Foley *et al.*, 2000). In contrast to work reported by Foley and colleagues (2000), Witte and colleagues (2001) has demonstrated ERβ expression in human colorectal cancer tissues (Witte *et al.*, 2001).

Consistent with the documented effects of estrogens on bone physiology, mRNA encoding ERα and ERβ has been detected in rat osteoblasts (Oreffo *et al.*, 1999; Windahl *et al.*, 2000). In addition, other studies have reported the expression of both ERα and ERβ in muscle tissues (Petersen *et al.*, 1998; Kalbe *et al.*, 2007).

The use of ERα and ERβ knockout mice have been employed to investigate the respective roles of both estrogen receptor subtypes, where the deletion of one of the ERs can be associated with changes in the effects of 17β-Estradiol in various tissues and on different responses (Couse *et al.*, 1995; Couse and Korach, 1999). For instance, ERα knockout female mice experience cystic hemorrhagic follicles leading to infertility (Lubahn *et al.*, 1993; Dupont *et al.*, 2000), abnormalities in reproductive behavior (Ogawa *et al.*, 1996) and abnormalities in breast development (Bocchinfuso and Korach, 1997). The ERα knockout male mice experience testicular atrophy, decreased spermatogenesis and inactive sperms leading to infertility irrespective of their motivation to mount female

mice (Lubahn *et al.*, 1993; Ogawa *et al.*, 1997). In addition, aggressive behaviors were considerably reduced and typical male offensive attacks were hardly displayed by ERα knockout male mice (Ogawa *et al.*, 1997).

Conversely, the ERβ knockout male mice have loss of abdominal fat yet are fully fertile. However, the ERβ knockout female mice show reduced fertility due to an obstruction in the follicle development before ovulation (Krege *et al.*, 1998). It has also been shown that ERβ knockout mice show several morphological abnormalities in the brain, such as neuronal hypocellularity (Wang *et al.*, 2001). Additionally, ERβ knockout mice seem to reveal smaller brains with fewer neurons than those of the wild-type littermates. They also encounter more apoptotic cells as well as fragmented processes of glial cells in the brain (Wang *et al.*, 2003). Both ERβ knockout male and female mice show profound memory and learning impairment (Day *et al.*, 2005).

2.4. Molecular Mechanisms of Estrogen Action

Nuclear actions of estrogens are usually determined by: (1) the structure of the ligands which may include endogenous estrogens or exogenous and synthetic estrogens, (2) the ER subtype involved, (3) the characteristics of the promoter and/or enhancer regions of target genes and finally (4) the balance of co-regulatory proteins (i.e. co-activators or co-repressors) that modulate the final transcriptional response following the ligand/ER complexes.

2.4.1. Classical Pathway via Estrogen Responsive Elements

17β-Estradiol exerts its effects mainly via a classical genomic mechanism of action involving the interaction of estrogen to ERs and subsequent regulation of gene transcription. Typically, the classical genomic pathway takes several hours for the effect to be manifested because of the time required for transcription and translation of estrogen-regulated genes (O'Lone *et al.*, 2004). In principle, ERs mainly exist in the cytoplasm in their unbound apoprotein state. The unbound cytoplasmic ER monomers are usually coupled with receptor-associated proteins that are largely located in the cytoplasm, such as heat shock proteins (hsp90 or hsp70) or immunophilins (**Figure 2-5**)

(Smith and Toft, 1993; Pratt and Toft, 1997). It has been proposed that heat shock proteins or other molecular chaperones play a structural role in: (1) stabilizing the ERs in their inactivated unbound state, (2) masking their hydrophobic ligand-binding domain to avoid inappropriate interactions and (3) allowing for high affinity-ligand binding conformation (Ellis *et al.*, 1989).

As illustrated in **Figure 2-5**, free 17β-Estradiol enters the cell by simple or facilitated diffusion; resulting in the dissociation of the cytoplasmic molecular chaperone as well as inducing a conformational change in the receptor. This change allows the receptor ligand-binding domain to be exposed for 17β-Estradiol interaction. The E2-ER complex then shuttles into the cell nucleus and binds simple sequences of EREs as either homodimers (either ERα-ERα or ERβ-ERβ) or heterodimers (ERα-ERβ) (Pettersson *et al.*, 1997; Gruber *et al.*, 2002). The exact mechanism of the nuclear translocation of E2-ER complex remains elusive. However, it is well-known that the cytosolic protein caveolin-1 stimulates the nuclear shuttling process through direct interaction with the receptor molecule (Schlegel *et al.*, 1999).

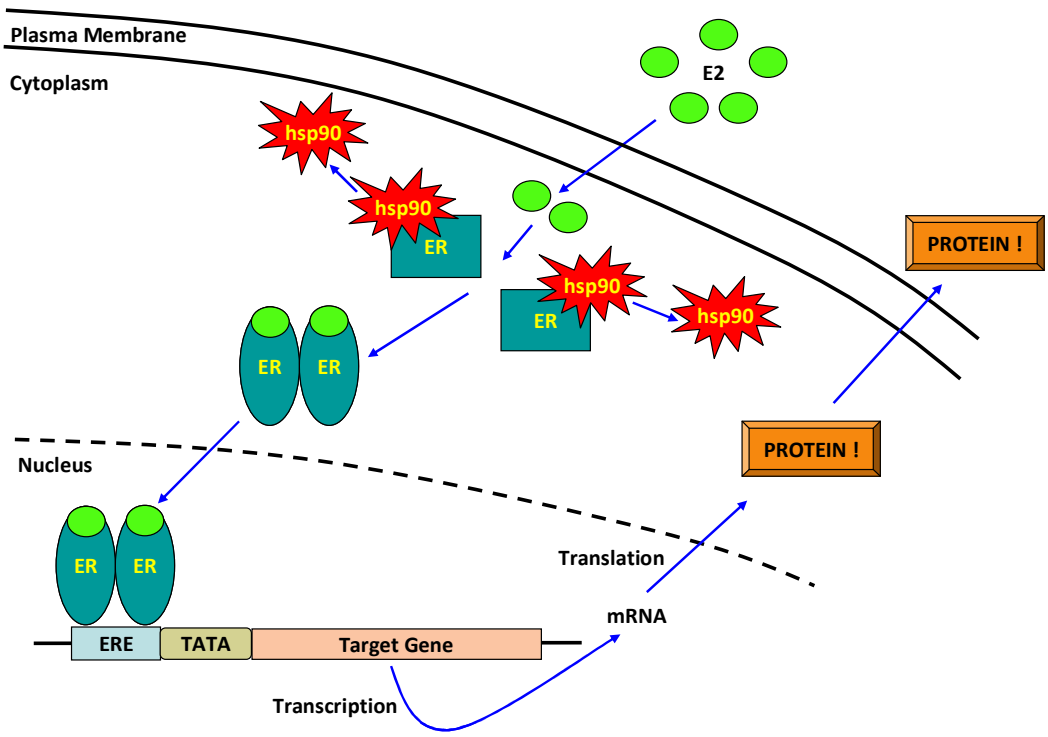

Figure 2-5: A simple schematic illustration representing the classical pathway of estrogen signaling via estrogen responsive elements. Abbreviations: E2, 17β-Estradiol; ER, Estrogen Receptor; hsp90, heat shock protein 90; ERE, Estrogen Responsive Element; mRNA, messenger RNA.

Only a small number of the most estrogen-inducible genes contain the common consensus of EREs (i.e. 5'-GGTCAnnnTGACC-3'). In some cases, alternative EREs have been described. For example, 5'-GGTCAnnnTG**G**CC-3' is a variant sequence differing from the consensus sequence by 1 bp. These variant sequences have been shown to bind ERs with less affinity, depending on the flanking bases (Driscoll *et al.*, 1998). Finally, the E2-ER complex binds to nuclear receptor co-activators or co-repressors (**Section 2.4.2**) to form a transcription-initiation complex, which includes the assembly of various factors; such as the TATA-box-binding protein and other associated factors that subsequently regulate the transcription and translation of target genes.

In humans, most of the genes regulated by ERs lack ERE-like sequences (O'Lone *et al.*, 2004). As a result, it has been extensively discussed whether estrogens can regulate the transcription of target genes that lack functional EREs by modulating the activity of other transcription factors. This action is often referred to as the alternative genomic pathways. These include regulation of target genes by ERs without directly binding to DNA, but rather via the formation of the pre-initiation complex through protein-protein interactions with transcription factors, such as the Activator Protein-1, Specificity Protein-1 and the Nuclear Factor-kappa B (Nilsson *et al.*, 2001; Bjornstrom and Sjoberg, 2005; Cheskis *et al.*, 2007).

Accumulating evidence suggests that E2 also exert non-genomic actions, i.e. actions that are very rapid and occur within minutes, hence cannot be attributed to a genomic mechanism of action. Non-genomic actions are a common property of all steroid hormones and are frequently associated with the activation of various protein-kinase cascades (Losel and Wehling, 2003). When ERs are targeted to the plasma membrane, it appears that functional domains, besides the ligand-binding domain, contribute to the level of non-genomic actions through protein-protein interactions (Kousteni *et al.*, 2001). It is more likely that the interaction of ERs with signaling molecules facilitates their activity. For example, it has been shown that ERs at the plasma membrane may associate with the scaffold protein caveolin-1 (Razandi *et al.*, 2002) in addition to a variety of proximal signaling molecules such as the G proteins (Wyckoff *et al.*, 2001). Non-genomic effects of E2 in neurons, for instance, leads to either changes in Ca^{+2} currents (Kurata *et*

al., 2001), changes in the cyclic AMP pathway (Gu and Moss, 1996), activation of mitogen-activated protein kinase pathway (Bulayeva *et al.*, 2004) or activation of protein kinase C pathway (Kelly *et al.*, 1999), which in turn greatly affects neuronal survival and transmission.

Even though evidence suggests that the classical ERs are capable of mediating many of the abovementioned events, more recent discoveries reveal the potential existence of a plasma membrane-associated receptor capable of responding to estrogens (Hasbi *et al.*, 2005). The proposed receptor is GPR30, a member of the G protein-coupled receptor superfamily that supposedly mediates the activation of estrogen-dependent kinase cascades in addition to gene transcriptional responses (Kelly *et al.*, 1999; Prossnitz *et al.*, 2008). Nevertheless, given the amount of perplexed data reported on the role of GPR30 as a membrane estrogen receptor from studies utilizing GPR30 knockout mice, further investigations shall be required to unravel such controversies [Reviewed in (Langer *et al.*, 2010; Maggiolini and Picard, 2010)].

2.4.2. Co-regulatory Proteins

The past decades have provided significant clarification of a large number of co-regulatory proteins associated with ERs and have been biochemically and functionally characterized as either co-activators or co-repressors of specific transcriptional machineries according to their mode of action (Malik and Roeder, 2005; Margueron *et al.*, 2005; Perissi and Rosenfeld, 2005).

The first are co-activator complexes that regulate promoter accessibility to various transcription factors and to basal transcriptional machinery to activate and initiate target gene expression (Dilworth and Chambon, 2001; Jenuwein and Allis, 2001). Most of them are characterized by the helical LXXLL motifs, known as nuclear receptor boxes. Those include the ATP-dependent chromatin remodeling factors, such as the SWI/SNF complex (Dilworth *et al.*, 2000); histone arginine methyltransferases, such as the p160/SRC 1-3 family (Steroid Receptor Co-activator family) that interacts with the AF-2 domain (Koh *et al.*, 2001); histone acetyltransferases, such as the CBP (CREB Binding Protein)/p300 proteins (Chan and La Thangue, 2001) in addition to factors of the so-called mediator

complex that mediate the interaction with the RNA polymerase II machinery, such as the TRAP/SMCC/DRIP/ARC complex (Rachez *et al.*, 1999).

The second are co-repressor complexes that inhibit gene activation and possibly turn off the expression of activated target genes. Those include basal or specific co-repressors. Basal co-repressors, such as NCoR (Nuclear Receptor Co-repressor) and SMRT (Silencing Mediator of Retinoid and Thyroid Receptors), function as platforms for the recruitment of other various subcomplexes that contain histone deacetylase activity (Li *et al.*, 2000). Specific co-repressors, such as LCoR (Ligand-dependent Co-repressor) and RIP140 (Receptor Interacting Protein of 140 kDa), interact with the AF-2 domain and function as a molecular scaffold that recruits several proteins that function in transcriptional repression in response to ligand induction (White *et al.*, 2004).

One important debate is whether or not ligand-bound ERα and ERβ recruit and contact different co-activators and/or co-repressors. Since both receptors show amino acid sequence homology in their AF-2 domain, it was expected that both ERs would show similar activity in co-activator recruitment, yet some differences have been pointed out. For instance, ERα shows higher affinity for SRC-3 than ERβ (Suen *et al.*, 1998). In contrast to ERα, ERβ strongly binds to the TRAP/SMCC/DRIP/ARC complex (Nilsson *et al.*, 2001).

The different binding specificities of the nuclear receptor box LXXLL motif could be one possible explanation associated with such differences (Darimont *et al.*, 1998; McInerney *et al.*, 1998). Additionally, since there are distinct ligand-binding specificities of the two ERs, and as ligands can alter receptor conformations, ligand-binding specificity is likely to affect co-regulator binding affinities and specificities. Affinity-selection approaches have been utilized to study such differences in receptor conformation. These set of experiments clearly revealed that different ER conformations are induced by different agonists and antagonists, which results in the recruitment of different ER-binding co-regulatory proteins (Norris *et al.*, 1999; Paige *et al.*, 1999).

2.5. Estrogen Receptor Ligands

The difference in the anatomical distribution between ERα and ERβ supports the possibility of achieving selectivity at the receptor level (Mosselman *et al.*, 1996; Kuiper *et al.*, 1997). Even though both ER subtypes are activated by binding 17β-Estradiol (Green *et al.*, 1986; Kuiper *et al.*, 1996), their ligand-binding domains share only 59 % of amino acid sequence identity (Shao and Brown, 2004). This implies that estrogen receptor ligands, besides the endogenous estrogens, will likely exist with different affinities, potencies and effects with regards to both ERα and ERβ (Kuiper *et al.*, 1998).

Besides the main endogenously synthesized estrogens, there exist numerous structurally diverse compounds that originate from both synthetic as well as natural sources and are known to possess estrogenic activity (**Figure 2-6**). Since these compounds interfere or alter functions of the endocrine system, they are often referred to as endocrine disrupting compounds or xenoestrogens. On one hand, humans are often exposed through the food chain to a selection of synthetic endocrine disrupting compounds, including, pesticides such as DDT and methoxychlor, industrial lubricants such as polychlorinated biphenyls as well as plasticizers such as phthalates and bisphenol A. Moreover, pharmaceutical estrogens such as ethinylestradiol can also be classified as synthetic xenoestrogens [Reviewed in (Cos *et al.*, 2003; Patisaul and Jefferson, 2010)]. It has been reported that synthetic xenoestrogens are often associated with female reproductive disorders and increasing rates of obesity and cancer (Fisher, 2004; Crain *et al.*, 2008).

On the other hand, most of the natural xenoestrogens are produced by fungi or plants and are therefore classified as mycoestrogens or phytoestrogens, respectively (**Figure 2-6**) (Cos *et al.*, 2003) . The most common mycoestrogen is zearalenone, which was reported to reduce the prevalence of breast cancer (Hilakivi-Clarke *et al.*, 1999). Based on the chemical structures of phytoestrogens, they are classified into three main groups, namely flavonoids, lignans and stillbenes (**Figure 2-6**) (Cos *et al.*, 2003). Phytoestrogens remain widely believed to provide a range of beneficial effects, including therapeutic actions in carcinogenesis, osteoporosis and atherosclerosis (Cassidy *et al.*, 2006; Kim, 2008). Nonetheless, the potential dangers of consuming high levels of these compounds have

raised concerns. As a result, phytoestrogens are currently under numerous investigations for their impact on human health (Abe, 1999). From the abovementioned natural xenoestrogens, the main focus of the present study will be the phytoestrogens particularly the flavonoids, where the isoflavones and the naringenin-type flavanones are classified.

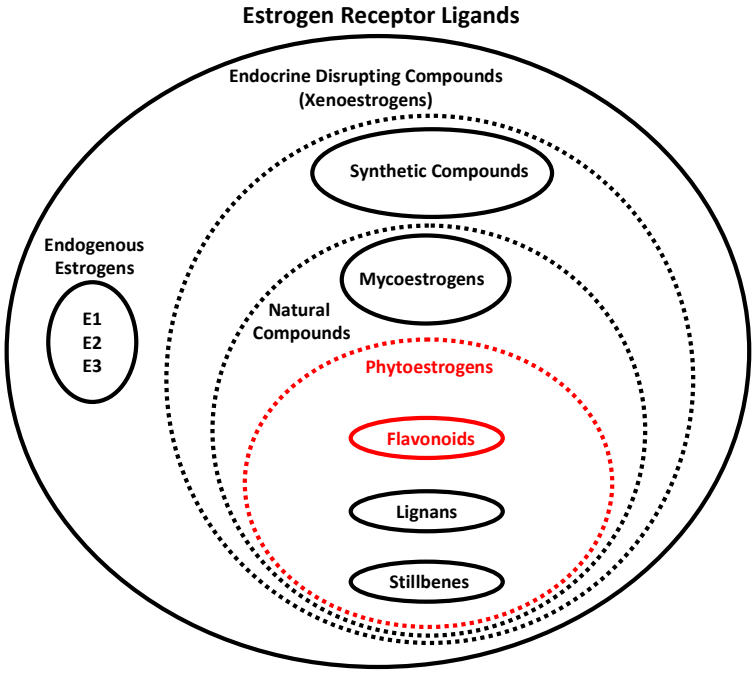

Figure 2-6: The classification of estrogen receptor ligands. Phytoestrogens, particularly the Flavonoids, are the main focus of the present study and are highlighted in red. Examples for each group are pointed out in the text.

2.5.1. Phytoestrogens: The Flavonoids

Phytoestrogens are polyphenolic naturally-occurring dietary compounds of plant origin that mostly resemble the structure of the mammalian steroidal endogenous estrogens. They cannot be classified as nutrients as lack in the diet does not lead to a deficiency syndrome; hence they are also known as plant-derived secondary metabolites (Patisaul and Jefferson, 2010). The potential use of phytoestrogens as therapeutic agents to overcome menopausal symptoms, which often lead to reduced quality of life for many women, has been receiving widespread interest due to their occurrence in medicinal plant extracts and a wide range of food items including dietary supplements with respective health claims (Brown and Setchell, 2001; Singleton and Khan, 2003).

The interest in phytoestrogens is mainly due to their estrogen-like bioactivity. They have the ability to bind both ERs and transactivate target genes. They also show both estrogenic or antiestrogenic properties depending on the circulating levels of endogenous estrogens (Cos *et al.*, 2003; Ososki and Kennelly, 2003). Medically, they have been studied as chemopreventors against various forms of cancers in addition to ameliorating symptoms in menopausal women. Their estrogenic effects vary according to the phytoestrogenic substance studied, the species and the experimental system (Davis *et al.*, 1999).

Numerous *in vitro* and *in vivo* mammalian model systems have been designed to elucidate gene expression profiles distinctive to substances with estrogenic activity as compared to 17β-Estradiol (Moggs *et al.*, 2004; Ise *et al.*, 2005). This indicates that estrogen-like substances of different origin may reveal similar molecular effects and perhaps share a significant potential for both beneficial and adverse health effects.

2.5.1.1. Isoflavones

Isoflavones are a group of bi-phenolic organic compounds with roughly 230 individual compounds and are most commonly found in legumes. Human exposures to such compounds primarily occurs through the consumption of soy-based food and beverage products, such as tofu and soy milk (Knight and Eden, 1996).

Genistein (GEN) (**Figure 2-7 A**) and Daidzein (DAI) (**Figure 2-7 B**) are the two best characterized isoflavones. Following oral uptake, the β-glucosides (i.e. Genistin and Daidzin) are broken down in the gut by intestinal glucosidases to their aglycones: Genistein and Daidzein, respectively. The aglycones can be either directly absorbed or metabolized by resident microflora in the gastrointestinal tract before absorption. Genistein is converted to several metabolites, such as dihydrogenistein, while Daidzein is converted to its main metabolite Equol (EQ) (**Figure 2-7 C**) (Axelson *et al.*, 1984; Munro *et al.*, 2003).

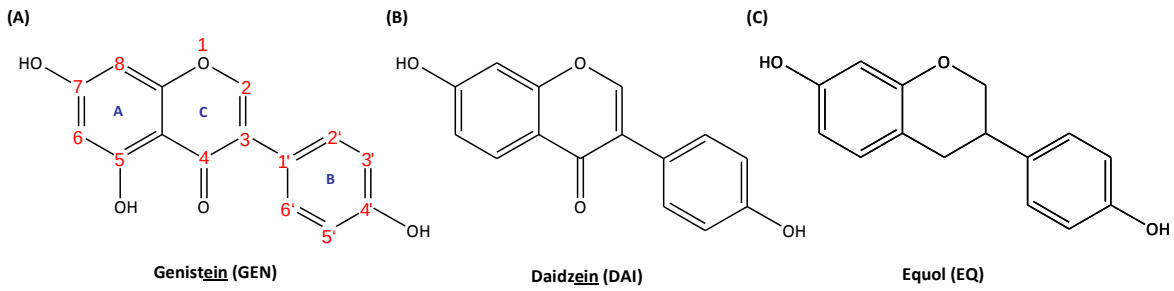

Figure 2-7: Chemical structure of the three isoflavones. Carbon atom numbering is denoted in red.

The chemical structure of isoflavones is similar to the chemical structure of 17β-Estradiol. The phenolic A-ring is one key structural feature of most compounds that bind to ERs. Another important key structural element that allows for binding to ERs is the distance between the hydroxyl groups at carbon-7 and carbon-4' of the isoflavone molecules, which is virtually identical to the 17β-Estradiol molecule (Zand *et al.*, 2000). It has been shown, using *in vitro* assays, that several isoflavones bind both ERα and ERβ, albeit to a lower affinity than 17β-Estradiol, thereby inducing or modulating the estrogen-signaling pathway, such as regulation of gene transcription and kinase pathways (Kuiper *et al.*, 1998). *In vitro* assays have shown that Genistein binds both ERs, with higher relative binding affinities for ERβ than for ERα (7.4 % and 0.017 %, respectively, where 17β-Estradiol has an affinity of 100 %) (Martin *et al.*, 1978; Muthyala *et al.*, 2004). Equol also reveals a higher relative binding affinity for ERβ than for ERα (3.2 % and 0.1 %, respectively, where 17β-Estradiol has an affinity of 100 %). Interestingly, Equol demonstrates an overall higher relative binding affinity values than its parent compound Daidzein (0.01 % for ERα and 0.04 % for ERβ, where 17β-Estradiol has an affinity of 100 %) (Markiewicz *et al.*, 1993; Muthyala *et al.*, 2004).

Epidemiological observations have indicated that high intake of isoflavones are associated with low incidences of breast cancer, cardiovascular diseases and osteoporosis (Adlercreutz and Mazur, 1997). However, data on isoflavones and their effects in brain cells are variable. On one hand, Zhao and colleagues (2002) reported that Genistein, Daidzein and Equol exerted a modest yet significant reduction in lactate dehydrogenase release, a marker of plasma membrane damage, in cultured hippocampal neurons. On the other hand, the isoflavones did not promote hippocampal neuron process outgrowth as opposed to 17β-Estradiol (Zhao *et al.*, 2002). Furthermore, it has recently been reported

that high concentrations of Genistein and Daidzein induce neurotoxicity in primary rat neuronal cultures (Jin *et al.*, 2007). Judging by these conflicting findings, biological properties of isoflavones in different brain cells are of significant interest, especially if it has been shown from a recent *in vivo* study that Genistein, for instance, has the ability to cross the blood brain barrier (Friso *et al.*, 2010).

2.5.1.2. Naringenin-type flavanones

A second recently described class of the flavonoids is the so-called naringenin-type flavanones. These are also bi-phenolic organic compounds where a large body of literature states their occurrence in various foodstuffs and medicinal plants, including Naringenin (NAR) (**Figure 2-8 A**) which is found in tomatoes (*Solanum lycopersicum)* and grapefruits (*Citrus grandis*). Additionally, 8-Prenylnaringenin (8-PN) (**Figure 2-8 B**) is a very potent naringenin-type flavanone in female hop cones (*Humulus lupulus)*, a beer flavoring agent (Milligan *et al.*, 2000; Zierau *et al.*, 2005). It can be prepared by direct prenylation of the naturally occurring Naringenin (Gester *et al.*, 2001). Finally 6-(1,1-Dimethylallyl)naringenin (6-DMAN) (**Figure 2-8 C**) is a naringenin-type flavanone that has been isolated from the leaves of the African tree *Monotes engleri* (Seo *et al.*, 1997). The analysis of naringenin-type flavanones for pharmacological applications has recently become more attractive because of the possibility to chemically synthesize naringenin derivatives using an efficient europium (III)-catalyzed Claisen rearrangement (Gester *et al.*, 2001; Tokalov *et al.*, 2004). This allowed access to larger quantities of the substances of interest as well as the development and synthesis of artificial structural variations, such as 7-(O-prenyl)naringenin-4'-acetate (7-O-PN) (**Figure 2-8 D**), which in contrast to the abovementioned compounds, has not yet been identified in any plant (Kretzschmar *et al.*, 2007).

ER binding studies have demonstrated the interaction of the most studied naringenin-type flavanones, Naringenin and 8-Prenylnaringenin, with both ERs. It has been shown that Naringenin binds both ERs, with higher relative binding affinity for ERβ than ERα (0.11 and 0.01, respectively) (Kuiper *et al.*, 1998). 8-Prenylnaringenin can strongly compete with E2 for binding both ERs, although there is no marked difference in the binding affinity for the two receptors (Milligan *et al.*, 2002). 8-Prenylnaringenin

reveals a strong ER-binding affinity that is only 0.5 orders of magnitude lower as compared to 17β-Estradiol (Effenberger *et al.*, 2005). In the case of 6-(1,1-Dimethylallyl)naringenin and 7-(O-prenyl)naringenin-4'-acetate, nothing is known about their relative binding affinities and receptor selectivity so far, however studies have shown that they have the ability to bind both ER subtypes in a cell- and tissue-specific manner (Zierau *et al.*, 2002; Zierau *et al.*, 2004; Kretzschmar *et al.*, 2007; Kretzschmar *et al.*, 2010).

Since the influence of naringenin-type flavanones on human health and their potential risks or benefits of usage are still debatable, they have lately gained considerable scientific interest. For instance, the estrogenic potency of Naringenin is highly controversial (Ruh *et al.*, 1995; Zand *et al.*, 2000). In addition, the estrogenic potency of 8-Prenylnaringenin is extensively discussed, yet its benefits and risks are poorly identified (Christoffel *et al.*, 2006). Moreover, nothing is known so far about the ability of the naringenin-type flavanones to cross the blood brain barrier. As a result, data on the biological effects of naringenin-type flavanones are of great interest.

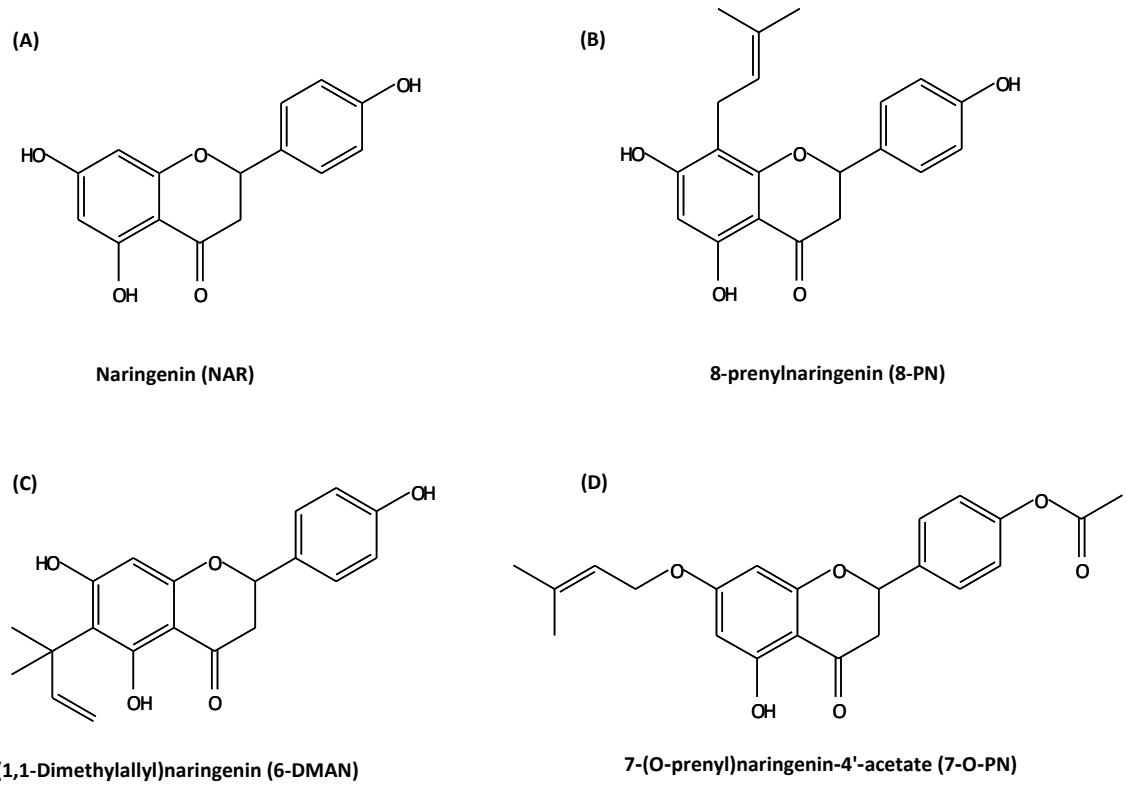

Naringenin (NAR)

8-prenylnaringenin (8-PN)

6-(1,1-Dimethylallyl)naringenin (6-DMAN)

7-(O-prenyl)naringenin-4'-acetate (7-O-PN)

Figure 2-8: Chemical structure of the four naringenin-type flavanones. Carbon atom numbering is the same as denoted in the isoflavone chemical structures in **Figure 2-7**.

2.5.2. Characterization of Other Selected Substances

2.5.2.1. Estrogen Receptor Agonists

A number of subtype-specific ER agonists have been developed as useful tools in understanding the differences in structure and biological function of each ER subtype. Propyl pyrazole triol (PPT) (**Figure 2-9 A**) is a synthetic triarylpyrazole that was reported to bind ERα with high affinity (approximately 50 % that of 17β-Estradiol) and has a 410-fold higher binding affinity preference for ERα than for ERβ. This high ERα binding selectivity is mediated through interactions between the pyrazole core with the ligand-binding pocket; where ERα has a smaller Leucine 384 residue than the Methionine 384 of ERβ (Stauffer *et al.*, 2000).

Diarylpropionitrile (DPN) (**Figure 2-9 B**) acts as an agonist for both ER subtypes. However, it exhibits a 70-fold relative binding preference and a 170-fold higher relative transactivational potency for ERβ than for ERα (Meyers *et al.*, 2001). The ERβ selectivity of DPN is mediated by the N-terminal region of the ERβ ligand-binding domain, specifically through helix 6. However, amino acid residues in helix 3 are also important in achieving ERβ selectivity of DPN. Using molecular modeling, it has been shown that the nitrile group is strongly engaged in stabilizing interactions with amino acid residues in the ligand-binding pocket of ERβ (Sun *et al.*, 2003).

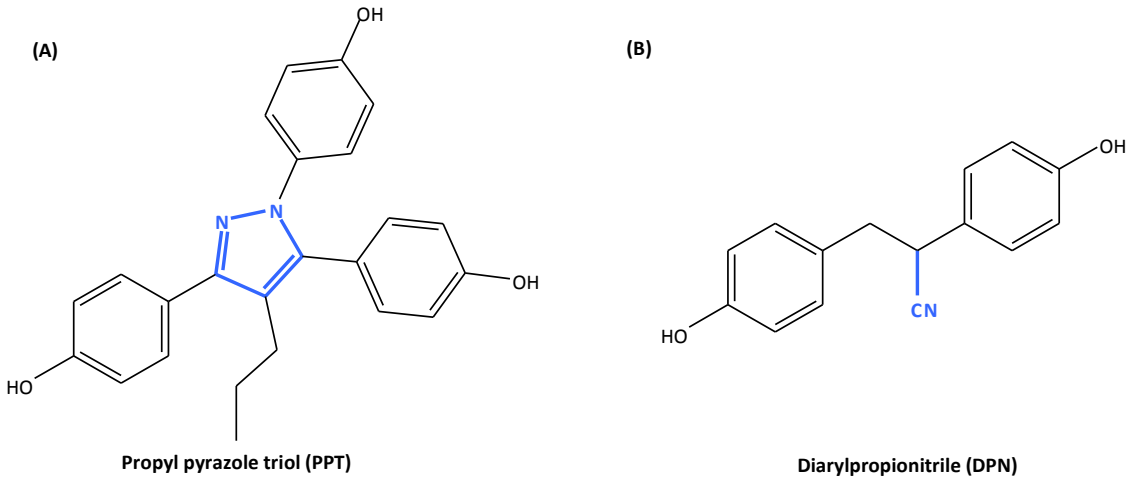

Figure 2-9: Chemical structure of the estrogen receptor selective agonists. The pyrazole core in PPT and the nitrile group in DPN are marked in blue.

2.5.2.2. Estrogen Receptor Antagonist or Antiestrogen

Antiestrogens are classified as substances that inhibit ER function. Fulvestrant (F) [also known as ICI 182,780 (FASLODEX®)] is considered a "pure" antiestrogen and a derivative of 17β-Estradiol containing a pentafluoropentylsulfinyl side extension in its 7α position (**Figure 2-10**) with no agonistic activities reported so far (Wakeling *et al.*, 1991).

The relative binding affinity of Fulvestrant is 0.89 as compared to 17β-Estradiol (1.0) (Bowler *et al.*, 1989; Wakeling *et al.*, 1991). At the molecular level, Fulvestrant competes with 17β-Estradiol for ER binding, inhibits the AF-1 and AF-2 transactivating domains, and prevents ER dimerization, thus disrupting its nuclear localization. Another property of Fulvestrant is that it down-regulates or reduces the steady-state levels of the ERs by increasing their turnover rate (Dauvois *et al.*, 1993; Johnston and Cheung, 2010).

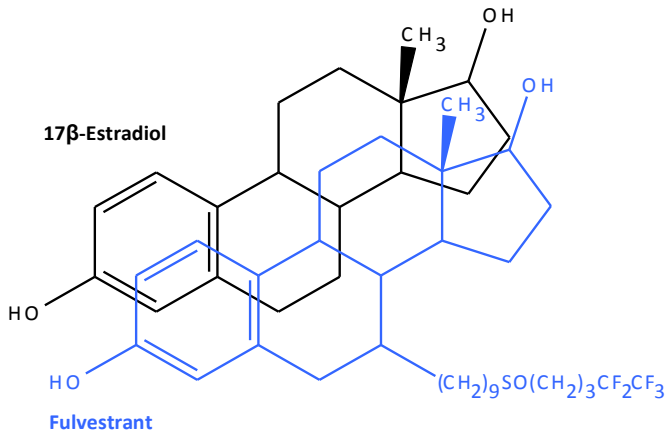

Figure 2-10: Comparison of the structure of Fulvestrant with that of 17β-Estradiol. The similarity of the two molecules is shown in planar spatial arrangement.

2.6. The Raphe Nuclei

The raphe nuclei are clusters of nuclei that are distributed near the midline of the brainstem along its rostrocaudal extension. Heterogeneous populations of neurons are located in the raphe nuclei, with distinct morphologies, projections and neurochemical characteristics. However, the major constituents of the raphe nuclei are cell bodies of serotonergic neurons which project to all cerebral regions and produce serotonin; a biogenic amine that functions as a neurotransmitter and as a hormone in the mammalian central nervous system and its periphery (Parent *et al.*, 1981; Hornung, 2003).

Serotonin is biochemically synthesized from the amino acid tryptophan by a short metabolic pathway that primarily involves the rate-limiting enzyme tryptophan hydroxylase (Walther *et al.*, 2003). It mediates various physiological functions such as appetite, thermoregulation, regulation of sleep-wake cycles, sexual behavior and memory. It also intervenes psychiatric behaviors including mood swings, depression and anxiety as well as panic disorders (Hoyer *et al.*, 2002). The large diversity of serotonin receptors is linked to the multiplicity of physiological functions and behaviors that serotonin participates in. Using molecular and pharmacological techniques, at least 15 distinct members of serotonin receptors have been determined. They represent one of the most complex families of neurotransmitter receptors that are classified into seven families according to their patterns of distribution, coupling mechanisms and pharmacological profiles (Julius, 1991). With the exception of the serotonin receptor subtype 3, which is a ligand-gated ion channel, all serotonin receptors belong to the G-protein coupled receptor superfamily (Kroeze *et al.*, 2002). Another important component of the serotonergic system is the serotonin re-uptake transporter; a monoamine transporter protein which functions in all serotonergic neurons by means of transporting serotonin from synaptic spaces into presynaptic neurons, thus terminating serotonin action. Changes in the serotonin re-uptake transporter may alter the expression and/or function of most, if not all, serotonin receptors in addition to the synthesis, metabolism and clearance of serotonin (Murphy *et al.*, 2008).

Neuroanatomical studies have shown that ERα and ERβ are widely distributed in different brain regions. In particular, ERβ immunoreactive cells were abundantly observed throughout the raphe nuclei (Shughrue *et al.*, 1996; Shughrue *et al.*, 1997; Perez *et al.*, 2003; Nomura *et al.*, 2005). Animal studies were also used to co-localize ERs and serotonin neurons. For instance, studies in macaques have shown the existence of ERβ mRNA as well as its protein in serotonin neurons (Gundlah *et al.*, 2001). Another group of researchers have pointed out the expression of ERβ in rat raphe nuclei (Lu *et al.*, 2001). Hence, the above observations support the general assumption that ERβ is more likely associated with the estrogenic regulation of serotonin neurons in the raphe nuclei than ERα.

A huge body of data has postulated a significant interaction between estrogens and serotonin (McEwen, 2001; Grigoriadis and Kennedy, 2002; Amin *et al.*, 2005). For instance, 17β-Estradiol acts through ERβ and increases the expression of tryptophan hydroxylase; the rate limiting-enzyme in the synthesis of serotonin (Pecins-Thompson *et al.*, 1996). Besides tryptophan hydroxylase, 17β-Estradiol may regulate other components of the serotonin system, such as increasing mRNA expression for the progesterone receptor (Bethea, 1994), while decreasing mRNA expression of serotonin re-uptake transporter (Pecins-Thompson *et al.*, 1998), the serotonin autoreceptor subtype 1 (Pecins-Thompson and Bethea, 1999) and the monoamine oxidase genes (Gundlah *et al.*, 2002). As a result, estrogen acts to serve towards serotonin neurotransmission, thereby regulating mood swings and depression as well as anxiety behaviors.

2.6.1. The RN46A-B14 Cell Line

RN46A-B14 is a rat serotonergic cell line and a sub-clone of the parent raphe nuclei-derived cell line, RN46A-V1. These have been isolated from a dissociated embryonic day 13 rat medullary raphe cells. They have been immortalized with the temperature-sensitive mutant of the Simian Virus 40 (SV40) large T-antigen. Based on this property, neuronal differentiation of this cell line is initiated in response to shifting cells from their proliferative conditions (i.e. permissive temperatures) to differentiation conditions (i.e. non-permissive temperatures); in which the cells are no longer under the mitotic drive of the temperature-sensitive mutant of the SV40 large T-antigen (White and Whittemore, 1992; Whittemore and White, 1993; White *et al.*, 1994). Potential markers for cellular differentiation can be represented by neurofilament proteins which are class IV intermediate 10 nm filamentous proteins composed of three subunits (low, medium and high). The names were designated according to their distinct molecular weights; where neurofilament low (NF-L) is 68-70 kDa, neurofilament medium (NF-M) is 145-160 kDa and finally neurofilament high (NF-H) is 200-220 kDa. Neurofilaments are found in neurons of vertebrates and are known to be formed in high concentrations during the development of neuronal axons (Cleverley *et al.*, 1998; Lalonde and Strazielle, 2003). Neuron specific enolase (NSE), an acid soluble protein of the glycolytic isoenzyme enolase that is composed of two gamma subunits, has been also utilized as an additional identifying neuronal molecular marker (White *et al.*, 1994). It is exclusively confined to

neurons of the central and peripheral nervous systems as well as cells of neuroendocrine origin and is thought to serve as a growth factor in neurons (Schmechel *et al.*, 1978; Schmechel *et al.*, 1980; Kirino *et al.*, 1983). It has been reported that RN46A-B14 cells should express the same complement of the nuclear ERβ as the rat raphe serotonin neurons, hence providing a convenient *in vitro* model that mimics the *in vivo* situation to help study estrogenic action in the raphe nuclei (Bethea *et al.*, 2003).

2.7. Aims of the Present Study

To evaluate the biological effects of the isoflavones and the naringenin-type flavanones within the raphe nuclei region of the brain, a region that plays a central role in regulating depression, mood swings and anxiety behavior, it is important to initially elucidate their transactivational activity on ERβ as well as their potential to regulate endogenous gene expression of estrogen responsive genes. To achieve this, RN46A-B14 cells were utilized as the main raphe nuclei-derived cellular model in the present study. However, preliminary findings have shown that the endogenous expression of ERβ in RN46A-B14 cells was insufficient for downstream investigations of estrogen-dependent activities (**Appendix 7-1**). As a result, the aims of the present study, as depicted in **Figure 2-11**, were proceeded as follows:

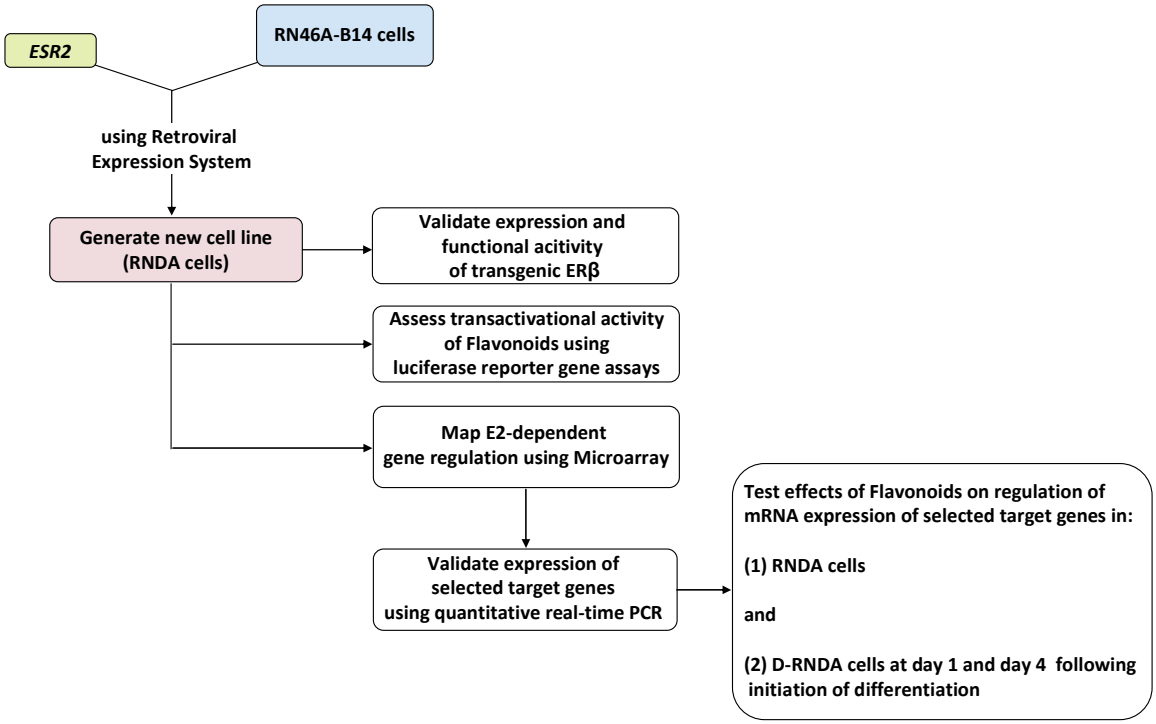

Figure 2-11: Schematic illustration representing the main workflow of the present study

(1) To stably integrate the human ERβ gene (*ESR2*) in RN46A-B14 cellular genome using a suitable Retroviral Expression System. The expression of the transgenic ERβ in the newly generated cell line (herein termed RNDA cells) as well as its functional activity shall be validated using standard Western blot techniques and firefly luciferase reporter gene

assays utilizing a plasmid containing the firefly luciferase reporter gene under the control of a double ERE-dependent promoter.

(2) To investigate the transactivational activity of selected flavonoids on the transgenic ERβ in RNDA cells using the same abovementioned reporter gene assay.

(3) To map the E2-dependent changes in the expression of the whole rat transcriptome in RNDA cells using a DNA microarray technique.

(4) To validate, using quantitative real-time PCR, the mRNA expression of E2-responsive genes that are specifically selected from the microarray according to specific features of estrogenic regulation of expression.

(5) To evaluate the effects of the flavonoids on the regulation of mRNA expression of the selected genes, including serotonin-related genes, using quantitative real-time PCR. Since RNDA cells encode a temperature-sensitive mutant of the SV40 large T-antigen, neuronal differentiation of these cells is constitutive upon shifting them from proliferative conditions (permissive temperature) to differentiation conditions (non-permissive temperature). Hence, the regulation of mRNA expression of the selected genes shall be investigated in: (a) RNDA cells (proliferating cells) and (b) D-RNDA cells (i.e. RNDA cells grown under differentiating conditions) at day 1 and day 4 following initiation of differentiation.

3. MATERIALS AND METHODS

3.1. Materials

3.1.1. Cell Lines

Besides the RN46A-B14 cell line, which was kindly provided by Professor Scott Whittemore (Department of Neurological Surgery; University of Miami School of Medicine, Miami), the following cell lines were also utilized in the present study:

- ***RNDA cell line*:**

RNDA cells are derivatives of the parent cell line RN46A-B14 cells, yet they are genetically modified to stably overexpress transgenic human ERβ using a suitable retroviral expression system. Like their parent cell line, the cells encode a temperature-sensitive mutant of the SV40 large T-antigen. Based on this property, neuronal differentiation is constitutive upon shifting them from proliferative conditions (permissive temperature) to differentiation conditions (non-permissive temperature) (White and Whittemore, 1992; Whittemore and White, 1993; White *et al.*, 1994). It is important to note that when RNDA cells are shifted to conditions promoting differentiation, cells are denoted as D-RNDA cells in the present study.

- ***HEK-293T cell line*:**

HEK-293T cells are human embryonic kidney cell line having a eukaryotic expression plasmid encoding the temperature-sensitive mutant of the SV40 large T-antigen (DuBridge *et al.*, 1987). In this study, they serve as the standard cell line for packaging and producing lentiviral particles. The cells were kindly provided by Professor Dirk Lindemann (Institute of Virology, Medical Faculty Carl Gustav Carus, TU-Dresden, Germany).

- ***HT-1080 cell line*:**

HT-1080 cells are human fibrosarcoma cell line commonly used as the reference cell line to verify efficiency of viral transduction (Rasheed *et al.*, 1974). The cells were also kindly provided by Professor Dirk Lindemann (Institute of Virology, Medical Faculty Carl Gustav Carus, TU-Dresden, Germany).

All outlined cell lines were grown in phenol-red free Dulbecco's Modified Eagle Medium/Nutrient Mixture F12 1:1 (DMEM/F12 1:1) containing L-Glutamine, sodium bicarbonate, 15 mM HEPES and high glucose (Biowest, Nuaillé, France). The medium was further supplemented with additional additives as shown in **Table 3-1**.

Table 3-1: Cell lines and their culture conditions

Cell Line	Media Additives / Final Concentration (including 1 % Penicillin / Streptomycin)		Temperature & 5 % CO_2
RN46A-B14 cells	Hygromycin B (50 mg/ml)	100 µg/ml	33 °C (permissive temperature)
	Geneticin® (G418) (50 mg/ml)	250 µg/ml	
	Fetal Calf Serum (FCS)	10 % (v/v)	
RNDA cells	Hygromycin B (50 mg/ml)	100 µg/ml	33 °C (permissive temperature: proliferation conditions)
	G418 (50 mg/ml)	250 µg/ml	
	FCS	10 % (v/v)	
	Zeocin™ (100 mg/ml)	60 µg/ml	
D-RNDA cells (Weigt, 2008)	Hygromycin B (50 mg/ml)	100 µg/ml	39 °C (non-permissive temperature: differentiation conditions)
	G418 (50 mg/ml)	250 µg/ml	
	B27 Supplement (50x)	1 % (v/v)	
	BSA Fraction V	1 % (w/v)	
HEK-293T cells	FCS	10 % (v/v)	37 °C
HT-1080 cells	FCS	10 % (v/v)	37 °C

3.1.2. Antibodies

Table 3-2: Primary antibodies used for either Western blot or Immunocytochemistry techniques

Primary Antibody	Catalogue No.	Distributor	City	Country
Mouse monoclonal anti NF-L	sc-58559	Santa Cruz Biotechnology®	Heidelberg	Germany
Mouse monoclonal anti NF-M	sc-58561	Santa Cruz Biotechnology®	Heidelberg	Germany
Mouse monoclonal anti NF-H	sc-133165	Santa Cruz Biotechnology®	Heidelberg	Germany

Primary Antibody (continued)	Catalogue No.	Distributor	City	Country
Mouse monoclonal anti NSE γγ	MAB314	Millipore GmbH	Schwalbach/ Ts.	Germany
Rabbit polyclonal anti ERβ	PA1-311	Thermo Fisher Scientific	Bonn	Germany
Rabbit polyclonal anti β-Actin	A5060	Sigma-Aldrich	Hamburg	Germany

Table 3-3: Secondary antibodies used for either Western blot or Immunocytochemistry techniques

Secondary Antibody	Catalogue No.	Distributor	City	Country
Alexa Flour 488 goat anti-mouse IgG (H + L)	A-11001	Molecular Probes	Darmstadt	Germany
HRPO-conjugated goat anti-rabbit IgG	303-035-003	Dianova	Hamburg	Germany

3.1.3. Enzymes

Table 3-4: Enzymes used for gene cloning techniques

Enzyme	Distributor	City	Country
*Age*1restriction enzyme	Fermentas	St. Leon-Rot	Germany
Calf Intestinal Alkaline Phosphatase (CIAP) Enzyme	Promega GmbH	Mannheim	Germany
*Eco*R1 restriction enzyme	Fermentas	St. Leon-Rot	Germany
T4-DNA-Ligase enzyme	Promega GmbH	Mannheim	Germany
*Xba*1 restriction enzyme	Fermentas	St. Leon-Rot	Germany

Table 3-5: Enzymes used for PCR and quantitative real-time PCR

Enzyme	Distributor	City	Country
10x Platinum® *Pfx* DNA Polymerase (2.5 U/µl)	Invitrogen	Karlsruhe	Germany
Moloney Murine Leukemia Virus Reverse Transcriptase (MMLV-RT) (200 U/µl)	Promega GmbH	Mannheim	Germany
Platinum® *Taq* DNA Polymerase (5 U / µl)	Invitrogen	Karlsruhe	Germany
RNaseOUT™ Recombinant Ribonuclease Inhibitor (40 U / µl)	Invitrogen	Karlsruhe	Germany
RQ1 RNase-Free DNase (1 U / µl)	Promega GmbH	Mannheim	Germany

Enzyme (continued)	Distributor	City	Country
Taq DNA Polymerase (Recombinant) (5 U / µl)	Invitrogen	Karlsruhe	Germany

3.1.4. Miscellaneous

Table 3-6: Lab Machines and Cell cultureware utilized throughout the study

Equipment	Distributor	City	Country
Agilent 2100 bioanalyzer	Agilent Technologies	Waldbronn	Germany
Agilent DNA Microarray Scanner employing SureScan High Resolution Technology	Agilent Technologies	Waldbronn	Germany
All cell cultureware	Techno Plastic Products (TPP®)	Trasadingen	Switzerland
Avanti® Centrifuge J-26 XP	BECKMAN COULTER™ GmbH	Krefeld	Germany
Biofuge fresco	Heraeus Instruments	Leipzig	Germany
Canon Power Shot G9 Digital Camera	Canon	Krefeld	Germany
Carl Zeiss Apotome camera	Carl Zeiss	Jena	Germany
Carl Zeiss Axiovert 200 Imaging Microscopy	Carl Zeiss	Jena	Germany
CFX96™ Real-Time System	BIO-RAD GmbH	Munich	Germany
EpiChemi^3 Benchtop Darkroom	UVP Ltd.	Cambridge	UK
FACSCalibur™ Flow Cytometer	BD Biosciences	Heidelberg	Germany
Gene Pulser II	BIO-RAD GmbH	Munich	Germany
HB-1000 Hybridizer	UVP Ltd.	Cambridge	UK
Infinite F200 spectrophotometer machine	TECAN	Männedorf	Switzerland
Megafuge 2.0R	Heraeus Instruments	Leipzig	Germany
Multifuge 3 S-R	Heraeus Instruments	Leipzig	Germany
NanoDrop® ND-1000 UV-Vis Spectrophotometer	NanoDrop® Technologies	Hilden	Germany
OLYMPUS® Culture Microscope Model CK40	OLYMPUS®	Hamburg	Germany
Primus 96 ^{plus} bench cycler	MWG-BIOTECH	Ebersberg	Germany
Trans-Blot® SD Semi-Dry Transfer Cell	BIO-RAD GmbH	Munich	Germany

Table 3-7: Software products utilized throughout the study

Software Product	Distributor	City	Country
Agilent Feature Extraction Software Version 9.5	Agilent Technologies	Waldbronn	Germany
Agilent Technologies GeneSpring GX 9 Software	Agilent Technologies	Waldbronn	Germany
AxioVert Software Release 4.8.1	Carl Zeiss	Jena	Germany
Becton Dickinson CellQuest™ Software	BD Biosciences	Heidelberg	Germany
Bio-Rad CFX Manager Version 1.6	BIO-RAD GmbH	Munich	Germany
Labworks™ Image Acquisition and Analysis Software Version 4.6.	UVP Ltd	Cambridge	UK
Magellan Software	TECAN	Männedorf	Switzerland
Microsoft Office Excel 2003	Microsoft Deutschland	Munich	Germany
Sigma Plot® Version 9.0	Systat Software	Erkrath	Germany

Table 3-8: Commercial kits utilized throughout the study

Kit	Distributor	City	Country
Agilent's Quick Amp Labelling Kit	Agilent Technologies	Waldbronn	Germany
Bicinchoninic Acid Protein Assay Kit	VWR	Darmstadt	Germany
Luciferase Assay System Kit	Promega	Mannheim	Germany
NucleoSpin® RNA/Protein Isolation Kit	MACHEREY-NAGEL	Düren	Germany
peqGOLD Gel Extraction Kit	PEQLAB Biotechnologie GmbH	Erlangen	Germany
QIAGEN® Plasmid Midi Kit (100)	QIAGEN GmbH	Hilden	Germany

Table 3-9: Reagents, solutions and supplies utilized throughout the study

Item	Distributor	City	Country
10,000 U/ml Penicillin and 10,000 µg/ml Streptomycin	Gibco-BRL	Eggenstein	Germany
17β-Estradiol crystalline	Sigma-Aldrich	Hamburg	Germany
50 bp DNA Ladder (1000 µg/ml)	NEW ENGLAND BioLabs GmbH	Frankfurt am Main	Germany
6-(1,1-Dimethylallyl)naringenin	Synthesized from Naringenin by a europium (III)-catalyzed Claisen rearrangement (Gester *et al.*, 2001)		
7-(O-prenyl)naringenin-4'-acetate	Byproduct of a Mitsunobu reaction used for the synthesis of 8-PN and 6-DMAN (Gester *et al.*, 2001; Tokalov *et al.*, 2004)		
8-Prenylnaringenin	Synthesized from Naringenin by a europium (III)-catalyzed Claisen rearrangement (Gester *et al.*, 2001)		
Amersham™ ECL Hyperfilm	GE Healthcare	Munich	Germany
Amersham™ ECL Plus Western Blotting Detection System	GE Healthcare	Munich	Germany
B27 Supplement (50x)	Gibco-BRL	Eggenstein	Germany
BSA Fraction V	SERVA Electrophoresis	Heidelberg	Germany
Collagen Type I from calf skin	Sigma-Aldrich	Hamburg	Germany
Daidzein	Sigma-Aldrich	Hamburg	Germany
DAPI	Santa Cruz Biotechnology®	Heidelberg	Germany
DEPC Solution	AppliChem GmbH	Darmstadt	Germany
Developing and Fixing Solution	Kodak	La Hulpe	Belgium
Diarylproprionitril	Tocris Biosciences	Bristol	UK
dibutyryl cyclic AMP	Sigma-Aldrich	Hamburg	Germany
dNTPs (100 mM each)	Invitrogen	Karlsruhe	Germany
DOTAP Liposomal Transfection Reagent	Roth	Karlsruhe	Germany
Equol	Sigma-Aldrich	Hamburg	Germany
Fulvestrant (ICI 182,780)	Tocris Biosciences	Bristol	UK
Geneticin® (G418) (50 mg/ml)	CALBIOCHEM®	Darmstadt	Germany
Genistein	Sigma-Aldrich	Hamburg	Germany

Item (continued)	Distributor	City	Country
HPLC water	AppliChem GmbH	Darmstadt	Germany
Hygromycin B (50 mg/ml)	Invitrogen	Karlsruhe	Germany
Mowiol 4-88 granules	Carl Roth GmbH	Karlsruhe	Germany
Naringenin	Sigma-Aldrich	Hamburg	Germany
n-Butyric Acid, Sodium Salt	Sigma-Aldrich	Hamburg	Germany
Non-fat dried milk powder	Merck KGaA,	Darmstadt	Germany
Oligo $(dT)_{18}$-primers (100 µM)	Eurogentec Germany GmbH	Cologne	Germany
PageRuler™ Prestained Protein Ladder	Fermentas	St. Leon-Rot	Germany
peqGOLD TriFast™ Reagent	PEQLAB Biotechnologie GmbH	Erlangen	Germany
Phenol-red free DMEM/F12 1:1 Medium	Biowest	Nuaillé	France
Polyethylenimine (PEI) Transfection Reagent	Sigma-Aldrich	Hamburg	Germany
Propyl pyrazole triol	Tocris Biosciences	Bristol	UK
PVDF Membrane (pore size: 0.45 µm)	Millipore GmbH	Schwalbach /Ts.	Germany
Quick Load 1 kb DNA Ladder (50 µg/ml)	NEW ENGLAND BioLabs GmbH	Frankfurt am Main	Germany
Rotiphorese® Gel 30	Carl Roth GmbH	Karlsruhe	Germany
SYBR® Green I	Sigma-Aldrich	Hamburg	Germany
TEMED	Carl Roth GmbH	Karlsruhe	Germany
Trypsin / EDTA (10x)	Biowest	Nuaillé	France
VS Membrane (pore size: 0.025 µm)	Millipore GmbH	Schwalbach /Ts.	Germany
Zeocin™ (100 mg/ml)	Invitrogen	Karlsruhe	Germany

3.2. Methods

3.2.1. Cell Culture

3.2.1.1. Trypsin Digestion, Counting and Preserving Cells

Adherent cells were washed twice with Phosphate Buffered Saline (PBS) (**Table 3-10**) and detached with 1x Trypsin / EDTA solution (Biowest, Nuaillé, France) for 5 minutes at either 33 °C, 37 °C or 39 °C and 5 % CO_2. Once detached, Trypsin was inactivated by adding a few milliliters of medium to cells. The cell suspension was then harvested using the Multifuge 3 S-R (Heraeus Instruments, Leipzig, Germany) at 900 rpm for 5 minutes. The cell pellet was subsequently re-suspended in 5 to 10 ml of medium. After re-suspension, cell count was determined using a Neubauer cell counting chamber and the exclusion dye Trypan blue (0.2 % w/v Trypan blue in 85 % w/v PBS). Cells were then plated at the desired density according to specified experimental design. The remaining cell suspension was centrifuged and the pellet was re-suspended in freezing medium (90 % FCS and 10 % DMSO) and placed in liquid nitrogen for long-term storage.

Table 3-10: PBS composition per 1 Liter (Sambrook *et al.*, 1989)

Component	Required Amount
Sodium Chloride	8.00 g
Disodium hydrogen phosphate dihydrated	1.44 g
Potassium Chloride	0.20 g
Potassium dihydrogen phosphate	0.24 g
Deionized distilled water	added up to 1 Liter
Autoclaved and stored at room temperature until use	

3.2.1.2. Phase Contrast Microscopy

Throughout this study, cells were visualized on an OLYMPUS® Culture Microscope Model CK40 (OLYMPUS®, Hamburg, Germany) to verify cell appearance before proceeding to the next steps. In particular, RNDA and D-RNDA cells were visualized and photographed via the Canon Power Shot G9 Digital Camera (Krefeld, Germany).

3.2.2. Genetic Engineering

Genetic engineering technologies using retroviral-based vectors have emerged in biomedical areas and basic research as an invaluable tool to manipulate target cellular genome. However, most of these retroviral vectors, such as oncoretroviral-based vectors, possess certain gene delivery limitations, including: (1) instability of the viral vector in the target cellular genome (Andreadis *et al.*, 1997), (2) production of low viral titers (Le Doux *et al.*, 1999) and (3) inability to transduce non-proliferating and possibly differentiating cells (Lewis and Emerman, 1994; Ryser *et al.*, 2007). To overcome these shortcomings, basic and applied research has focused their interest on utilizing lentiviral-based vectors to stably integrate transgenic DNA into any cellular target and eventually manipulate its original function according to the researcher's needs (Bukrinsky *et al.*, 1993). Lentiviral-based vectors have superior transduction efficiencies in modifying cells *in vitro* and *in vivo*, leading to the most desirable feature that is long-term gene expression (Park, 2007). DNA insertional mutagenesis is also induced at lower frequencies as opposed to other retroviral-based systems. Finally, lentiviral-based vectors are capable of stably transducing quiescent non-dividing cells (Naldini *et al.*, 1996; Breckpot *et al.*, 2004).

In this study, the lentiviral expression vector, p6NST50 (**Figure 3-1**), was the method of choice to insert and stably integrate the human ERβ gene (*ESR2*) into the RN46A-B14 cellular genome. This vector was kindly provided by Professor Dirk Lindemann (Institute of Virology, Medical Faculty Carl Gustav Carus, TU-Dresden, Germany). Cloning of human *ESR2* fragment into p6NST50 was initially conducted prior to viral transduction / infection.

Figure 3-1: Schematic linear illustration of the lentiviral transfer vector construct employed in the present study. Self-inactivating HIV-1 based retroviral transfer vector p6NST50 contains an internal spleen focus forming virus (SFFV) U3 promoter with downstream multiple cloning site (MCS) and an internal ribosomal entry site (IRES) driven enhanced green fluorescent protein-Zeocin marker gene cassette (EGFP-Zeo). **Abbreviations:** Ψ: packaging sequence; RRE: rev-responsive-element; cPPT: central poly purine tract; WPRE: Woodchuck hepatitis virus posttranscriptional regulatory element; CMV: cytomegalo virus immediate early enhancer-promoter; R: long terminal repeat (LTR) region; U5: LTR unique 5' region; ΔU3: enhancer-promoter deleted LTR unique 3' region.

3.2.2.1. Dialysis of p6NST50 and Transformation of Escherichia coli with p6NST50 by Electroporation

Initially, the provided p6NST50 was dialysed to eliminate any inhibitory substances, such as salts, that could obstruct the process of transformation of *Escherichia coli* (*E. coli*) using electroporation. Deionized distilled water was poured into a Petri dish and a 25 mm diameter VS Membrane (pore size = 0.025 µm) (Millipore GmbH, Schwalbach/Ts., Germany) was allowed to float with shiny side facing upwards while avoiding any bubbles. The floating membrane was kept on water for 5 minutes. 10 µl of the provided p6NST50 was carefully pipetted onto the centre of the filter and allowed to incubate for 15 minutes. Carefully, the vector droplet was retrieved for subsequent steps.

Bacterial stocks of p6NST50 were prepared by adding 1 µl of the dialysed p6NST50 to 40 µl electrocompetent DH10B *E. coli* cell suspension and allowed to stand on ice for 1 minute. The mixture was then transferred to a 0.2 cm gap sterile electroporation cuvette and electroporated with Gene Pulser II (BIO-RAD, Munich, Germany) using a single impulse at 2.5 volts, 25 µF, 200 Ω for 4.5 – 5.0 ms. 1 ml of Super Optimal Broth medium (**Table 3-11**) was immediately added to the cuvette and the content was transferred to a new Eppendorf tube and incubated at 37 °C for 1 hour. Finally, 100 µl of the transformed *E. coli* was plated on Lysogeny Broth (LB)-Agar-containing ampicillin (**Table 3-12**) and incubated overnight at 37 °C.

Table 3-11: Super Optimal Broth medium per 100 ml (Sambrook *et al.*, 1989)

Component	Final Concentration
Bacto-Tryptone	2 % (w/v)
Bacto-Yeast Extract	0.5 % (w/v)
Sodium Chloride	10 mM
Potassium Chloride	2.5 mM
Magnesium Chloride	10 mM
Glucose	20 mM
Deionized distilled water	added up to 100 ml
Aliquots were autoclaved and stored at -20 °C until use	

Table 3-12: LB-Agar-containing ampicillin (Sambrook *et al.*, 1989)

Component	Required Amount
Sodium Chloride	1 % (w/v)
Peptone	1 % (w/v)
Bacto-Yeast Extract	0.5 % (w/v)
Agar	1.5 % (w/v)
Autoclaved and left to cool down. Later, ampicillin was added at a dilution of 1:1000	
Aseptically poured in 10-cm Petri dishes and left to solidify. Finally, stored at 4 °C until use	

Following overnight incubation, glycerol stocks of DH10B *E. coli* cells carrying the p6NST50 lentiviral vector were prepared. A single bacterial colony was picked from the plate into 6 ml LB medium-containing ampicillin (**Table 3-13**) and allowed to grow overnight at 37 °C with constant shaking (approximately 200 rpm). The bacterial suspension was subsequently centrifuged at 11,000 x g for 1 minute and bacterial pellet was re-suspended in bacterial freezing medium (**Table 3-14**). The mixture was transferred to cryovials and stored at -80 °C until further use.

Table 3-13: LB medium-containing ampicillin (Sambrook *et al.*, 1989)

Component	Required Amount
Sodium Chloride	1 % (w/v)
Peptone	1 % (w/v)
Yeast Extract	0.5 % (w/v)
Autoclaved and left to cool down. Later, ampicillin was added at a dilution of 1:1000	
Stored at 4 °C until use	

Table 3-14: Bacterial freezing medium

Component	Required Amount
Glycerol	40 % (v/v)
LB medium-containing ampicillin	60 % (v/v)
Stored at 4 °C until use	

3.2.2.2. Cloning of Human ESR2 into p6NST50

- ***1st step: Amplification of human ESR2***

A 1.5-kb DNA fragment encoding human ERβ (*ESR2*) (**Appendix 7-2**), kindly provided by Dr. Luisella Toschi (Schering AG, Berlin), was amplified using standard polymerase chain reaction (PCR). The reason for amplifying and subsequently cloning human *ESR2* instead of a rat *Esr2* in the studied rat cell line was due to two reasons: (1) availability of human *ESR2* DNA fragment in the lab and (2) human ERβ shows approximately 89% identity in its translated region to the rat ERβ as compared to any other mammalian ERβ (Enmark and Gustafsson, 1999). Specific primer sequences used during amplification were designed to include *ESR2* fragment flanked by *Age*1 – *Xba*1 restriction sites of the 9-kb p6NST50 (**Appendix 7-3**). Primer pairs (Forward (Fwd) and Reverse (Rev)) were commercially synthesized by Biomers.net GmbH (Ulm, Germany) and the delivered lyophilized primers were re-suspended in High Performance Liquid Chromatography (HPLC) water (Applichem, Darmstadt, Germany) such that stock concentrations were adjusted to 100 pmol/µl (100 µM) each. A primer mix was further prepared in which the final concentration of the forward and reverse primers was 10 pmol/µl (10 µM) each. The reaction mixture was set as shown in **Table 3-15**. The reaction took place in the Primus 96 *plus* bench cycler (MWG-BIOTECH, Ebersberg, Germany) under cycling conditions recommended for Platinum® *Pfx* DNA Polymerase (Invitrogen, Karlsruhe, Germany) as shown in **Table 3-16**.

Table 3-15: PCR amplification of *ESR2* fragment (100 µl total volume per reaction)

Component	Required Volume
10x *Pfx* Amplification Buffer (supplied with the Platinum® *Pfx* enzyme)	10 µl
Deoxyribonucleotide triphosphate (dNTP) mixture (Final Concentration: 10 mM each)	3 µl
50 mM Magnesium Sulphate	2 µl
Human *ESR2* Primer Mix (Final Concentration: 10 µM each) **Fwd**: TAT ATA ACC GGT CCA TGG ATA TAA AAA ACT CAC CAT CTA G **Rev**: TAT ATA TCT AGA TCA CTG AGA CTG TGG GTT CT	3 µl
Human *ESR2* DNA template	2 µl
10x Platinum® *Pfx* DNA Polymerase (2.5 U/µl)	1 µl
HPLC water	added up to 100 µl

Table 3-16: Cycling conditions for Platinum® *Pfx* DNA Polymerase

Step	Temperature [°C]	Required Time	Number of Cycles
1. Initial Denaturation	94.0	2 minutes	1x
2. Denaturation of dsDNA	**94.0**	**15 seconds**	**35x**
3. Annealing	**51.0**	**30 seconds**	
4. Extension	**68.0**	**1 minute and 40 seconds**	
5. Further Extension	68.0	10 minutes	1x

Subsequently, successful PCR verification was confirmed by agarose gel electrophoresis. 0.2 volumes of 6x loading buffer (**Table 3-17**) was added to 5 µl of the resultant PCR reaction and the mixture was loaded on a 1 % agarose gel (+ 0.004 % ethidium bromide) against a Quick Load 1 kb DNA Ladder (50 µg/ml) (NEW ENGLAND BioLabs GmbH, Frankfurt am Main, Germany). The gel was left to run at 100 volts for 30 minutes in 1x Tris-Acetate-EDTA Buffer (TAE buffer) (**Table 3-18**). Gel visualization took place under the UV-light (EpiChemi^3 Benchtop Darkroom, UVP Ltd, Cambridge, UK) and gel image was captured using Labworks™ Image Acquisition and Analysis Software Version 4.6.

Table 3-17: 6x loading stock buffer per 10 ml (Sambrook *et al.*, 1989)

Component	Required Amount
Sucrose	4 g
Bromophenol Blue	25 mg
Xylene Cyanol	25 mg
Deionized distilled water	added up to 10 ml
Aliquots were stored at 4 °C	

Table 3-18: 50x TAE stock buffer per 1 Liter (Sambrook *et al.*, 1989)

Component	Required Amount / Volume
Tris	242 g
Glacial acetic acid	57.1 ml
0.5 M EDTA	100 ml
Deionized distilled water	added up to 1 Liter
pH adjusted to 8.0 and stored at 4 °C	

- ***2nd step: Digestion of p6NST50 and ESR2 fragment using restriction enzymes***

After verifying the correct size of the *ESR2* fragment, the remaining PCR product was purified using the peqGOLD Gel Extraction Kit (PEQLAB Biotechnologie GmbH, Erlangen, Germany) as per manufacturer's protocol. The kit was used to purify the amplified *ESR2* fragment for further cloning steps. Concentration of the purified *ESR2* fragment was then measured using the NanoDrop® ND-1000 UV-Vis Spectrophotometer (Tab: Nucleic Acid; Sample type: DNA-50). Finally, p6NST50 and the purified *ESR2* fragment were digested by *Age*1 and *Xba*1 restriction enzymes (Fermentas, St. Leon-Rot, Germany) according to the reaction parameters shown below in **Table 3-19**.

Table 3-19: Restriction enzyme digestion (100 µl total volume per reaction)

Component	Required Amount / Volume
Purified *ESR2* fragment / p6NST50 vector	up to 6 µg each
10x Restriction Buffer (supplied with restriction enzyme)	10 µl
Restriction Enzyme	1 – 2 µl
Deionized distilled water	added up to 100 µl
Incubated overnight at 37 °C	

Successful digestion was further verified by running the samples on a 1 % agarose gel, as previously described. Once again, the remaining products of the restriction enzyme digestion were purified using the peqGOLD Gel Extraction Kit (PEQLAB Biotechnologie GmbH, Erlangen, Germany).

- ***3rd step: Dephosphorylation of p6NST50 and ligation of ESR2 into p6NST50***

The purified linearized vector was dephosphorylated (i.e. removing phosphate group from the vector's sticky ends to ensure proper ligation of the *ESR2* fragment) using the Calf Intestinal Alkaline Phosphatase (CIAP) Enzyme (Promega GmbH, Mannheim, Germany). The dephosphorylation reaction was set up as shown in **Table 3-20**.

Table 3-20: Vector dephosphorylation (100 µl total volume per reaction)

Component	Required Volume
Linearized p6NST50	The whole purified sample volume
10x Phosphatase Buffer (supplied with enzyme)	10 µl
CIAP Enzyme	2 µl
Deionized distilled water	added up to 100 µl
Incubated at 37 °C for 30 minutes. Later, reaction was inactivated at 85 °C for 15 minutes	

Following vector dephosphorylation, DNA ligation was set up such that the vector to fragment molar ratio is 1:3. The reaction was prepared as shown in **Table 3-21** using the T4-DNA-Ligase enzyme (Promega GmbH, Mannheim, Germany). For a negative control setup, an identical reaction mixture was arranged but devoid of any DNA fragment.

Table 3-21: DNA fragment ligation into vector (10 µl total volume per reaction)

Component	Required Volume / Amount
p6NST50 to *ESR2* molar ratio	1 : 3
10x T4-DNA-Ligase Buffer (supplied with enzyme)	1 µl
T4-DNA-Ligase Enzyme (3U/µl)	0.3 µl
Deionized distilled water	added up to 10 µl
Incubated overnight at 4 °C	

The resulting ligation product was then dialysed and transformed into DH10B *E. coli* cells (**Section 3.2.2.1**) and later plated on an LB-Agar-containing ampicillin. To verify successful ligation, ten bacterial colonies were randomly chosen for another restriction enzyme digestion (**Table 3-19**) using a different restriction enzyme, such as *Eco*R1 (Fermentas, St. Leon-Rot, Germany). The digestion product was visualized on a 1 % agarose gel, as previously described. From at least two positive clones, the new p6NST50 encoding *ESR2* (herein termed p6NST50 + ERβ) (**Figure 3-2**) was sequenced at MWG-BIOTECH (Ebersberg, Germany) to confirm sequence identity.

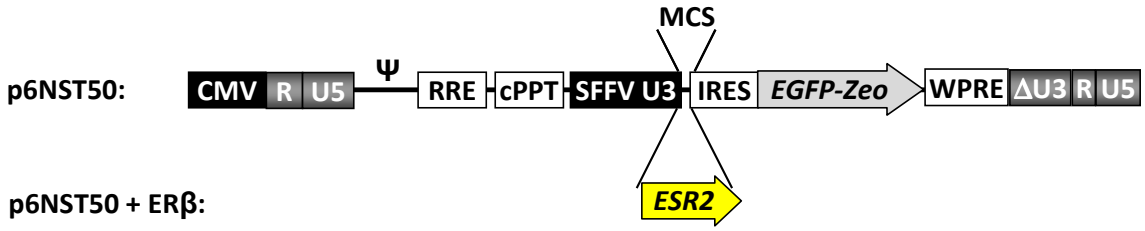

Figure 3-2: Schematic linear illustration of p6NST50 encoding human ERβ transgene (*ESR2*). The transgenic human ERβ was cloned into *Age*1 - *Xba*1 restriction site of the parent lentiviral vector (p6NST50). The new vector is named p6NST50 + ERβ. **Abbreviations:** refer to **Figure 3-1**.

3.2.2.3. Plasmid Midi-Preparation

Plasmid stocks were prepared according to QIAGEN® Plasmid Midi Kit (100) standard protocol (QIAGEN GmbH, Hilden, Germany). A transformed *E. coli* glycerol streak or a single bacterial colony from a streaked LB-Agar-containing ampicillin was inoculated into 100 ml LB medium-containing ampicillin (**Table 3-13**) and grown at 37 °C for 16 hours with constant shaking (approximately 200 rpm). Bacterial cells were harvested using the Avanti® Centrifuge J-26 XP (BECKMAN COULTER™ GmbH, Krefeld, Germany) at 6000 x g for 15 minutes at 4 °C. Next, the bacterial pellet was re-suspended in 4 ml of the supplied Re-suspension Buffer. 4 ml of the supplied Lysis Buffer was then added with vigorous mixing (without vortexing). The mixture was incubated at room temperature for 5 minutes. Then, 4 ml of chilled supplied Neutralization Buffer was added and the mixture was vigorously shaken and kept on ice for further 15 minutes. Subsequently, the mixture was centrifuged at 20,000 x g for 1 hour at 4 °C. Supernatant-containing plasmid DNA was promptly removed and centrifuged again at 20,000 x g for 15 minutes at 4 °C. The supernatant was then applied to the pre-equilibrated supplied QIAGEN-tip100 and bound to the resin by gravity flow. The QIAGEN-tip was washed twice with 10 ml of the supplied Wash Buffer and the plasmid DNA was eluted with 5 ml of the supplied Elution Buffer. To precipitate the eluted plasmid DNA, 3.5 ml 100 % isopropanol was added at room temperature and mixed well prior to centrifugation at 15,000 x g for 30 minutes at 4 °C. The supernatant was then discarded and the pellet-containing plasmid DNA was washed with 2 ml of 70 % ethanol and centrifuged at 15,000 x g for 10 minutes at 4 °C. Finally, plasmid DNA was air-dried and re-dissolved in 300 µl of Tris-EDTA (TE) Buffer, pH 8.0 (**Table 3-22**) and stored at -20 °C until further use.

Table 3-22: TE Buffer per 1 Liter (Sambrook *et al.*, 1989)

Component	Required Amount
1 M Tris pH 8.0	10 ml
0.5 M EDTA pH 8.0	2 ml
Deionized distilled water	added up to 1 Liter
pH adjusted to 8.0 and stored at room temperature	

3.2.3. Production of Viral Particles and Transduction of Target Cells

All viral-related experiments were conducted according to Level 2 Biosafety requirements and in collaboration with Professor Dirk Lindemann's laboratory (Institute of Virology, Medical Faculty Carl Gustav Carus, TU-Dresden, Germany).

3.2.3.1. Determination of Zeocin™ Sensitivity

Since the employed lentiviral-based plasmids encode a Zeocin marker gene cassette (**Figure 3-1 and Figure 3-2**), minimal Zeocin™ concentration (Invitrogen, Karlsruhe, Germany) required to kill almost 100 % of RN46A-B14 cells had to be initially established. RN46A-B14 cells were grown in two 6-well cell culture plates for 24 hours. The medium was then replaced with fresh medium-containing Zeocin™ in a concentration gradient (500, 250, 125, 60, 30, 15, 8, 4, 2, 1, 0.5 and 0 µg/ml). Medium-containing Zeocin™ was replenished every 3 - 4 days and the percentage of surviving cells was roughly determined under the microscope. Finally, the Zeocin™ concentration that killed almost 100 % of cells within 2 weeks was defined and subsequently used to culture raphe nuclei-derived cells bearing p6NST50 or p6NST50 + ERβ.

3.2.3.2. Production of Viral Particles

Infectious lentiviral particles are generally produced via three main lentiviral genes that are encoded in the retroviral genome. Those include: (1) *Gag*: encodes a polyprotein required for viral capsid assembly, (2) *Pol*: encodes four main enzymes, such as protease, integrase, reverse transcriptase and RNase H required for reverse transcription of the RNA genome and finally (3) *Env*: encodes the necessary viral glycoproteins required for budding at cellular membranes (Richter *et al.*, 2009). Since p6NST50 and p6NST50 + ERβ

lack all of the aforementioned viral structural genes, two additional plasmids encoding the lentiviral structural genes were employed, as illustrated in **Figure 3-3**.

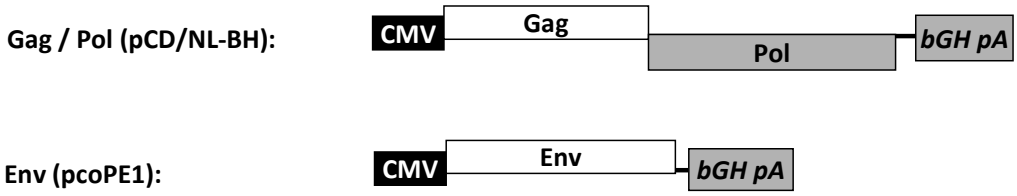

Figure 3-3: Schematic linear illustration of the lentiviral packaging constructs employed in the present study. Both Gag and Pol are represented in one construct, namely pCD/NL-BH. The Env is represented in a different construct, namely pcoPE1. Both constructs were kindly provided by Professor Dirk Lindemann. **Abbreviations:** CMV: cytomegalo virus immediate early enhancer-promoter; bGH pA: Bovine Growth Hormone and Polyadenylation element serving as a sequence for termination of transcription.

Stocks of all viral plasmids were prepared using QIAGEN® Plasmid Midi-Preparation Kit (**Section 3.2.2.3**) and stock concentrations were adjusted to 1 µg/µl. Production of viral particles was conducted over a period of four days as follows:

- ***Day 1: Plating the viral packaging cell line***

The HEK-293T cells were used as the standard cell line for packaging and producing infectious viral particles. HEK-293T cells were plated at a density of 6 x 10^6 cells in a 10-cm cell culture dish in 8 ml aliquots of medium and were left to grow overnight at 37 °C and 5 % CO_2.

- ***Day 2: Transfection of HEK-293T cells with all viral plasmids***

HEK-293T cells were transfected with all employed viral plasmids using the standard polyethylenimine (PEI) transfection reagent (Sigma-Aldrich, Hambrug, Germany). PEI is an organic polymer with a high cationic-charge potential. PEI binds to nucleic acids and ionically condenses them to aid binding to anionic surface receptors; hence promoting the process of endocytosis (Boussif *et al.*, 1995). At first, basal phenol red-free DMEM / F12 medium (i.e. medium with no FCS and other additives) was used to prepare the transfection solution. Stock and working PEI solutions were prepared as shown in **Table 3-23** and **Table 3-24**, respectively. Subsequently, the transfection solution for each 10-cm cell culture dish was set up as shown in **Table 3-25**.

Table 3-23: PEI stock solution (100 mg/ml) per 10 ml

Component	Required Amount / Volume
PEI	1 g
Deionized distilled water	added up to 10 ml
Filter sterilized and stored at 4 °C	

Table 3-24: PEI working solution (1 mg/ml) per 10 ml

Component	Required Volume
PEI stock solution (100 mg/ml)	100 µl
Deionized distilled water	added up to 10 ml
Aliquots were stored at 4 °C	

Table 3-25: Transfection solution per 10-cm cell culture dish

Component	Required Volume
PEI working solution (1 mg/ml)	45 µl
Basal phenol red-free DMEM / F12 medium	955 µl
Total Volume	**1000 µl**

Meanwhile, all viral plasmids (i.e. p6NST50 or p6NST50 + ERβ together with the Gag/Pol/Env plasmids) were also prepared in basal phenol red-free DMEM / F12 medium such that the total plasmid concentration per 10-cm cell culture dish was 15 µg. The required co-transfection mixture was prepared as shown in **Table 3-26**.

Table 3-26: Co-transfection mixture per 10-cm cell culture dish

Viral plasmid (Stock Concentration: 1 µg/µl)	Required Amount / Volume
p6NST50 / p6NST50 + ERβ	7 µg each
pcoPE1 encoding the *Env* gene	1 µg
pCD/NL-BH encoding the *Gag* and *Pol* genes	7 µg
Basal phenol red-free DMEM / F12 medium	985 µl
Total Volume	**1000 µl**

Rapidly, the prepared PEI solution was added to the viral plasmid mixture at a ratio of 1:1 and vortexed. The mixture was incubated at room temperature for 20 minutes. Meanwhile, culture medium was aspirated from the HEK-293T cells and replaced with 4 ml of phenol red-free DMEM / F12 medium containing 15 % FCS only and no further supplements. After 20 minutes, the 2 ml transfection mixture was added to the dish in a drop-wise fashion and cells were finally incubated overnight at 37 °C and 5 % CO_2.

- ***Day 3: Induction of HEK-293T cells***

Since every third atom of PEI is a protonable amino nitrogen, amine protonation results in counter-ion influx followed by lowering of the cell's osmotic potential once the cationic complex (i.e. PEI + plasmids) has been endocytosed by the cell. Osmotic swelling bursts the vesicle releasing the polymer-plasmid complex into the cytoplasm (Akinc *et al.*, 2005). Based on the publication of Olsen and Sechelski (1995), an adapted step was included to increase retroviral production prior to harvesting of viral particles (Olsen and Sechelski, 1995). 120 µl of 500 mM sodium butyrate (**Table 3-27**) was added to each 10-cm cell culture dish to obtain a final working concentration of 10 mM sodium butyrate per dish. Cells were further incubated for 6 - 8 hours at 37 °C and 5 % CO_2. Induction was then stopped by aspirating out medium and adding, in a drop-wise fashion, new phenol red-free DMEM / F12 medium containing 10 % FCS only and no further supplements. Cells were finally incubated overnight before harvesting supernatant-containing viral particles.

Table 3-27: 500 mM stock solution of sodium butyrate in 50 ml PBS

Component	Required Amount / Volume
n-Butyric Acid, Sodium Salt	2.75 g
PBS	added up to 50 ml
Filter sterilized and aliquots were stored at 4 °C	

- ***Day 4: Harvesting of viral particles and storage***

HEK-293T supernatants-containing infectious viral particles were filter-sterilized using a 0.45 µm nitrocellulose filter and aliquots of the sterilized cell-free supernatants were stored at -80 °C until further use.

3.2.3.3. Transduction (Infection) of Target Cells

In virology, transduction or infection means the incubation of target cells with the produced infectious viral particles resulting in the entry of the virus into the host cell and eventually integrating in its cellular genome. This process proceeded as follows:

- ***Day 1: Plating target cells***

RN46A-B14 cells and HT-1080 cells (the reference cell line) were plated in 12-well cell culture plates at a density of 1×10^5 and 2×10^4 cells per well, respectively, in 1 ml aliquots of medium and allowed to grow overnight.

- ***Day 2: Transduction of target cells***

For transduction of target cells, all viral stock dilutions were prepared in phenol red-free DMEM / F12 medium containing 10 % FCS only and no further supplements. Medium was aspirated and replaced with either 2 ml of undiluted (UD) viral stocks or 1:10 dilution of viral stocks. For the negative controls (i.e. untransduced cells), viral particles were omitted. Cells were incubated for 6 - 8 hours. Transduction was ultimately stopped by incubating cells in their own medium (**Table 3-1**) for 72 hours prior to cell harvesting and flow cytometry analysis.

To downgrade transduced cells from Biosafety Level 2 to Biosafety Level 1, supernatants of cultured transduced cells were harvested after 72 hours of transduction and filter-sterilized using 0.45 µm nitrocellulose filters. The cell-free filtrate was later subjected to flow cytometry analysis.

3.2.3.4. Fluorescence-Activated Cell Sorting Analysis

Fluorescence-Activated Cell Sorting (FACS) is a technique used to multiparametrically analyze cells by suspending them in a liquid stream and passing them through a beam of laser light (Givan, 2004). In principle, detectors are placed such that one lies in line with the beam of laser light to measure forward scatter and another lies perpendicular to the beam to measure the side scatter. Additionally, one or more built-in fluorescent detectors are set to measure emitted fluorescence intensity from fluorescently-labeled cells.

Scattered and emitted light from cells are then converted to digital values. By analyzing these values, it is possible to measure and analyze the physical and chemical properties of the cells in addition to the intensity of fluorescence emitted from labeled cells (Basu *et al.*, 2010).

Here, the efficiency of the transduction process was analyzed according to the percentage of target cells expressing the reporter gene, enhanced green fluorescent protein (EGFP), encoded in the employed lentiviral transfer vectors (**Figure 3-1 and Figure 3-2**). Following 72 hours of transduction, cells were harvested in non-sterile FACS tubes (i.e. polypropylene round-bottom tubes) at 1500 rpm for 5 minutes. The resulting supernatant was carefully discarded and cells were re-suspended in 200 µl FACS Buffer (PBS containing 1 % (v/v) FCS). Cell suspensions were ultimately analyzed via the Becton Dickinson FACSCalibur™ Flow Cytometer (BD Biosciences, Heidelberg, Germany). Data were processed using the Becton Dickinson CellQuest™ Software (BD Biosciences, Heidelberg, Germany). During the data processing, EGFP-expressing cells were gated in Region (R2) to distinguish them from the flow of heterogeneous cell population.

3.2.4. Luciferase Reporter Gene Assays

The functional activity of both endogenous ERβ and transgenic human ERβ in the rat raphe nuclei-derived cell lines were assessed using standard reporter gene assays. The degree of estrogenicity (i.e. the transactivational activity) of the flavonoids was also examined. In principle, the assay basically tests for the initiation of a successful ligand-dependent activation of ERβ via the classical ERE pathway through the expression of a reporter plasmid (**Figure 3-4**). In this study, the 2x-ERE-tk-Luc plasmid, which contains the firefly luciferase reporter gene under the control of a double ERE-dependent promoter was utilized. The plasmid was kindly provided by Dr. Luisella Toschi (Schering AG, Berlin).

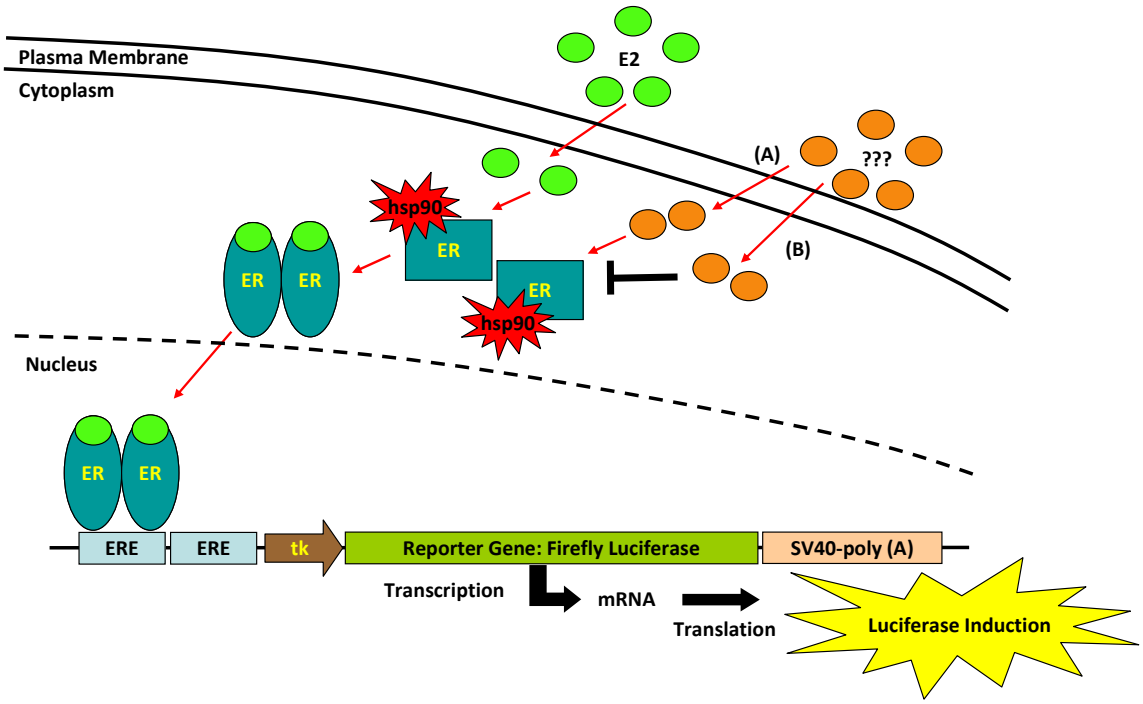

Figure 3-4: A simple schematic model of the reporter gene assay utilized in the present study. 17β-Estradiol (presented in bright green) enters the cell and binds to respective hsp90-inactivated ERs, where a conformational change occurs. Free hsp90-activated bound ERs shuttle to the nucleus and binds to respective EREs, hence activating the transcriptional machinery of the firefly luciferase reporter gene. Alternatively, test substances (represented in orange) can enter the cell and either act as **(A)** estrogenic or **(B)** non-estrogenic substances, hence assessing their affinity for ERs and downstream estrogenicity. **Abbreviations:** E2, 17β-estradiol; hsp90, heat shock protein 90; ER, estrogen receptor; ERE, estrogen responsive elements; tk, thymidine kinase promoter; SV-40, Simian Virus-40; mRNA, messenger RNA.

3.2.4.1. Day 1: Plating Target Cells

RN46A-B14 cells (either untransduced or transduced with p6NST50) or RNDA cells (i.e. the RN46A-B14 cells transduced with p6NST50 + ERβ) were initially washed three times with PBS. In 24-well cell culture plates, cells were plated at a density of 1 x 10^5 cells per well in 500 µl aliquots of medium. The medium was prepared as shown in **Table 3-28**. As noticed, the 10 % FCS component in the original medium was replaced by 5 % DCC-FCS (FCS pre-treated with dextran-coated charcoal) to eliminate any steroid background generated from FCS.

Table 3-28: Phenol red-free DMEM / F12 medium containing 5 % DCC-FCS

Cell Line	Media Additives / Final Concentration (in phenol red-free DMEM / F12 medium)		Temperature & 5 % CO_2
RN46A-B14 cells or RNDA cells	Hygromycin B (50 mg/ml)	100 µg/ml	33 °C
	G418 (50 mg/ml)	250 µg/ml	
	DCC-FCS	5 % (v/v)	
	Penicillin / Streptomycin	1 % (v/v)	

3.2.4.2. Day 2: Transient Transfection of Target Cells

Initially, stock concentrations of reporter plasmid (2x-ERE-tk-Luc) were prepared using QIAGEN® Plasmid Midi-Preparation Kit (**Section 3.2.2.3**) and concentration was measured using the NanoDrop® ND-1000 UV-Vis Spectrophotometer (Tab: Nucleic Acid; Sample type: DNA-50). Transfection mixture was prepared using 1x Serum-Free Defined Medium (SFDM) (**Table 3-29**). Cells were transiently transfected with 0.6 µg reporter plasmid per well. 1,2-Dioleoyl-3-Trimethylammonium-Propane (DOTAP) was used as the standard liposomal transfection reagent, such that ratio of reporter plasmid to DOTAP was 1 µg : 3 µl, respectively (**Table 3-30**). The transfection mixture was incubated for 12 minutes at room temperature. Meanwhile, cells were washed twice with PBS. Finally, 500 µl of the transfection mixture was added to each well and incubated at 33 °C and 5 % CO_2 for 6 hours. Transfection medium was then aspirated and cells were incubated overnight in medium-containing 5 % DCC-FCS.

Table 3-29: 10x SFDM per 500 ml DMEM / F12 medium

Component	Required Amount
Insulin-Transferrin-Sodium Selenite Media Supplement solution	-
1 mM hydrocortisone solution (Final Concentration: 10^{-8} M) (prepared using deionized distilled water)	50 µl
Putrescine dihydrochloride (Final Concentration: 1 mg/l)	5 mg
Filter sterilized and aliquots were stored at -20 °C	

Table 3-30: Standardized reporter gene transfection mixture

Component	Required Amount / Volume (per well per 500 µl)
Reporter Plasmid	0.6 µg
DOTAP	1.8 µl
1x SFDM	added up to 150 µl
Incubated for 12 minutes at room temperature	
Completed volume to 500 µl using 1x SFDM	

3.2.4.3. Day 3: Treatment of Target Cells

Stock concentrations of all control and test substances (**Table 3-31**) were initially dissolved in DMSO. Final concentrations were prepared in medium containing 5 % DCC-FCS ensuring that the final DMSO concentration used was 0.1 %. In all experiments, DMSO treatment served as the standard carrier control treatment. RNDA cells were initially treated with increasing concentrations of E2 (100 fM - 100 nM) to establish a sigmoidal E2-dose response relationship and determine the optimal E2 concentration that shall be used as the positive control concentration in subsequent experiments. Accordingly, 10 nM E2 served as the standard positive control treatment in all experiments.

Untransduced RN46A-B14 cells as well as RNDA cells were treated with 0.1 % DMSO or 10 nM E2 to verify the expression levels of endogenous ERβ versus expression levels of transgenic ERβ. To further exclude non-specific transgenic ERβ effects, RN46A-B14 cells transduced with p6NST50 and RNDA cells were treated with 0.1 % DMSO or 10 nM E2. To further examine whether the observed effects were exclusively mediated by the activated transgenic ERβ, RNDA cells were treated with increasing concentrations (1 nM - 1 µM) of the ERα agonist (Propyl pyrazole triol) or the ERβ agonist (Diarylproprionitril).

The transactivational activity of the flavonoids (i.e. the isoflavones and the naringenin-type flavanones) on the transgenic ERβ in RNDA cells was then scrutinized using an increasing range of concentrations (10 nM - 10 µM) to obtain dose-response relationships. Moreover, to determine whether the observed effects involve the interaction of the flavonoid with the transgenic ERβ, RNDA cells were co-treated with

1 µM of each flavonoid and 500 nM of the pure estrogen receptor antagonist, Fulvestrant. The Fulvestrant dose represented a 50-fold molar excess of 10 nM E2, which corresponded to 10x effective excess of antagonist (Wakeling and Bowler, 1987; Wakeling and Bowler, 1992). To further examine possible antiestrogenic properties, cells were co-treated with 10 nM E2 and 1 µM of each flavonoid. Total final volume of all reactions was 500 µl per well and cells were treated for 24 hours.

Table 3-31: Substances used in luciferase reporter gene assays

Substances	Stock Concentration	Final Concentration
DMSO (Carrier Control Treatment)	-	0.1 %
17β-Estradiol	**Dose Response:** 100 pM - 100 µM **Positive Control:** 10 µM	100 fM - 100 nM 10 nM
Fulvestrant	1 mM	500 nM
Propyl pyrazole triol	1 µM - 1 mM	1 nM - 1 µM
Diarylproprionitril	1 µM - 1 mM	1 nM - 1 µM
Genistein	10 µM - 10 mM	10 nM - 10 µM
Daidzein	10 µM - 10 mM	10 nM - 10 µM
Equol	10 µM - 10 mM	10 nM - 10 µM
Naringenin	10 µM - 10 mM	10 nM - 10 µM
8-Prenylnaringenin	10 µM - 10 mM	10 nM - 10 µM
7-(O-prenyl)naringenin-4'-acetate	10 µM - 10 mM	10 nM - 10 µM
6-(1,1-Dimethylallyl)naringenin	10 µM - 10 mM	10 nM - 10 µM

3.2.4.4. Day 4: Measurement of Luciferase Activity

Treated cells were washed twice with PBS then lysed by adding 100 µl 1x Promega reporter lysis buffer (diluted from a supplied 5x stock solution using deionized distilled water) (Promega, Mannheim, Germany). Plates were then incubated at -80 °C for 30 minutes. Cells were allowed to thaw at room temperature and cell lysates were collected into Eppendorf tubes.

To normalize the data, protein concentration was determined using the bicinchoninic acid (BCA) standard assay (VWR, Darmstadt, Germany). For protein determination, BSA stock solution with 1 µg/µl BSA (dissolved in 0.15 M sodium chloride solution) was initially prepared and a BSA standard series was arranged as shown in **Table 3-32**. 10 µl of each standard (1 to 7) was pipetted horizontally and in triplicates into a clear 96 well flat-bottomed plate. 10 µl of the sample cell lysates and the 1x Promega reporter lysis buffer (negative control) were also pipetted in the same plate and in the same manner. Subsequently, 250 µl of the BCA mixture (supplied BCA solution and copper (II) sulphate solution used at a ratio of 50:1, respectively) was added to each well and incubated at 37 °C for 30 minutes. BCA was then measured at an absorbance of 565 nm using the Infinite F200 spectrophotometer machine and the Magellan Software (TECAN, Männedorf, Switzerland).

Table 3-32: BSA standard series used for luciferase reporter gene assays

Tube #	0.15 M NaCl	1 µg/µl BSA solution (dissolved in 0.15 M NaCl)	Final BSA Concentration per well
1	-	10 µl	1 µg/µl
2	2 µl	8 µl	0.8 µg/µl
3	4 µl	6 µl	0.6 µg/µl
4	6 µl	4 µl	0.4 µg/µl
5	8 µl	2 µl	0.2 µg/µl
6	9 µl	1 µl	0.1 µg/µl
7	10 µl	-	0 µg/µl

To measure luciferase activity using the standard Luciferase Assay System (Promega, Mannheim, Germany), 10 µl of cell lysates were pipetted vertically and in duplicates into a white 96 well flat-bottomed plate. Subsequently, 50 µl of the supplied Promega Luciferase Assay Substrate (delyophilized using the supplied Promega Luciferase Assay Buffer) was added to each well and was measured immediately using the Infinite F200 spectrophotometer machine; however no absorbance was specified in this case since the reaction is bioluminescent. Data analyses and statistical procedures were conducted as explained in **Section 3.2.9.1**.

3.2.5. Gene Expression Analysis

Quantitative real-time PCR has proven to be a highly sensitive approach to amplify and simultaneously quantify the expression and regulation of target mRNA in cells or tissues. The general idea of quantitative real-time PCR is initiated by converting small amounts of RNA into cDNA by reverse transcription. The resulting cDNA is further amplified over a specified number of cycles. The newly synthesized PCR products are easily detected via the use of SYBR® Green I fluorescence dye that specifically binds double-stranded DNA. By plotting fluorescence against the cycle number on a logarithmic scale, relative concentrations of the amplified DNA are determined during the exponential phase of the reaction. A threshold is usually determined to detect fluorescence above background. The cycle at which the fluorescence from a sample crosses the threshold is usually determined by the Cycle Threshold Value (C_T-value) [Reviewed in (VanGuilder *et al.*, 2008)].

Quantitative real-time PCR also determines the melting temperature of the synthesized PCR products following the amplification reactions. The nucleotide composition as well as the length of the synthesized DNA product determines the melting temperature of the product. In principle, all PCR products for the same primer pair should show the same melting temperature. Since SYBR® Green I indiscriminately binds to double-stranded DNA including primer dimers, similar melting temperatures amongst all samples act as a reliable quality control (Nolan *et al.*, 2006).

For accurate quantification of gene expression, it is necessary to correct the expression of the gene of interest to a ubiquitously expressed gene, referred to as the internal reference gene. This correction allows for accurate comparison of gene expression amongst various samples, given that the expression of the internal reference gene is stable across all test samples, even under experimental conditions (Eisenberg and Levanon, 2003). In this study, the rat ribosomal protein S18 (*Rps-18*) (Chan *et al.*, 1991) was used as the standard internal reference gene.

3.2.5.1. RNA Isolation from Adherent Rat Raphe Nuclei-Derived Cells

RNA isolation was carried out using peqGOLD TriFast™ standard protocol (http://www.peqlab.com/wcms/en/pdf/30-2010_m.pdf) (PEQLAB Biotechnologie GmbH,

Erlangen, Germany). Unless otherwise stated, all steps were carried out at room temperature and all working surfaces were sprayed with RNAse-Exitus Plus™ (Applichem, Darmstadt, Germany) to eliminate any RNase contaminations.

- ***Homogenization:***

Adherent cells were trypsinized and harvested (**Section 3.2.1.1**). Cell pellet was re-suspended in 1 ml peqGOLD TriFast™ reagent and incubated for 5 minutes at room temperature to dissociate nucleoprotein complexes.

- ***Phase separation:***

The re-suspended cell pellet was transferred to an appropriate Eppendorf tube and 200 µl of pure chloroform was added. The mixture was then vigorously shaken (by hand) for 15 seconds at room temperature and left for a minimum of 10 minutes till a visual separation of phases was noticed. At this point, samples were centrifuged using the Biofuge fresco (Heraeus Instruments, Leipzig, Germany) at 12,000 x g for 5 minutes at 4 °C. Centrifugation clearly separated the mixture into a lower red phase (phenol-chloroform phase), an interphase and a colourless upper aqueous phase.

- ***Precipitation of RNA:***

Since the RNA is exclusively separated into the aqueous upper phase, the aqueous phase was collected into a new Eppendorf tube and the other two phases were kept at -80 °C. RNA was then precipitated with 500 µl 100 % isopropanol. Samples were briefly vortexed and kept at 4 °C for a minimum of 15 - 20 minutes. Samples were then centrifuged at 12,000 x g for 10 minutes at 4 °C. The RNA pellet formed a white gel-like precipitate on the bottom and sides of the tube.

- ***Washing of RNA:***

Supernatant was carefully removed and RNA pellet was washed twice with 1 ml 75 % ethanol and further centrifuged at 12,000 x g for 10 minutes at 4 °C. The 75 % ethanol in this step was prepared using diethylpyrocarbonate (DEPC)-treated water to inactivate possible RNase enzymes.

- ***Solubilization of RNA:***

RNA pellet was allowed to air-dry. Pellet was then re-suspended using 20 - 50 µl DEPC-treated water (depending on pellet size). Samples were stored at -80 °C until further use.

- ***Measuring RNA concentration and RNA quality control:***

RNA concentration was measured using the NanoDrop® ND-1000 UV-Vis Spectrophotometer (Tab: Nucleic Acid; Sample type: RNA-40). To further assess the quality of the isolated RNA sample, 0.2 volumes of 6x loading buffer (**Table 3-17**) was added to 0.5 - 1 µg of each isolated RNA sample and the mixture was loaded onto a 1 % agarose gel (+ 0.004 % ethidium bromide). The gel was left to run at 100 volts for 30 minutes in 1x TAE buffer (**Table 3-18**). Gel visualization took place under the UV-light (EpiChemi^3 Benchtop Darkroom, UVP Ltd, Cambridge, UK) and gel image was captured using Labworks™ Image Acquisition and Analysis Software Version 4.6.

3.2.5.2. DNase Digestion and Quantitative Real-Time PCR

Genomic rat DNA was eliminated from the isolated RNA samples by incubating the sample with RQ1 RNase-Free DNase (Promega, Mannheim, Germany) for 30 minutes at 37 °C in Primus 96 ^{plus} bench cycler (MWG-BIOTECH, Ebersberg, Germany). Reaction mixture was prepared as shown in **Table 3-33**. Following the incubation, the thermostable *Taq* DNA polymerase (Recombinant) (5 U / µl) (Invitrogen, Karlsruhe, Germany) was used in a quantitative real-time PCR (**Table 3-34**) to verify proper digestion of any genomic rat DNA via the cycling conditions described in **Table 3-35**. An independent positive control rat cDNA was included for quality control. A piece of the rat internal reference gene, *Rps-18*, was amplified as a test for the completeness of the digest. The reaction was carried out in low 96-well white un-skirted PCR plates (BIO-RAD, Munich, Germany). The plate was briefly centrifuged using the Megafuge 2.0R (Heraeus Instruments, Leipzig, Germany) and subsequently placed in the CFX96™ Real-Time System (BIO-RAD, Munich, Germany) and results were analyzed using the Bio-Rad CFX Manager Version 1.6.

Table 3-33: DNase digestion (10 µl total volume per reaction)

Component	Required Amount / Volume per reaction
RNA sample	3 µg
10x PCR Buffer (Sambrook *et al.*, 1989)	1 µl
RNaseOUT™ Recombinant Ribonuclease Inhibitor (40 U / µl)	0.5 µl
RQ1 RNase-Free DNase (1 U / µl)	1 µl
HPLC water	added up to 10 µl
Incubated at 37 °C for 30 minutes	

Table 3-34: Quantitative real-time PCR (20 µl total volume per reaction)

Component	Required Volume per reaction
Quantitative real-time PCR Product	1 µl
10x PCR Buffer (without Magnesium Chloride) (Invitrogen) including 2.4x SYBR® Green I (Sigma)	2 µl
50 mM Magnesium Chloride	0.8 µl
dNTP mixture (Final Concentration: 2.5 mM each)	0.8 µl
Rat *Rps-18* primer mix (Final Concentration: 10 µM each) **Fwd**: CGT GAA GGA TGG GAA GTA TAG C **Rev**: TAT TAA CAG CAA AGG CCC AAA G	0.6 µl
Taq DNA Polymerase (Recombinant) (5 U / µl)	0.06 µl
HPLC water	added up to 20 µl

Table 3-35: Cycling conditions for quantitative real-time PCR in CFX96™ Real-Time System

Step	Temperature [°C]	Required Time	Number of Cycles
1. Initial Denaturation	95.0	3 minutes	1x
2. Denaturation of dsDNA	**95.0**	**10 seconds**	**40x**
3. Annealing	**60.0**	**10 seconds**	
4. Extension	**72.0**	**20 seconds**	
5. Melting of dsDNA	95.0	10 seconds	1x
6. Melt Curve	65.0 - 95.0 in 0.5 steps	5 seconds	1x

3.2.5.3. DNase Inactivation, cDNA Synthesis and Quantitative Real-Time PCR

1 µl EDTA was added to the DNase digestion product to inactivate the RQ1 RNase-Free DNase. The samples were incubated at 80 °C for 3 - 5 minutes in Primus 96 *plus* bench cycler (MWG-BIOTECH, Ebersberg, Germany). Then, 10 µl of cDNA synthesis reaction mixture (**Table 3-36**) was added and samples were incubated at 42 °C for 1 hour in Primus 96 *plus* bench cycler (MWG-BIOTECH, Ebersberg, Germany).

20 µl of HPLC water was finally added to each reaction and once again, the thermostable *Taq* DNA polymerase (Recombinant) (5 U / µl) was used in a quantitative real-time PCR (**Table 3-34**) to verify successful cDNA synthesis using the same cycling conditions described in **Table 3-35**. Again, an independent positive control rat cDNA was included for quality control. A piece of the rat internal reference gene, *Rps-18*, was also amplified as a test for the completeness of the synthesis. Prepared rat cDNA samples were then stored at -20 °C until further use.

Table 3-36: cDNA synthesis reaction mixture (10 µl total volume per reaction)

Component	Required Volume
Product of DNase digestion reaction	10 µl
Oligo $(dT)_{18}$-primers (Final Concentration: 100 µM)	1 µl
dNTP mixture (Final Concentration: 10 mM each)	2 µl
10x PCR Buffer (Sambrook *et al.*, 1989)	1 µl
50 mM Magnesium Chloride	1 µl
RNaseOUT™ Recombinant Ribonuclease Inhibitor (40 U / µl)	0.5 µl
MMLV-RT (200 U/µl)	1 µl
HPLC water	added up to 20 µl
Incubated at 42 °C for 1 hour	
20 µl HPLC water was further added (i.e. final total volume per cDNA sample was 40 µl)	

3.2.5.4. Primer Design

Genomic DNA sequences of target genes (**Table 3-37**) were extracted from the UCSC Genome Browser Database (http://genome.ucsc.edu/) (Kent *et al.*, 2002; Rhead *et al.*, 2010). The sequences were employed in Primer3 Version 2.2.3 (http://frodo.wi.mit.edu/primer3/) (Rozen and Skaletsky, 2000) for primer design. Primers were designed to flank the last intron at the 3' end of the sequence. The most prominent parameters for the primer design in the Primer3 program were: (1) melting temperature (59 °C - 61 °C), (2) amplicon size (150 - 220 bp), (3) primer length (18 - 20 bp) and (4) at least one GC-clamp at the 3' end of the primer

Using the *Blat*- and *in silico* PCR tools provided within the UCSC Genome Browser website, a primer sequence match search against the rat genome was performed to evaluate the specificity of the designed primers and their exact location on the genomic sequence. Finally, the primer pairs of each target gene (**Table 3-37**) were commercially synthesized by Biomers.net GmbH (Ulm, Germany).

Table 3-37: Primer sequences utilized throughout the study

Gene Symbol: Description	Accession ID	Primer Sequences (Fwd and Rev)
ESR2: Human estrogen receptor-beta *	NM_001040276	**Fwd:** GGC ATC TCC TCC CAG CAG CAA TCC **Rev:** TCA GCA TCT CCA GCA GCA GGT CAT A
Esr2: Rat estrogen receptor-beta *	NM_012754	**Fwd:** CTA CAG AGA GAT GGT CAA AAG TGG A **Rev:** GGG CAA GGA GAC AGA AAG TAA GT
Rps-18: Rat ribosomal protein S18 *	NM_213557	**Fwd:** CGT GAA GGA TGG GAA GTA TAG C **Rev:** TAT TAA CAG CAA AGG CCC AAA G
Cml-5: Rat camello-like 5	NM_080884	**Fwd:** GGA TAG CGA AAG CAC TGG TC **Rev:** AGC AGA AGG GAA AGC ATA CG
Sox-18: Rat sex determining region Y-box 18	NM_001024781	**Fwd:** CTT TAT GGT GTG GGC GAA G **Rev:** AGG CCG GTA CTT GTA GTT GG
Krt-19: Rat keratin, type I cytoskeletal 19	NM_199498	**Fwd:** ATG AGC TGA ACA CCC AGG TC **Rev:** CAC CTT GGA TGT GTG ACA GC
Nefm: Rat neurofilament, Medium polypeptide	NM_017029	**Fwd:** ATC GAG ATC GCC GCA TAT AG **Rev:** TGT GTT GGA CCT TGA GCT TG
Zdhhc-2: Rat zinc finger, DHHC-type containing 2	NM_145096	**Fwd:** GCA ACC CTG CAT TAA CTA TGG **Rev:** TTG ATC CCC ATC ACT GAA GAC
Slc6a4: Rat solute carrier family 6 member 4	NM_013034	**Fwd:** TCT TGG GCT ACT GCA TAG GG **Rev:** CCT CTC CCA GGG TGT GTT AC

* Previously designed primer pairs in the lab

3.2.5.5. PCR Optimization and PCR Efficiency

As previously mentioned, the delivered lyophilized primers were re-suspended using a given volume of HPLC water such that stock concentrations were adjusted to 100 pmol/µl (100 µM) each. For each gene, a primer mix was prepared in which the final concentration of the forward and reverse primers was 10 pmol/µl (10 µM) each. For optimal PCR conditions, primer and magnesium chloride volumes were optimized such that 3.36 µl of the reaction mixture (**Table 3-38**) were pipetted into each well of a 96-well white un-skirted PCR plate (BIO-RAD, Munich, Germany) using a 4 x 4 matrix scheme **Table 3-39**.

Table 3-38: Reaction mixture per well for the primer / magnesium chloride optimization

Component	Required Volume
10x PCR Buffer (without Magnesium Chloride) (Invitrogen) including 2.4x SYBR® Green I (Sigma)	2 µl
dNTP mixture (Final Concentration: 2.5 mM each)	0.8 µl
A rat cDNA sample	0.5 µl
Taq DNA Polymerase (Recombinant) (5 U / µl)	0.06 µl
Total Volume	**3.36 µl**

Table 3-39: 4 x 4 matrix scheme for the primer / magnesium chloride optimization

Magnesium Chloride (50mM) in µl

Primer Mix in µl (Fwd + Rev) (10 µM each) [µl]	0.8	1.2	1.6	2
0.4	15.44	15.04	14.64	14.24
0.6	15.24	14.84	14.44	14.04
0.8	15.04	14.64	14.24	13.84
1.2	14.64	14.24	13.84	13.44

HPLC water [µl] pipetted to complete total volume per well to 20 µl

The PCR reaction was carried out in the CFX96™ Real-Time System (BIO-RAD, Munich, Germany) using the cycling conditions described in **Table 3-35**. Via the Bio-Rad CFX Manager Version 1.6, the quantification and melting curve of each well was analyzed. First, the melting curve was analyzed such that a well-defined peak was observed at a specific melting temperature. Accordingly, conditions with primer and magnesium chloride concentrations were selected. Subsequently, the quantification curves were analyzed.

Concentrations with the lowest C_T-values were chosen and concentrations with the lowest primer consumption were finally selected. The appropriate size of PCR products was confirmed by agarose gel electrophoresis. 0.2 volumes of 6x loading buffer (**Table 3-17**) was added to 5 µl of the resulting PCR reaction and the mixture was loaded on a 2 % agarose gel (+ 0.004 % ethidium bromide) against a 50 bp DNA Ladder (1000 µg/ml) (NEW ENGLAND BioLabs GmbH, Frankfurt am Main, Germany). The gel was left to run at 100 volts for 45 minutes in 1x TAE buffer (**Table 3-18**).

The optimal primer and magnesium chloride concentrations were used for further determination of PCR efficiency. 1 µl of each of the standard dilution series (ranging from 10^{-3} to 10^{-10}) of the PCR product with the optimal conditions was pipetted in duplicates in low 96-well white un-skirted PCR plates (BIO-RAD, Munich, Germany) for evaluation of primer efficiency. The same abovementioned cycling conditions (**Table 3-35**) were used and efficiencies normally ranged from 85 – 110 % (i.e. indicating best PCR optimization). The primers and their PCR optimized conditions required for further mRNA expression analyses are presented in **Table 3-40**.

Table 3-40: PCR conditions required for mRNA expression analyses

Gene Symbol	Description	Amount of 50 mM $MgCl_2$ per reaction per 20 µl total volume	Amount of Primer Mix per reaction per 20 µl total volume	Amplicon Size	Melting Temperature	Efficiency
ESR2 *	Human estrogen receptor-beta	0.8 µl	0.4 µl	153 bp	87 °C	95 %
Esr2 *	Rat estrogen receptor-beta	1.6 µl	0.4 µl	215 bp	86.5 °C	89 %
Rps-18 *	Rat ribosomal protein S18 (Internal reference gene)	0.8 µl	0.6 µl	218 bp	90 °C	92 %
Cml-5	Rat camello-like 5	0.8 µl	0.6 µl	214 bp	85 °C	106 %
Sox-18	Rat sex determining region Y-box 18	0.8 µl	0.8 µl	195 bp	89.5 °C - 90 °C	98.7 %
Krt-19	Rat keratin, type I cytoskeletal 19	0.8 µl	0.8 µl	195 bp	87 °C	108 %
Nefm	Rat neurofilament, Medium Polypeptide	0.8 µl	0.6 µl	168 bp	85 °C	102 %
Zdhhc-2	Rat zinc finger, DHHC-type containing 2	0.8 µl	0.8 µl	173 bp	83 °C	111 %
Slc6a4	Rat solute carrier family 6 member 4	0.8 µl	0.4 µl	182 bp	85 °C	97 %

* Previously optimized primers in the lab

3.2.5.6. mRNA Expression Analyses Using Quantitative Real-Time PCR

Quantitative mRNA expression analyses were performed with all of the abovementioned genes. Since an optimal specificity and sensitivity of enzymatic action is required, each reaction was carried out using the Platinum® *Taq* DNA Polymerase (5 U / µl) (Invitrogen, Karlsruhe, Germany). Reaction mixtures were prepared as shown in **Table 3-41**.

Table 3-41: Quantitative mRNA analyses reaction mixture (20 µl total volume per reaction)

Component	Required Volume per reaction
Rat cDNA solution	0.5 µl
10x PCR Buffer (without Magnesium Chloride) (Invitrogen) including 2.4x SYBR® Green I (Sigma)	2 µl
50 mM Magnesium Chloride	**Table 3-40**
dNTP mixture (Final Concentration: 2.5 mM each)	0.8 µl
Gene's primer mix (Fwd and Rev Final Concentration: 10 µM each)	**Table 3-40**
Platinum® *Taq* DNA Polymerase (5 U / µl)	0.06 µl
HPLC water	added up to 20 µl

The quantitative real-time PCR reaction was carried out using the cycling conditions described in **Table 3-35**. As always mentioned, the rat *Rps-18* was used as the standard internal reference gene. The reaction was carried out in low 96-well white un-skirted PCR plates (BIO-RAD, Munich, Germany). Each plate was briefly centrifuged using the Megafuge 2.0R (Heraeus Instruments, Leipzig, Germany) and subsequently placed in the CFX96™ Real-Time System (BIO-RAD, Munich, Germany) and results were analyzed via the Bio-Rad CFX Manager Version 1.6. Data analyses and statistical procedures were conducted as explained in **Section 3.2.9.2**.

3.2.6. One-Colour Microarray-Based Gene Expression Analysis

DNA microarray is a high throughput technology that is widely used to simultaneously measure changes in the expression of thousands of genes in any given biological sample. The core principle behind DNA microarrays is the binding of fluorescently-labelled copies of nucleic acids from target samples onto immobilized gene-specific probes fixed on a

solid state matrix, such as microscopic glass slides or ceramic chips. The amount of target sample binding to the probes defines the total strength of the generated signal from a spot or so-called feature (Freeman *et al.*, 2000).

There exist two general hybridization strategies in DNA microarray. The first and the most commonly known approach is the two-colour microarray where two different target samples are allowed to hybridize to the same microarray chip because they are both labeled with two different flourophores (usually Cyanine-3 and Cyanine-5) having two different emission wavelengths. The second recently used approach is the one-colour microarray where one single sample is labeled with one flourophore (usually Cyanine-3 only) per array (Knapen *et al.*, 2009). Both approaches have certain advantages and disadvantages. Yet, studies comparing one-colour and two-colour microarrays show that both approaches perform equally well regarding data quality and accuracy of measuring expression ratios (Patterson *et al.*, 2006; Peixoto *et al.*, 2006). Thus, the decision whether to use either approaches is mainly determined by experimental design considerations, costs and the researcher's preference. In the present study, the one-colour microarray approach provided by Agilent Technologies (Waldbronn, Germany) was employed to globally assess E2-induced gene expression in RNDA cells due to two main reasons: (1) cost considerations and (2) avoiding the drawback of using Cyanine-5 as its susceptibility to environmental ozone levels leads to a decrease in quality of data (Fare *et al.*, 2003).

All microarray experiments were conducted under the guidance of the DNA Microarray Facility at the Max Planck Institute for Molecular Cell Biology and Genetics (Dresden, Germany). Cells were plated at a density of 1×10^6 cells per 75-cm^2 cell culture flask. At approximately 70 % confluence, cells were treated with either 0.1 % DMSO (control carrier treatment) or 10 nM E2 (positive control treatment) for 24 hours. Cells were then trypsinized and harvested (**Section 3.2.1.1**) for RNA isolation using the peqGOLD TriFast™ standard protocol (**Section 3.2.5.1**). Three independent cell culture experiments were conducted.

All isolated RNA samples were subjected to stringent quality control procedures using the Agilent 2100 bioanalyzer (http://www.chem.agilent.com/Library/applications/5989-

1086EN.pdf) (Agilent Technologies, Waldbronn, Germany). By evaluating the resulting bioanalyzer electropherograms, a good RNA quality was indicated by well-defined peaks for 18s and 28s ribosomal RNA with an RNA Integrity Number of at least 7.00.

Using the Agilent's Quick Amp Labelling Kit (Agilent Technologies, Waldbronn, Germany) and following the standard Agilent's One-Colour Microarray-Based Gene Expression Analysis Manual Version 5.7 (http://www.chem.agilent.com/Library/usermanuals/Public/G4140-90041_One-Color_Tecan.pdf), 500 ng of total isolated RNA was used to pursue microarray experimental steps, as illustrated in **Figure 3-5**.

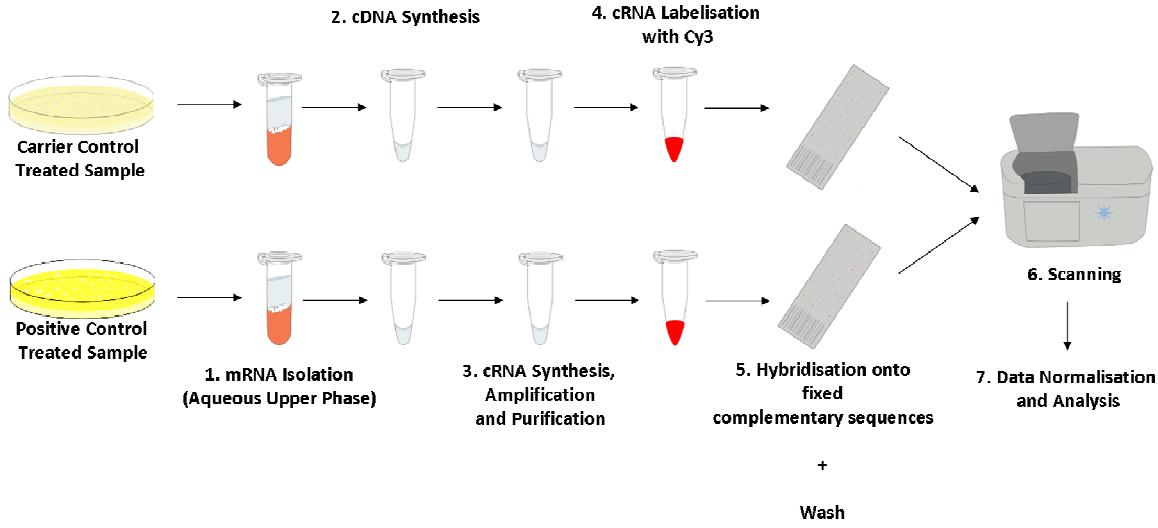

Figure 3-5: Workflow of one-colour microarray approach for Cy3-labelled cRNA sample preparation and array processing. Abbreviations: mRNA, messenger RNA; cDNA, complementary DNA; cRNA, complementary RNA; Cy3, Cyanine-3.

The resulting cyanine 3-labelled amplified and purified complementary RNA was further linearized and fragmented into smaller pieces to enhance the hybridization process onto probes on the Agilent microarray (4 x 44K) slide format of the whole rat transcriptome. The Agilent microarray slides were placed in an appropriate slide holder and loaded into the carousel of the Agilent DNA Microarray Scanner employing SureScan High Resolution Technology (Agilent Technologies, Waldbronn, Germany). Generated data were extracted using the Agilent Feature Extraction Software Version 9.5 (Agilent Technologies, Waldbronn, Germany). Following the manufacturer's user guide (http://www.chem.agilent.com/Library/usermanuals/Public/UserGuide_050415.pdf), information from probe features were extracted from the microarray scanned data in order

to measure gene expression of the given biological samples. Finally, the microarray raw data files (tab-delimited text format) were uploaded to the Agilent Technologies GeneSpring GX 9 Software (http://www.chem.agilent.com/cag/bsp/products/gsgx/manuals/GeneSpringGX9_QuickStartGuide.pdf). Probe sets that were undetectable in all treatment groups were eliminated. The remaining probe sets were first filtered on expression (20^{th}-100^{th}) percentile on normalized data. Finally, probe sets that exhibited at least two-fold change of expression in response to DMSO- and E2-treated samples were selected.

3.2.7. Treatment of Raphe Nuclei-Derived Cells for Gene Expression Studies

The regulation of mRNA expression of selected estrogen responsive genes (identified from the microarray-based analysis) was scrutinized in response to E2 or the flavonoids. Because RNDA cells encode a temperature-sensitive mutant of the SV40 large T-antigen, neuronal differentiation is constitutive upon shifting them to non-permissive temperature (White and Whittemore, 1992; Whittemore and White, 1993; White *et al.*, 1994). Based on this property, the regulation of mRNA expression was investigated in RNDA cells grown under permissive temperature (proliferative conditions) or under non-permissive temperature (differentiation conditions) (i.e. denoted as D-RNDA cells).

3.2.7.1. Treatment of RNDA Cells

RNDA cells were plated at a density of 5×10^5 cells per 25-cm^2 cell culture flask. At approximately 80 % confluence, cells were treated for 24 hours with the control or test substances (**Table 3-42**) prior to RNA isolation and gene expression analysis (**Section 3.2.5**). Three independent cell culture experiments were performed.

Table 3-42: Treatment of RNDA cells for gene expression studies

Substances	Stock Concentration (dissolved in DMSO)	Final Concentration (prepared in medium)
DMSO (Carrier Control Treatment)	-	0.1 %
17β-Estradiol (Positive Control)	10 µM	10 nM
8-Prenylnaringenin, Naringenin, 6-(1,1-Dimethylallyl)naringenin, Genistein, Daidzein or Equol	10 mM	10 µM

3.2.7.2. Treatment of D-RNDA Cells

To treat D-RNDA cells, RNDA cells were first plated at a density of 2 x 10^6 cells per 75-cm^2 cell culture flask at 33 °C and 5 % CO_2. At approximately 80 % confluence, one 75-cm^2 cell culture flask was treated for 24 hours with 0.1 % DMSO prior to RNA isolation and gene expression analysis (**Section 3.2.5**) (referred to as the day 0 sample). As depicted in **Figure 3-6**, the remaining 18 flasks were shifted to differentiation conditions at day 0 (i.e. day of initiation of differentiation).

Media was changed every other day and cells were treated for 24 hours with the control or test substances (**Table 3-43**) prior to RNA isolation and gene expression analysis (**Section 3.2.5**). Two different collection time points were chosen: at day 1 and day 4 following initiation of differentiation. Three independent cell culture experiments were performed.

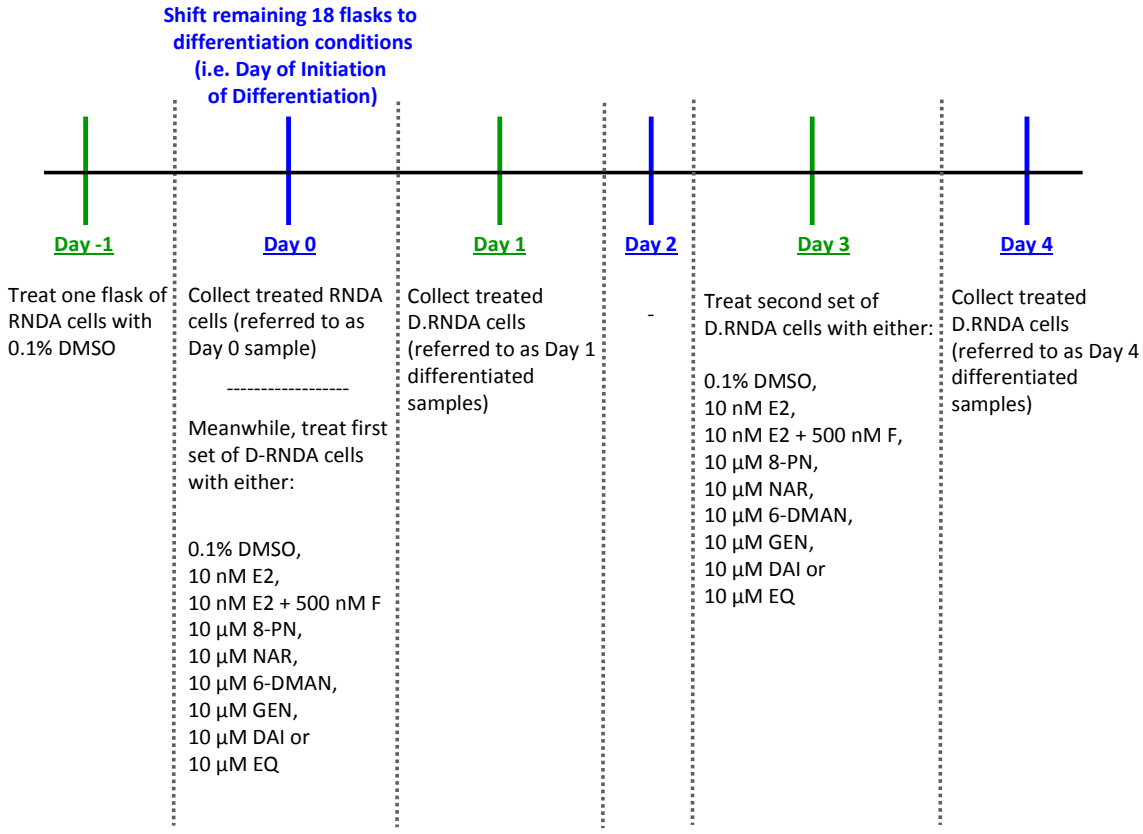

Figure 3-6: Time plan and experimental design pursued to treat D-RNDA cells for gene expression studies.
Total number of flasks per experiment is 19 flasks.

Table 3-43: Treatment of D-RNDA cells for gene expression studies

Substances	Stock Concentration (dissolved in DMSO)	Final Concentration (prepared in medium)
DMSO (Carrier Control Treatment)	-	0.1 %
17β-Estradiol (Positive Control)	10 µM	10 nM
Fulvestrant	1 mM	500 nM
8-Prenylnaringenin, Naringenin, 6-(1,1-Dimethylallyl)naringenin, Genistein, Daidzein or Equol	10 mM	10 µM

3.2.8. Protein Expression Analysis

3.2.8.1. Western Blotting

Western Blot analytical techniques were employed to detect and verify the successful expression of the transgenic human ERβ protein in RNDA cells.

- ***Protein isolation:***

Protein fractions were initially isolated from RN46A-B14 cells (either untransduced or transduced with p6NST50) and RNDA cells. The rat raphe nuclei-derived cells were grown to 80 % confluence in 75-cm^2 cell culture flasks. Using the NucleoSpin® RNA/Protein Kit (MACHEREY-NAGEL, Düren, Germany), cytosolic protein fractions were isolated as per manufacturer's instructions.

Briefly, cells were collected and lysed using 350 µl of the supplied Lysis Buffer RP1 and 3.5 µl of β-mercaptoethanol (Sigma-Aldrich, Hamburg, Germany). Next, viscous cell lysates were vigorously vortexed and lysate viscosity was further reduced by filtration through the supplied NucleoSpin® Filter at 11,000 x g for 1 minute. Subsequently, RNA binding conditions were adjusted by adding 350 µl of 70 % ethanol to the homogenized lysate. For each preparation, the lysate was loaded onto the supplied NucleoSpin® RNA/Protein Column and centrifuged at 11,000 x g for 30 seconds. At this step, protein fractions were isolated by recovering the flow-through. 100 µl were transferred into a fresh supplied collection tube and the supplied Protein Precipitator was added at a ratio of 1:1. The mixture was vigorously shaken and kept at room temperature for

approximately 10 minutes and subsequently centrifuged at 11,000 x g for 5 minutes. The resulting protein pellet was then washed using 500 µl of 50 % ethanol and further centrifuged at 11,000 x g for 1 minute. Ultimately, protein pellet was air-dried for 5 - 10 minutes and the pellet was dissolved by adding 100 µl of the supplied pre-warmed Protein Solving Buffer containing reducing agent (PSB-TCEP). Finally, protein samples were incubated at 95 °C - 98 °C for 3 minutes and eventually stored at -20 °C until protein quantification and further analysis.

- ***Protein quantification:***

Following protein isolation, protein quantification is occasionally required prior to protein analysis. However, most protein quantification procedures are incompatible with sodium dodecyl sulphate (SDS), an anionic detergent that denatures secondary and tertiary protein structures and is commonly present in the sample buffer, as in the case with protein samples dissolved in PSB-TCEP. Hence, protein samples prepared using the NucleoSpin® RNA/Protein Kit (MACHEREY-NAGEL, Düren, Germany) were quantified as per manufacturer's instructions based on the method described by Karlsson and colleagues (Karlsson *et al.*, 1994). Briefly, BSA stock solution with 40 µg/µl BSA dissolved in deionized distilled water was initially prepared and a BSA standard series was arranged as shown in **Table 3-44**.

Table 3-44: Standard BSA dilution series (adapted from the NucleoSpin® Kit)

Tube #	Supplied PSB-TCEP	40 µg/µl BSA solution (dissolved in deionized distilled water)	Final BSA Concentration in 100 µl total volume per well
1	75 µl	25 µl	10 µg/µl
2	80 µl	20 µl	8 µg/µl
3	85 µl	15 µl	6 µg/µl
4	90 µl	10 µl	4 µg/µl
5	95 µl	5 µl	2 µg/µl
6	97.5 µl	2.5 µl	1 µg/µl
7	50 µl	-	0 µg/µl

20 µl of each standard (1 to 7) was pipetted in duplicates into a clear 96 well flat-bottomed plate. In addition, 20 µl of protein samples (each dissolved in PSB-TCEP) as well as PSB-TCEP buffer (serving as the negative control) were also pipetted in the same plate and in the same manner. Subsequently, 40 µl of the supplied PSB-TCEP buffer was added to all wells. Finally, 40 µl of 60 % trichloracetic acid was added to each well to end up with a final total volume of 100 µl per well. The plate was then mixed until color changed from blue (corresponds to color of PSB-TCEP) to bright yellow. Plate was left at room temperature for 30 minutes and eventually absorption was measured at a wavelength of 570 nm using the Infinite F200 spectrophotometer machine and the Magellan Software (TECAN, Männedorf, Switzerland). Protein concentrations were then calculated from the resulting standard curve. Accordingly, aliquots of 20 µg of protein were prepared and stored at -20 °C until further analysis.

- ***Protein detection:***

Following protein isolation and quantification, target protein was detected using the Western blot analytical technique, which proceeded as follows:

⇨ *1st step: SDS-PolyAcrylamide Gel Electrophoresis (SDS-PAGE)*

Protein samples were first separated using SDS-PAGE, where the SDS component maintains polypeptides in their denatured state and applies a negative charge to the proteins in proportion to their mass, thus allowing the separation by their molecular weight (Weber and Osborn, 1969). Initially, all stock solutions of required buffers for SDS-PAGE were prepared as shown in **Table 3-45** up to **Table 3-48**.

Table 3-45: 4x Stacking gel buffer per 500 ml

Component	Required Amount
Tris	30.25 g
SDS	2 g
Deionized distilled water	added up to 500 ml
pH adjusted to 6.8 and stored at room temperature	

Table 3-46: 4x Separating gel buffer per 500 ml

Component	Required Amount
Tris	90.75 g
SDS	2 g
Deionized distilled water	added up to 500 ml
pH adjusted to 8.8 and stored at room temperature	

Table 3-47: 10x Electrophoresis buffer per 1 Liter (Stock Solution)

Component	Required Amount
Tris	30 g
99 % Glycine	144 g
Deionized distilled water	added up to 1 Liter
Stored at 4 °C	

Table 3-48: 1x Electrophoresis buffer per 1 Liter (Working Solution)

Component	Required Volume
10x Electrophoresis Buffer stock solution	100 ml
10 % SDS	10 ml
Deionized distilled water	added up to 1 Liter
Stored at 4 °C	

At first, 10 % separating gel mixture was prepared (**Table 3-49**) and poured in a 1.5 mm thick gel chamber. The mixture was covered with a thin layer of 100 % isopropanol to ensure a very straight border between the two types of gels as well as facilitating fast polymerization by blocking oxygen contact. After approximately 30 minutes, the isopropanol was discarded and 4 % stacking gel mixture (**Table 3-49**) was poured on top of the polymerized separating gel. A 1.5 mm comb was then placed to spare for sample wells. After polymerization, the gel chamber was placed in its electrophoresis apparatus provided by Bio-Rad (BIO-RAD, Munich, Germany). The apparatus was filled with 1x electrophoresis buffer and sample wells were further rinsed and cleared by a thin needle using the 1x electrophoresis buffer. For sample loading, 20 µg of prepared protein

samples were heated up for 5 minutes at 95 °C and loaded into respective wells against 7 µl of PageRuler™ Prestained Protein Ladder (Fermentas GmbH, St. Leon-Rot, Germany) to estimate protein size. The protein separation was carried out at 100 volts for approximately 2 hours.

Table 3-49: SDS-PAGE composition (1.5 mm thickness)

Component	Required Volume (10 % Separating Gel)	Required Volume (4 % Stacking Gel)
4x Separating Gel Buffer	2.393 ml	-
4x Stacking Gel Buffer	-	750 µl
Rotiphorese® Gel 30	3.218 ml	450 µl
4 % Ammonium Persulfate solution (APS)	154 µl	60 µl
Tetramethylethylenediamine (TEMED)	8.25 µl	13 µl
Deionized distilled water	3.850 ml	1.75 ml

⇨ *2nd step: Protein transfer*

In order to make the proteins accessible to antibody detection, they were transferred from within the gel onto a Polyvinylidene difluoride (PVDF) membrane (pore size = 0.45 µm) (Millipore GmbH, Schwalbach/Ts., Germany), which was initially activated by 100 % methanol for 10 minutes at room temperature and constant rotation. Meanwhile, stacks of blot paper (BIO-RAD, Munich, Germany) were pre-soaked in chilled transfer buffer (**Table 3-50**). The transfer was conducted in the Trans-Blot® SD Semi-Dry Transfer Cell (BIO-RAD, Munich, Germany) for 2 hours at a constant current of 0.8 mA per cm^2 of PVDF membrane.

Table 3-50: Transfer buffer per 1 Liter

Component	Required Volume
10x Electrophoresis Buffer	100 ml
10 % SDS	10 ml
100 % Methanol	100 ml
Deionized distilled water	added up to 1 Liter
Stored at 4 °C	

⇨ *3rd step: Protein immunostaining and detection*

1x PBS-Tween 20 (1x PBST) (**Table 3-51 and Table 3-52**) was freshly prepared for all necessary washing steps. Following protein transfer, the PVDF membrane was incubated in 10 % non-fat dried milk powder (blocking buffer) (**Table 3-53**) for 1 hour at room temperature with constant shaking. The blocking buffer was used to avoid any unspecific antibody binding to the membrane. The membrane was then incubated with the primary antibody against ERβ (**Table 3-54**) overnight at 4 °C with constant shaking. The next day, the membrane was washed 3 times for 5 minutes each with 1x PBST and antibody-antigen complexes were detected by incubating the membrane with a horseradish peroxidase (HRPO)-conjugated secondary antibody (**Table 3-54**) for 1 hour at room temperature with constant shaking. Afterwards, the membrane was washed 3 times for 5 minutes each with 1x PBST and the ERβ protein was visualized using the Amersham ECL Plus™ Western Blotting Detection System (GE Healthcare, Munich, Germany).

All immunodetection steps were conducted in the dark room. First, the ECL solution (chemiluminescence reagent) was prepared by adding 25 µl of the supplied solution B to 975 µl of the supplied solution A (dilution 1:40, respectively). The PVDF membrane was then incubated in the ECL solution for 5 minutes. Next, the reagent was slowly wiped off and an Amersham ECL Hyperfilm (GE Healthcare, Munich, Germany) was placed on the membrane for 30 minutes exposure time. The film was then (1) placed in developing solution (Kodak, La Hulpe, Belgium), (2) rinsed with deionized distilled water, (3) placed in fixing solution (Kodak, La Hulpe, Belgium) and finally (4) rinsed again with deionized distilled water.

To allow for a second protein detection, the PVDF membrane was briefly rinsed with 1x PBST and the antibody was stripped using a strip buffer (**Table 3-55**). The membrane was incubated in 20 ml strip solution for 30 minutes at 50 °C with constant rotation in the HB-1000 Hybridizer (UVP Ltd., Cambridge, United Kingdom). The membrane was then washed twice in 1x PBST for 10 minutes each with constant shaking, re-activated in 100 % methanol and re-blocked in 10 % blocking buffer for 1 hour at room temperature with constant shaking. The membrane was then incubated for 1 hour at 4 °C with a specific

antibody against the reference protein β-Actin (**Table 3-54**). Antibody-antigen complexes were detected by incubating the membrane with the same abovementioned HRPO-conjugated secondary antibody (**Table 3-54**) for 1 hour at room temperature with constant shaking. Afterwards, the membrane was washed 3 times for 5 minutes each with 1x PBST and the β-Actin protein was visualized using the same aforementioned detection procedure.

Resulting blots were left to dry and pictures were captured under the white light (EpiChemi^3 Benchtop Darkroom, UVP Ltd, Cambridge, UK) and blot images were captured using Labworks™ Image Acquisition and Analysis Software Version 4.6.

Table 3-51: 10x washing stock solution per 1 Liter

Component	Required Amount
Disodium hydrogen phosphate dihydrated	142.4 g
Sodium dihydrogen phosphate monohydrated	27.6 g
Sodium Chloride	5.84 g
Deionized distilled water	added up to 1 Liter
Stored at 4 °C	

Table 3-52: 1x washing working solution (1x PBST) per 1 Liter

Component	Required Volume
10x washing stock solution (**Table 3-51**)	100 ml
Tween® 20	1 ml
Deionized distilled water	added up to 1 Liter
Stored at 4 °C	

Table 3-53: 10 % blocking buffer per 10 ml (Freshly Prepared)

Component	Required Amount
Non-fat dried milk powder	1 g
1x PBST	added up to 10 ml

Table 3-54: Immunodetection antibodies (freshly prepared in 10 % blocking buffer)

Primary Antibody	Host	Dilution	Protein Size
Polyclonal anti ERβ	Rabbit	1:2,000	55 kDa
Polyclonal anti β-Actin	Rabbit	1:4,000	42 kDa
Secondary Antibody	**Host**	**Dilution**	
HRPO-conjugated anti-rabbit IgG	Goat	1:20,000	

Table 3-55: Strip buffer per 200 ml

Component	Required Amount / Volume
Tris	1.51 g
SDS	4 g
Deionized distilled water	180 ml
	pH adjusted to 6.7
β-Mercaptoethanol	1.4 ml
Deionized distilled water	added up to 200 ml
	Stored at room temperature

3.2.8.2. Immunocytochemistry

To confirm the switch of RNDA cellular status from proliferation to differentiation, a protein-based technique was sought to detect the expression of neuronal differentiation markers. By using standard ICC techniques, intracellular markers such as NF-L, NF-M, NF-H and NSE were labeled and visualized in RNDA cells and D-RNDA cells.

RNDA cells were grown to 80 % confluence on autoclaved glass coverslips 18 x 18 mm (DIAGONAL GmbH, Münster, Germany) placed in 6-well cell culture plates. To initiate differentiation, RNDA cells were grown to 80 % confluence on autoclaved glass coverslips 18 x 18 mm placed in 6-well cell culture plates. Cells were then shifted to differentiation conditions (**Table 3-1**). Cells were left to grow under differentiation conditions for four days followed by the addition of 10 µM dibutyryl cyclic AMP for an additional three days to enhance differentiation (White *et al.*, 1994).

On the day of assessment, cells were rinsed twice with PBS (**Table 3-10**) and cell morphology was preserved in pre-warmed 4 % paraformaldehyde solution (**Table 3-56**) for 20 minutes at 37 °C. Following fixation, cells were rinsed twice with PBS and antigenicity was enhanced by incubating the cells in 50 mM ammonium chloride solution freshly prepared from a stock solution of 1 M (**Table 3-57**) for 10 minutes at room temperature. Subsequently, cells were rinsed twice with PBS and permeabilized in cold 0.1 % Triton X-100 freshly prepared from a cold stock solution of 10 % (**Table 3-58**) for 5 minutes at 4 °C to enhance antibody penetration during immunostaining. Prior to immunostaining, cells were rinsed twice with PBS and incubated in 3 % BSA solution (blocking buffer) (**Table 3-59**) for 1 hour at room temperature. For immunostaining, primary antibodies against NF-L, NF-M, NF-H and NSE were freshly prepared in cold 3 % BSA solution (**Table 3-60**). Cells were immunostained for 1 hour at room temperature in a dark humidified chamber. Cells were then rinsed twice with PBS for 5 minutes each and further incubated in 3 % BSA solution for 10 minutes at room temperature. Next, cells were incubated with a secondary antibody carrying the Alexa Flour® dye, a green fluorescent dye. The antibody was also freshly prepared in cold 3 % BSA (**Table 3-61**). Cells were incubated with the secondary antibody for 30 minutes at room temperature in a dark humidified chamber and ultimately rinsed three times with PBS for 5 minutes each and once with deionized distilled water to eliminate excess fluorescent phosphate crystals. Control samples were additionally included to test for antibody specificities by omitting incubation with either the primary or the flourochrome-coupled secondary antibody.

Glass coverslips were inversely mounted on the anti-fade mounting mixture (**Table 3-62**) composed of the anti-fade medium, Mowiol 4-88 (**Table 3-63**) including DAPI (4',6-diamidino-2-phenylindole), which is a fluorescent stain that binds strongly to DNA, hence staining cell nucleus. Coverslips were mounted on DIAGONAL microscopic slides 76 x 26 mm (DIAGONAL GmbH, Münster, Germany). Slides were left to dry in the dark at room temperature overnight. The next day, slides were kept at 4 °C until imaging.

Imaging took place at the BIOTEC Microscope Facility (Biotechnology Centre, TU-Dresden, Dresden, Germany). Cell samples were viewed on a Carl Zeiss Axiovert 200 Imaging Microscopy via the Plan-Apochromat 63x / 1.40 Oil DIC objective. Control samples were

viewed on the same microscope but using the Plan-Apochromat 20x / 0.4 (Ph2). Photographs were captured using the Carl Zeiss Apotome camera (Carl Zeiss, Jena, Germany) and the AxioVert Software Release 4.8.1.

Table 3-56: 4 % (w/v) paraformaldehyde per 50 ml (prepared under a fume hood)

Component	Required Amount / Volume
Paraformaldehyde	2 g
PBS	30 ml
2 - 3 drops of 1 M NaOH was added with constant stirring and heating at 70 °C to clear suspension	
pH was adjusted to 7.4	
PBS	added up to 50 ml
Aliquots were stored at -20 °C	

Table 3-57: 1 M ammonium chloride solution per 50 ml (Stock Solution)

Component	Required Amount
Ammonium Chloride	2.675 g
PBS	added up to 50 ml
Filter sterilized and stored at room temperature	

Table 3-58: 10 % (v/v) Triton X-100 per 50 ml (Stock Solution)

Component	Required Volume
Triton X-100	5 ml
PBS	added up to 50 ml
Stored at 4 °C	

Table 3-59: Blocking buffer 3 % (w/v) BSA per 50 ml

Component	Required Amount
BSA Fraction V	1.5 g
PBS	added up to 50 ml
Filter sterilized and aliquots were stored at -20 °C	

Table 3-60: Primary antibodies used in ICC (freshly prepared in cold 3 % BSA)

Primary Antibodies	Host	Dilution
Monoclonal anti NF-L	Mouse	1:25
Monoclonal anti NF-M	Mouse	1:25
Monoclonal anti NF-H	Mouse	1:25
Monoclonal anti NSE γγ	Mouse	1:25

Table 3-61: Secondary antibody used in ICC (freshly prepared in cold 3 % BSA)

Secondary Antibody	Host	Dilution
Alexa Flour 488 anti-mouse IgG (H + L)	Goat	1:500

Table 3-62: Anti-fade mounting mixture used in ICC per 1 ml

Component	Required Amount
Mowiol 4-88 medium (**Table 3-63**)	996 µl
DAPI	added at a dilution of 1:250
Hint: mixture was not vortexed to avoid bubbles	
Each coverslip required 35 - 40 µl mixture to ensure full coverage on microscopic slides	

Table 3-63: Mowiol 4-88 medium composition

Component	Required Amount / Volume
Glycerol	6 g
Mowiol 4-88 granules (yellow in colour)	2.4 g
Stirred to mix	
Deionized distilled water	6 ml
Stirred for 4 hours at room temperature	
0.2 M Tris (pH 8.5)	12 ml
Heated in a water bath at 50 °C for 10 minutes	
After dissolving, centrifuged at 500 x g for 15 minutes	
Aliquots were stored at -20 °C	

3.2.9. Data Analyses and Statistical Procedures

Unless otherwise stated, all generated data were handled and plotted using Microsoft Office Excel 2003. Arithmetic mean and standard deviation values were calculated from three independent cell culture experiments with independent passage numbers. A paired two-sample *t*-test was applied when data from test groups with a defined standard deviation were compared to a control group bearing no standard deviation. Ultimately, an adapted Student's *t*-test, Welch's *t*-test, was applied when data with unequal variances were compared (Welch, 1938).

3.2.9.1. Analysis of Data Generated from Luciferase Reporter Gene Assays

Within the luciferase reporter gene assays, treatments were performed in triplicates. For each treatment, luciferase bioluminescent activity was calculated in relative luciferase units per amount of protein per well. Values were expressed as arithmetic mean ± standard deviation. Asterisks indicate values differing significantly from the DMSO carrier control treatment (which was always set to 100 %):

*	:	$p \leq 0.05$	:	significant
**	:	$p \leq 0.01$	:	very significant
***	:	$p \leq 0.001$	:	highly significant

Hash signs indicate values differing significantly from the positive control treatment (E2 10 nM):

#	:	$p \leq 0.05$	:	significant
###	:	$p \leq 0.001$	:	highly significant

Plus signs indicate values differing significantly from the 1 µM single dose treatment of the flavonoids:

++	:	$p \leq 0.01$	:	very significant
+++	:	$p \leq 0.001$	:	highly significant

- **Measuring the value of the half maximal effective concentration (EC_{50}):**

The value of EC_{50} refers to the concentration of a given substance that induces a half maximal response following specified exposure duration that finally reaches a plateau. It is commonly used to measure the substance's estrogenic potency (http://www.graphpad.com/curvefit/introduction89.htm).

In this study, the EC_{50} was calculated from the sigmoidal dose-response relationship curve using the statistical software Sigma Plot® Version 9.0. The following steps were conducted to calculate the EC_{50}:

(1) Right click on the curve of interest
(2) Select "Fit Curve". A "Regression Wizard" window will pop-up
(3) For the "Equation Category", select " Standard Curve" from the drop-down menu
(4) For the "Equation Name", select "Four Parameter Logistic Curve". The value of EC_{50} appears after clicking "Next"

3.2.9.2. Analysis of Data Generated from Quantitative Real-Time PCRs

Three independent rat cDNA samples were synthesized from three independent cell culture experiments. Relative gene expression levels of target genes were corrected with the expression of the rat internal reference gene, *Rps-18*. Relative quantification was performed using the ΔΔ cycle threshold ($\Delta\Delta C_T$) calculation method to describe the change of expression of a target gene relative to a reference group by using the C_T-values (Winer *et al.*, 1999; Pfaffl, 2001). In this study and unless otherwise stated, data were either normalized against the DMSO carrier control treatment for RNDA cells or the day 0 sample treated with DMSO for D-RNDA cells. A series of mathematical equations were exploited for data analysis. At first, the difference in average C_T-values for the target gene of interest and the internal reference gene was calculated as follows:

Equation 3-1: $$\Delta C_T = C_T \text{ average}_{\text{target gene}} - C_T \text{ average}_{\text{rat } Rps18}$$

Next, subtraction of the test treatment ΔC_T from the control treatment ΔC_T yielded the ΔΔCT. Since the reaction doubles the amount of product per cycle, the ΔΔCT value was used as the exponent of 2 as shown below:

Equation 3-2: $2^{\Delta\Delta CT} = 2^{(\Delta CT \text{ control treatment} - \Delta CT \text{ test treatment})}$

$2^{\Delta\Delta CT}$ values were expressed as arithmetic mean ± standard deviation of all PCR reactions. For RNDA cells, plus signs indicate values differing significantly from the DMSO carrier control treatment:

+	:	$p \leq 0.05$	:	significant
++	:	$p \leq 0.01$	:	very significant
+++	:	$p \leq 0.001$	:	highly significant

For D-RNDA cells, asterisks indicate values differing significantly from the day 1 differentiated sample treated with DMSO. In addition, hash sign indicates values differing significantly from the day 4 differentiated sample treated with DMSO:

*	:	$p \leq 0.05$	:	significant
**	:	$p \leq 0.01$	:	very significant
#	:	$p \leq 0.05$	:	significant

4. RESULTS

4.1. Transduction Efficiency and Generation of RNDA Cells

The efficiency of viral transduction was determined from the percentage of target cells expressing EGFP using standard flow cytometry techniques due to the fact that p6NST50 and p6NST50 + ERβ lentiviral vectors encode EGFP as a reporter gene (**Figure 3-1 and Figure 3-2**). Two different viral stock dilutions (either UD or 1:10 diluted) were used to transduce RN46A-B14 cells as well as the reference control cell line HT-1080 (**Section 3.2.3.3**). As depicted in **Figure 4-1**, the resulting red dot density FACS charts represent percentage of either HT-1080 or RN46A-B14 cells expressing EGFP as compared to their untransduced counterparts.

Region 2 (R2) of each FACS chart in **Figure 4-1** was set to distinguish or "gate" the flow of the EGFP-expressing cells from the heterogeneous cell population. Hence, the efficiency of viral transduction was determined from the percentage of gated cells in Region 2 (R2) (signifying the percentage of cells expressing EGFP). After 72 hours of viral transduction, transduction of HT-1080 cells revealed that both lentiviral particles (i.e. p6NST50 and p6NST50 + ERβ) were infectious with efficacies reaching almost 93 % (**Figure 4-1, Panel A**). RN46A-B14 cells were generally transduced but with a relatively reduced efficacy if compared to HT-1080 cells (**Figure 4-1, Panel B**).

There was no difference in the percentage of RN46A-B14 cells transduced with either the undiluted p6NST50 or 1:10 diluted p6NST50 viral particles (67.32 % vs. 68.12 %, respectively). An obvious difference was only noticed when RN46A-B14 cells were transduced with the viral vector encoding the ERβ, where the percentage of RN46A-B14 cells transduced with 1:10 diluted p6NST50 + ERβ was 3.8-fold higher than the percentage of cells transduced with undiluted p6NST50 + ERβ (24.48 % vs. 6.39 %, respectively). Accordingly, RN46A-B14 cells transduced with the 1:10 diluted lentiviral particles were considered for this study. The cells were then propagated using the medium of untransduced RN46A-B14 cells but containing 60 µg/ml Zeocin™ (**Table 3-1**), as deduced from the Zeocin™ kill-curve (**Section 3.2.3.1**).

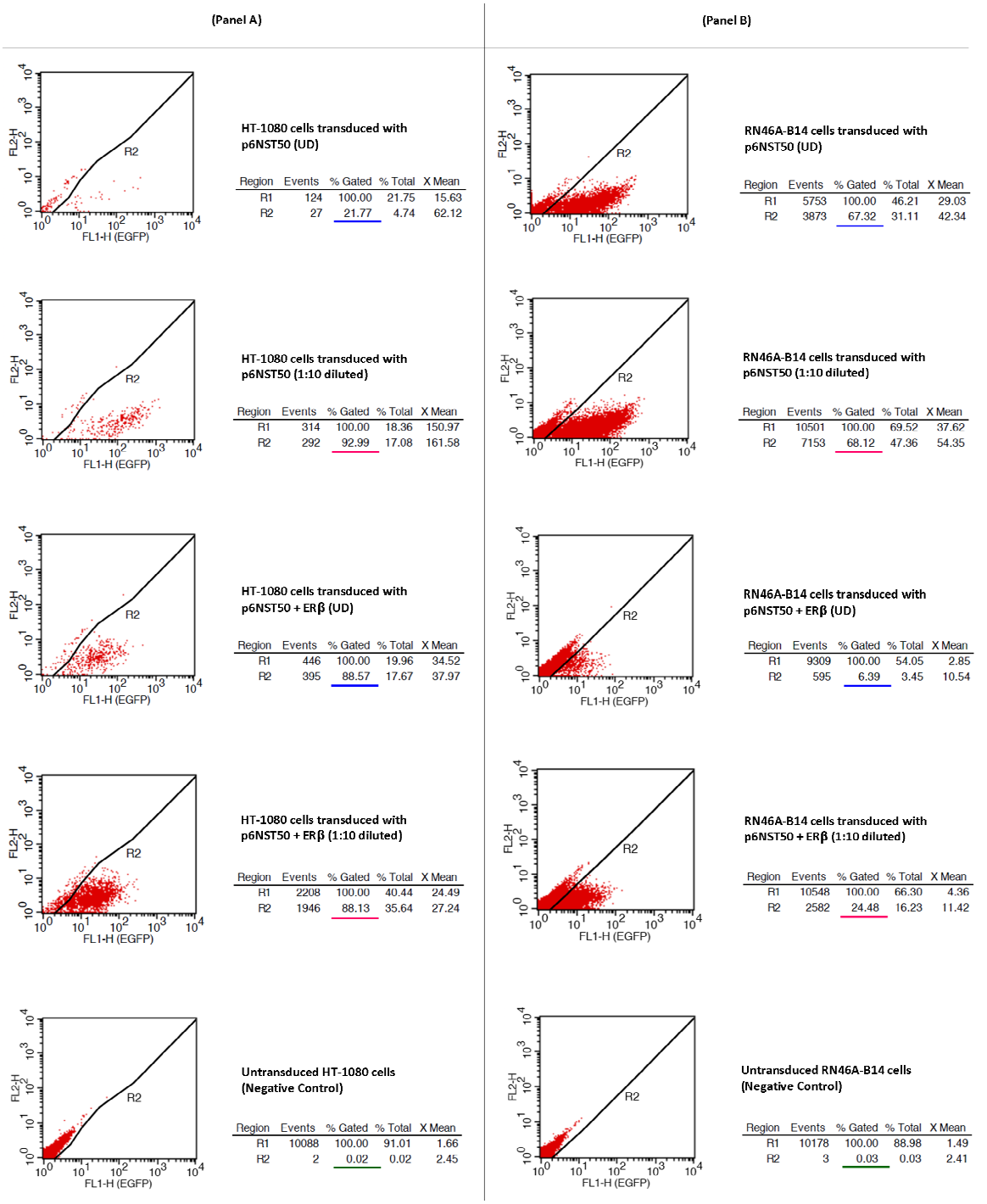

Region	Events	% Gated	% Total	X Mean
R1	124	100.00	21.75	15.63
R2	27	21.77	4.74	62.12

Region	Events	% Gated	% Total	X Mean
R1	5753	100.00	46.21	29.03
R2	3873	67.32	31.11	42.34

Region	Events	% Gated	% Total	X Mean
R1	314	100.00	18.36	150.97
R2	292	92.99	17.08	161.58

Region	Events	% Gated	% Total	X Mean
R1	10501	100.00	69.52	37.62
R2	7153	68.12	47.36	54.35

Region	Events	% Gated	% Total	X Mean
R1	446	100.00	19.96	34.52
R2	395	88.57	17.67	37.97

Region	Events	% Gated	% Total	X Mean
R1	9309	100.00	54.05	2.85
R2	595	6.39	3.45	10.54

Region	Events	% Gated	% Total	X Mean
R1	2208	100.00	40.44	24.49
R2	1946	88.13	35.64	27.24

Region	Events	% Gated	% Total	X Mean
R1	10548	100.00	66.30	4.36
R2	2582	24.48	16.23	11.42

Region	Events	% Gated	% Total	X Mean
R1	10088	100.00	91.01	1.66
R2	2	0.02	0.02	2.45

Region	Events	% Gated	% Total	X Mean
R1	10178	100.00	88.98	1.49
R2	3	0.03	0.03	2.41

Figure 4-1: Red dot density FACS charts representing the efficiency of lentiviral transduction by determining the percentage of HT-1080 cells or RN46A-B14 cells expressing the reporter gene EGFP as compared to their untransduced counterparts. Cells were harvested 72 hours after transduction. EGFP is detected by the FL1 sensor (assigned to the x-axis). All other scattered light is detected by the FL2 sensor (assigned to the y-axis). Transduced cells expressing EGFP are gated in Region 2. The percentage of cells expressing EGFP is denoted by a coloured underline. **(Panel A)** transduction analysis of the reference control cell line HT-1080 cells incubated with undiluted or 1:10 diluted lentiviral particles and **(Panel B)** transduction analysis of RN46A-B14 cells incubated with undiluted or 1:10 diluted lentiviral particles.

Subsequently, supernatants of cultured transduced RN46A-B14 cells were tested for the absence of infectious viral particles. The purpose of this step was to ensure the safe transfer of the transduced cells from Biosafety Level 2 to Biosafety Level 1. Cell-free supernatants were harvested and checked for any EGFP expression using standard flow cytometry techniques (**Section 3.2.3.3**). As depicted in **Figure 4-2**, supernatants harvested from cultured RN46A-B14 cells transduced with 1:10 diluted p6NST50 (**Figure 4-2 A**) or 1:10 diluted p6NST50 + ERβ (**Figure 4-2 B**) was devoid of any cells expressing EGFP (0.00 %) as compared to supernatants harvested from cultured untransduced RN46A-B14 cells (0.01 %) (**Figure 4-2 C**). Therefore, this indicated that cultured transduced RN46A-B14 cells do not produce any further infectious lentiviral particles in their supernatants. Thus, cells were successfully and safely downgraded from Biosafety Level 2 to Biosafety Level 1 and the newly generated RN46A-B14 cells transduced with 1:10 diluted p6NST50 + ERβ were given the new notation, RNDA cells.

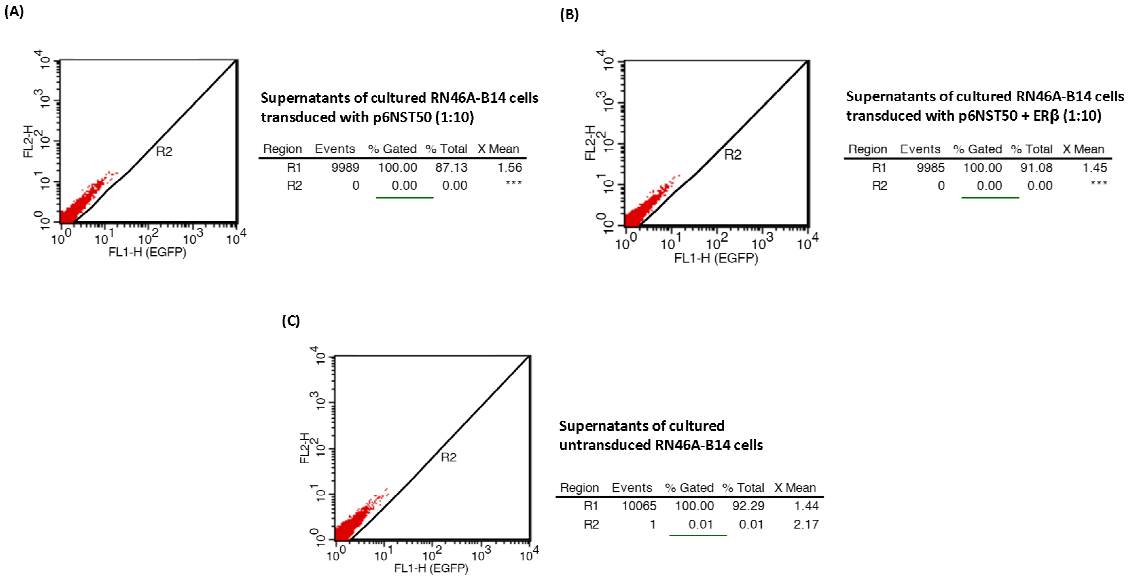

Figure 4-2: Red dot density FACS charts representing the absence of infectious lentiviral particles in supernatants of cultured RN46A-B14 cells transduced with 1:10 diluted lentiviral vectors. EGFP is detected by the FL1 sensor (assigned to the x-axis). All other scattered light is detected by the FL2 sensor (assigned to the y-axis). Transduced cells expressing EGFP are gated in Region 2. Absence of infectious lentiviral particles in the supernatants were determined by the absence of cells expressing EGFP; values denoted by a green underline. **(A)** analysis of cell-free supernatants of cultured RN46A-B14 cells transduced with 1:10 diluted p6NST50, **(B)** analysis of cell-free supernatants of cultured RN46A-B14 cells transduced with 1:10 diluted p6NST50 + ERβ and **(C)** analysis of cell-free supernatants of cultured untransduced RN46A-B14 cells.

4.2. Successful Transcription and Translation of Transgenic Human *ESR2* in RNDA Cells

As previously mentioned, the reason for cloning and stably integrating human *ESR2* instead of a rat *Esr2* in the studied rat cell model was due to two reasons: (1) availability of human *ESR2* DNA fragment in the lab and (2) human ERβ shows approximately 89% identity in its translated region to the rat ERβ as compared to any other mammalian ERβ (Enmark and Gustafsson, 1999). Using the first passage number of the newly generated RNDA cells, successful transcription of the transgenic human *ESR2* was verified by quantitative real-time PCR using its specified primer sequences and PCR conditions (**Table 3-37 and Table 3-40**). As depicted from the 1 % agarose gel in **Figure 4-3 A**, amplified human *ESR2* cDNA with an amplicon size of 153 bp was successfully detected in RNDA cells (**Figure 4-3 A, Lane 2**) as opposed to RN46A-B14 cells transduced with p6NST50 (**Figure 4-3 A, Lane 1**) or untransduced RN46A-B14 cells (**Figure 4-3 A, Lane 3**).

Following the transcription analysis of the transgenic human *ESR2*, successful translation of human ERβ was verified using Western blot techniques. From RNDA cell protein extracts, an ERβ-immunoreactive band was detected at 55 kDa (**Figure 4-3 B, Lane 3**) as opposed to protein extracts from untransduced RN46A-B14 cells (**Figure 4-3 B, Lane 1**) or protein extracts from RN46A-B14 cells transduced with p6NST50 (**Figure 4-3 B, Lane 2**).

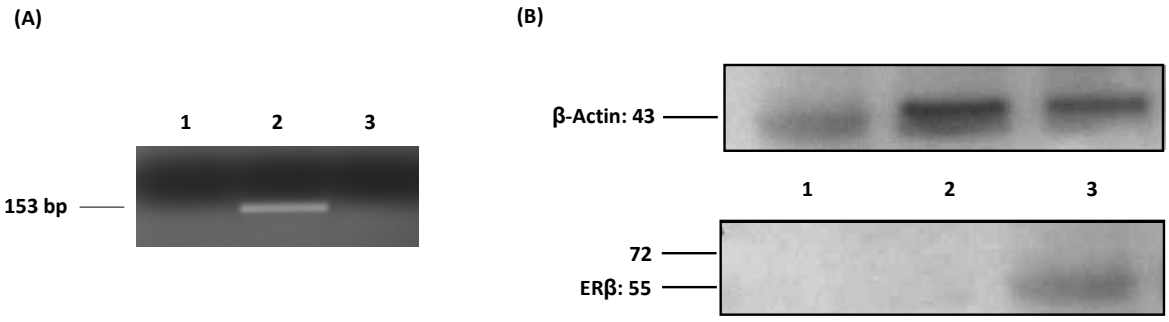

Figure 4-3: Verification of successful transcription and translation of transgenic human *ESR2* in RNDA cells. (A) A 1% agarose gel depicting the correct amplicon size of an amplified cDNA of transgenic human *ESR2* in RNDA cells (Lane 2) as opposed to RN46A-B14 cells transduced with p6NST50 (Lane 1) or untransduced RN46A-B14 cells (Lane 3), **(B)** An immunoblot verifying protein expression of transgenic human ERβ against the reference protein (β-Actin) in RNDA cells (Lane 3) as opposed to untransduced RN46A-B14 cells (Lane 1) or RN46A-B14 cells transduced with p6NST50 (Lane 2). Molecular mass of protein ladder (Fermentas, St. Leon-Rot, Germany) are indicated in kDa.

4.3. Functional Characterization of Transgenic Human ERβ in RNDA Cells

Following the validation of successful transcription and translation of the transgenic human *ESR2* in RNDA cells, luciferase reporter gene assays (**Section 3.2.4**) were utilized to determine whether the transgenic human ERβ is functional for downstream investigations of estrogen-dependent activities. Accordingly, transient transfection assays with the firefly luciferase regulated by a double ERE as an estrogen-responsive reporter gene were employed in RNDA cells (**Figure 3-4**).

The ability of increasing concentrations of E2 (100 fM - 100 nM) to evoke a specific response in RNDA cells was initially investigated. Results revealed a significant sigmoidal dose-response relationship in luciferase expression following E2 treatment (**Figure 4-4 A**). From this concentration-dependent regression curve and by using the statistical software Sigma Plot® Version 9.0, the EC_{50} of E2 was calculated to be 4.0×10^{-10} M (**Section 3.2.9.1**). Moreover, the maximum response evoked by E2 was at a concentration of 10 nM. This concentration was further used in all subsequent experiments as the standard positive control treatment.

As depicted in **Figure 4-4 B**, a highly significant increase in luciferase output was noticed in RNDA cells as opposed to the untransduced RN46A-B14 cells in response to 10 nM E2 treatment. Proof of excluding non-specific transgenic ERβ effects was further scrutinized where a highly significant increase in luciferase activity was observed in RNDA cells following 10 nM E2 treatment as opposed to the RN46A-B14 cells transduced with p6NST50 only (**Figure 4-4 C**). Additionally, the specific transcriptional activation of luciferase via the transgenic human ERβ was demonstrated by treating RNDA cells with increasing concentrations (1 nM - 1 μM) of Diarylproprionitril (the selective ERβ agonist) or Propyl pyrazole triol (the selective ERα agonist). RNDA cells significantly responded in a concentration-dependent manner to Diarylproprionitril (**Figure 4-4 D**) but not to Propyl pyrazole triol (**Figure 4-4 E**).

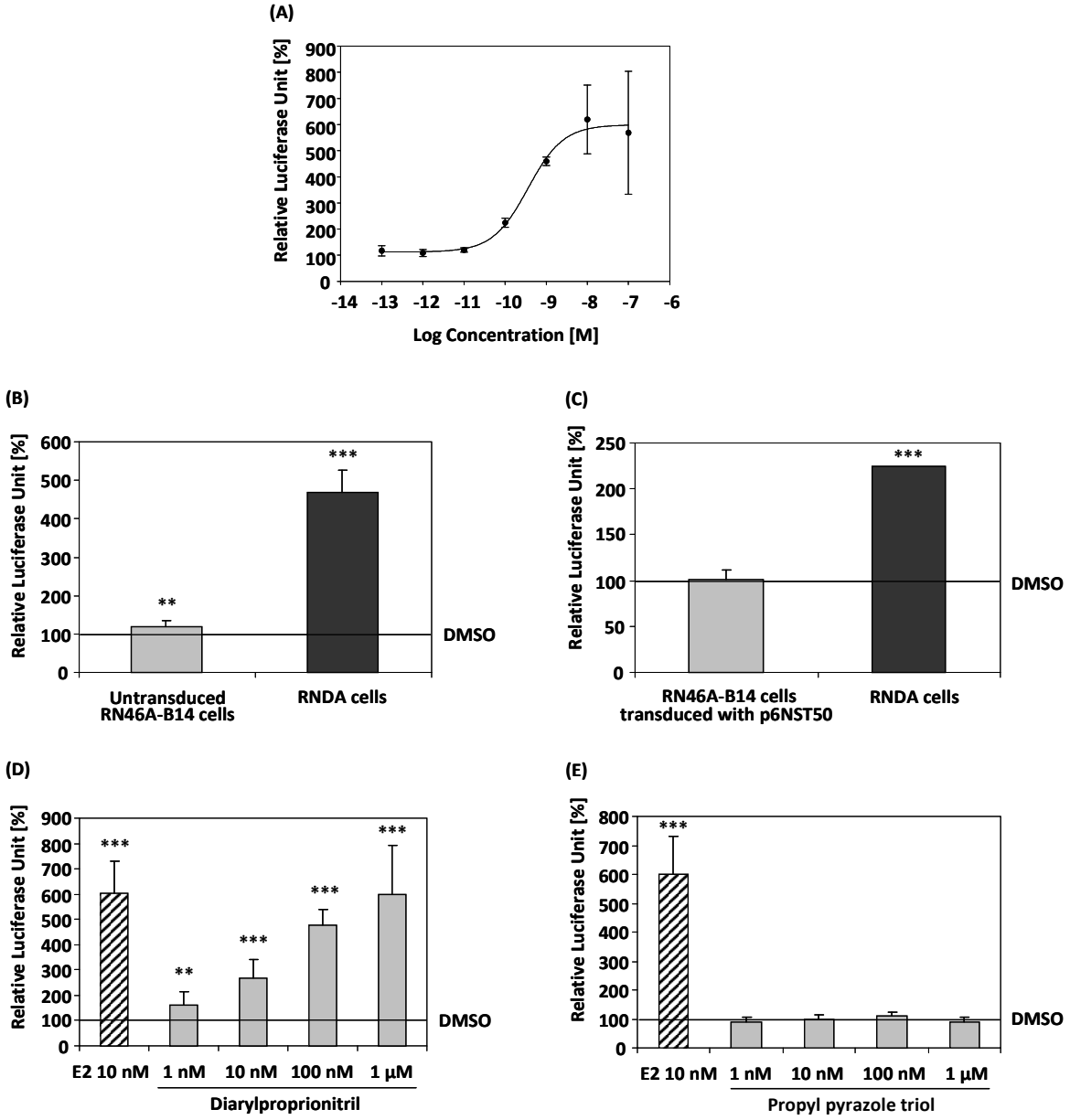

Figure 4-4: Transgenic human ERβ is functional in RNDA cells by inducing significant luciferase activity. Normalized luciferase output observed in RNDA cells in response to **(A)** increasing concentrations of E2 (100 fM - 100 nM), **(B)** 10 nM E2 as opposed to untransduced RN46A-B14 cells, **(C)** 10 nM E2 as opposed to RN46A-B14 cells transduced with p6NST50, **(D)** increasing concentrations (1 nM - 1µM) of the selective ERβ agonist (Diarylproprionitril) and **(E)** increasing concentrations (1 nM - 1µM) of the selective ERα agonist (Propyl pyrazole triol). The luciferase output in response to DMSO treatment is represented by a black horizontal line set to 100 %. Effects differ significantly from DMSO treatment: ** $p \leq 0.01$ and *** $p \leq 0.001$.

4.4. Transactivational Activity of Flavonoids in RNDA Cells

Following the verification of stable integration of transgenic human *ESR2* in RNDA cells and the significant functional activity of the transgenic human ERβ in RNDA cells, the

transactivational activity of the flavonoids on the transgenic ERβ was initially investigated in same studied cell line. These substances are sold as medicinal plant remedies or as dietary supplements and have reached quite remarkable market shares. Nevertheless, sufficient data regarding their activity as well as their efficacy and safety in different body organs, including the raphe nuclei region of the brain, remains to be unavailable.

In this study, seven different flavonoids were tested for their transactivational activity on ERβ in the newly established RNDA cell model using the luciferase reporter gene assay. First, RNDA cells were treated with increasing concentrations of the three isoflavones: Genistein, Daidzein and Equol. RNDA cells were also treated with increasing concentrations of the second tested group of flavonoids, namely the naringenin-type flavanones. These include Naringenin, 8-Prenylnaringenin, 7-(O-prenyl)naringenin-4'-acetate and 6-(1,1-Dimethylallyl)naringenin.

4.4.1. Transactivational Activity of Isoflavones in RNDA Cells

RNDA cells were treated with increasing concentrations of the isoflavones (10 nM - 10 µM). A co-treatment of 1 µM of each isoflavone with either 500 nM Fulvestrant or the effective dose of E2 (10 nM) was further tested in RNDA cells (**Section 3.2.4.3**).

As depicted in all panels of **Figure 4-5**, a highly significant luciferase output was noticed in RNDA cells following 10 nM E2 treatment as compared to the DMSO treatment (black horizontal line set to 100 %). This high significant luciferase output was also noticed in a concentration-dependent manner starting at the lowest concentration of 10 nM when cells were treated with increasing concentrations of Genistein, Daidzein or Equol as compared to the DMSO treatment (**Figure 4-5 A, B and C**). Additionally, a co-treatment of Genistein, Daidzein or Equol with Fulvestrant completely antagonized effects elicited by 1 µM of each isoflavone; indicating that all three substances act by binding to and activating the transgenic ERβ. Moreover, additional significant effects were observed in RNDA cells in response to a co-treatment of 10 nM 17β-Estradiol with 1 µM of either Genistein or Daidzein, but not Equol, if compared to the E2 single-dose treatment (**Figure 4-5 A, B and C**). Based on the tested doses of the isoflavones in this study

(i.e. 10 nM - 10 µM), calculation of the EC_{50} was not possible mathematically due to the fact that the data do not fit in sigmoidal dose-response relationship, where a plateau does not seem to be reached at 10 µM.

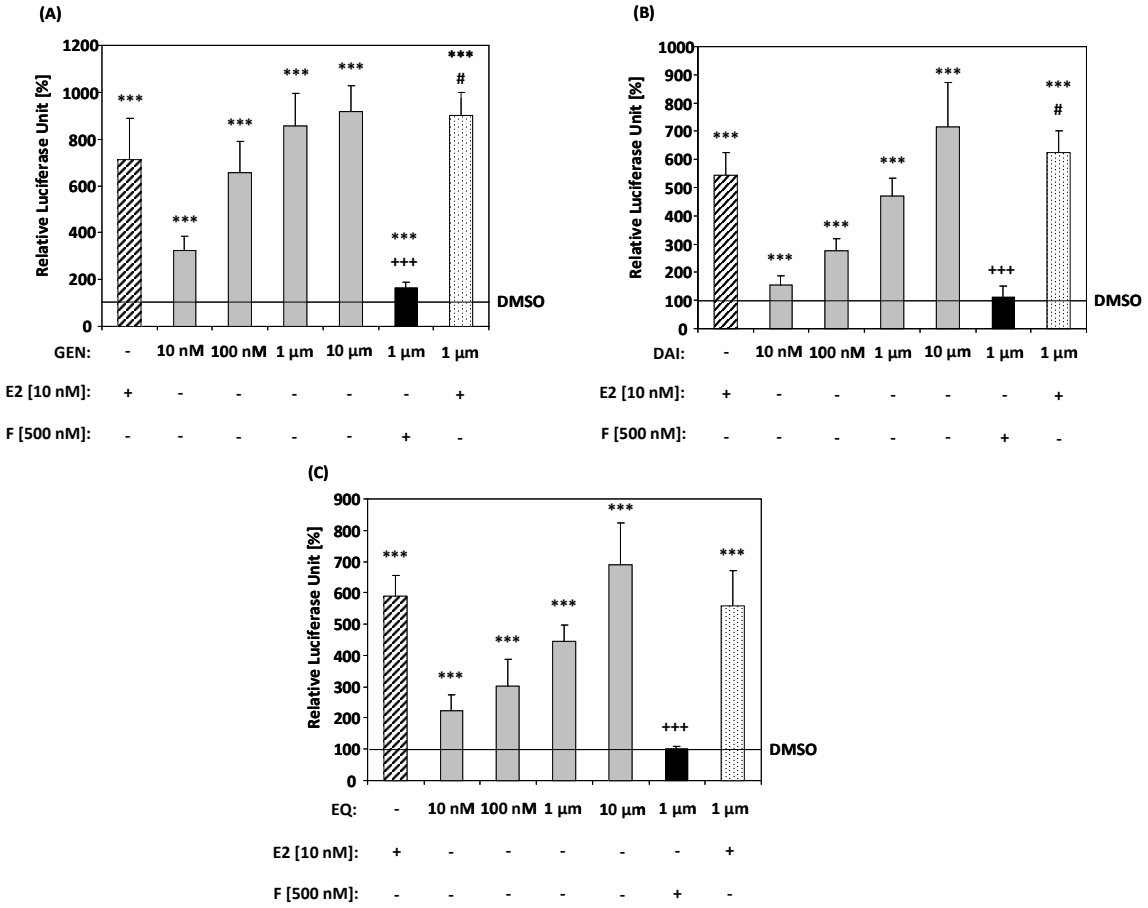

Figure 4-5: Effect of isoflavones on luciferase activity in RNDA cells. Normalized luciferase output observed in RNDA cells in response to **(A)** increasing concentrations of Genistein or co-treatment of 1 µM Genistein with either 500 nM Fulvestrant or 10 nM E2, **(B)** increasing concentrations of Daidzein or co-treatment of 1 µM Daidzein with either 500 nM Fulvestrant or 10 nM E2 and **(C)** increasing concentrations of Equol or co-treatment of 1 µM Equol with either 500 nM Fulvestrant or 10 nM E2. The luciferase output in response to DMSO treatment is represented by a black horizontal line set to 100 %. Effects differ significantly from either DMSO treatment: *** $p \leq 0.001$, E2 single-dose treatment: # $p \leq 0.05$ or 1 µM single-dose treatment of the isoflavone: +++ $p \leq 0.001$.

4.4.2. Transactivational Activity of Naringenin-type Flavanones in RNDA Cells

RNDA cells were treated with increasing concentrations of the naringenin-type flavanones (10 nM - 10 µM). A co-treatment of 1 µM of each with either 500 nM Fulvestrant or the effective dose of E2 (10 nM) was further tested (**Section 3.2.4.3**).

As illustrated in all panels of **Figure 4-6**, a highly significant luciferase output was noticed in RNDA cells following 10 nM E2 treatment as compared to the DMSO treatment (black horizontal line set to 100 %). This significant luciferase output was also noticed in a concentration-dependent manner starting at a concentration of 100 nM when cells were treated with increasing concentrations of Naringenin as compared to the DMSO treatment (**Figure 4-6 A**). Moreover, a co-treatment with Fulvestrant completely antagonized effects elicited by 1 µM Naringenin, indicating that Naringenin acts by binding to and activating the transgenic ERβ. However, no significant additional effects were noticed when RNDA cells were co-treated with 10 nM 17β-Estradiol and 1 µM Naringenin if compared to the E2 single-dose treatment.

A similar pattern was noticed in response to 8-Prenylnaringenin (**Figure 4-6 B**), where a highly significant increase in luciferase output was displayed in a concentration-dependent manner starting at a concentration of 100 nM as compared to the DMSO treatment. As expected, co-treatment with Fulvestrant completely antagonized effects elicited by 1 µM 8-Prenylnaringenin, indicating that 8-Prenylnaringenin also acts by binding to and activating the transgenic ERβ. In contrast to the parent molecule Naringenin, 1 µM 8-Prenylnaringenin was able to significantly antagonize effects elicited by 10 nM E2 if compared to the E2 single-dose treatment.

As depicted in **Figure 4-6 C**, only the high concentrations of 7-(O-prenyl)naringenin-4'-acetate (1 µM and 10 µM) caused a highly significant increase in luciferase output in RNDA cells as compared to the DMSO treatment. Co-treatment with Fulvestrant completely antagonized effects elicited by 1 µM 7-(O-prenyl)naringenin-4'-acetate, which again indicates that 7-(O-prenyl)naringenin-4'-acetate also acts by binding to and activating the transgenic ERβ. Similar to 8-Prenylnaringenin, 1 µM 7-(O-prenyl)naringenin-4'-acetate was also able to significantly antagonize effects elicited by 10 nM E2 if compared to the E2 single-dose treatment.

In contrast to the abovementioned naringenin-type flavanones, no significant luciferase activity was detected in RNDA cells in response to increasing concentrations of 6-(1,1-Dimethylallyl)naringenin (**Figure 4-6 D**). Moreover, co-treatment with either

500 nM Fulvestrant or 10 nM E2 did not reveal any significant change in luciferase output if compared to the single-dose treatment of either the substance or E2, respectively. Once again, based on the tested doses of the naringenin-type flavanones in this study (i.e. 10 nM – 10 µM), calculation of the EC_{50} was not possible mathematically due to the fact that the data do not fit in sigmoidal dose-response relationship, where a plateau does not seem to be reached at 10 µM.

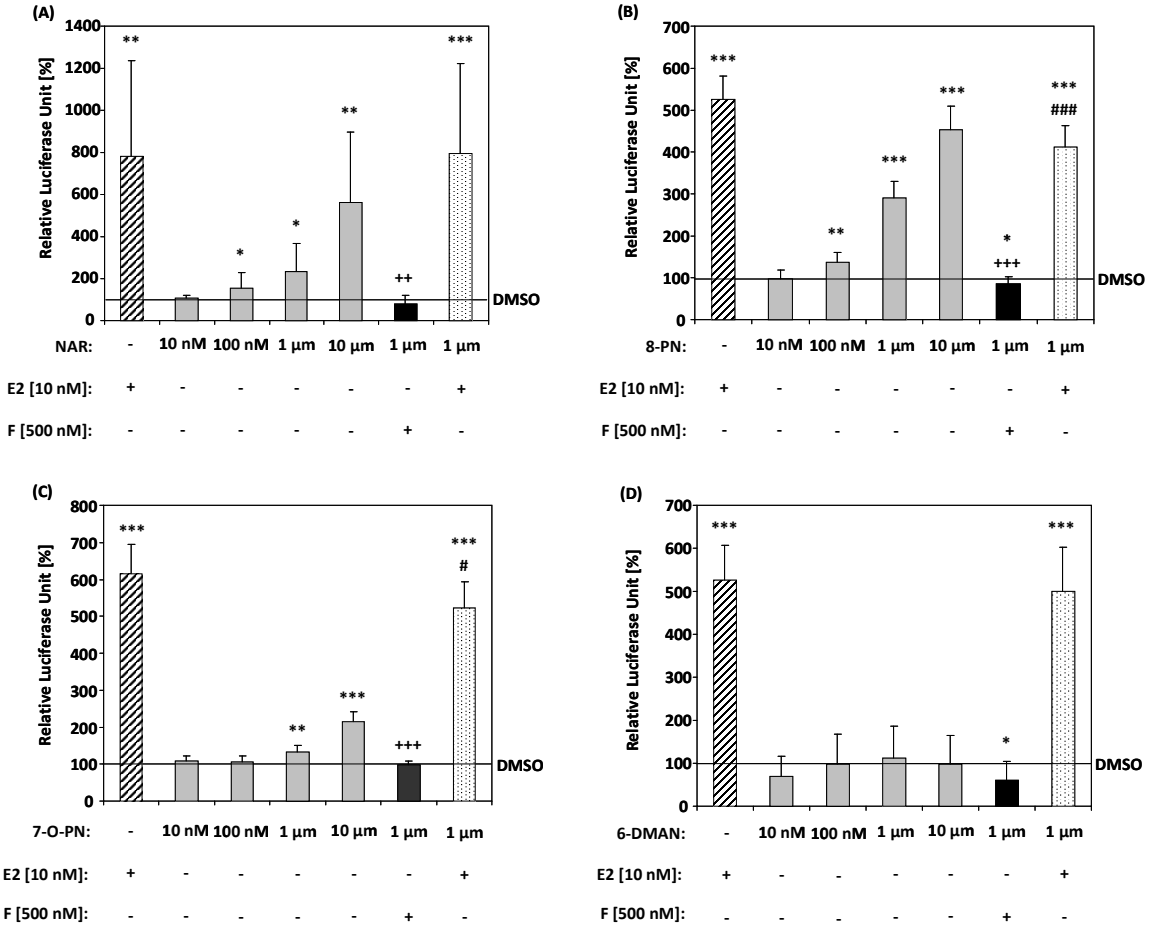

Figure 4-6: Effect of naringenin-type flavanones on luciferase activity in RNDA cells. Normalized luciferase output observed in RNDA cells in response to **(A)** increasing concentrations of Naringenin or co-treatment of 1 µM Naringenin with either 500 nM Fulvestrant or 10 nM E2, **(B)** increasing concentrations of 8-Prenylnaringenin or co-treatment of 1 µM 8-Prenylnaringenin with either 500 nM Fulvestrant or 10 nM E2, **(C)** increasing concentrations of 7-(O-prenyl)naringenin-4'-acetate or co-treatment of 1 µM 7-(O-prenyl)naringenin-4'-acetate with either 500 nM Fulvestrant or 10 nM E2 and **(D)** increasing concentrations of 6-(1,1-Dimethylallyl)naringenin or co-treatment of 1 µM 6-(1,1-Dimethylallyl)naringenin with either 500 nM Fulvestrant or 10 nM E2. The luciferase output in response to DMSO treatment is represented by a black horizontal line set to 100 %. Effects differ significantly from either DMSO treatment: * $p \leq 0.05$, ** $p \leq 0.01$ and *** $p \leq 0.001$, E2 single-dose treatment: # $p \leq 0.05$ and ### $p \leq 0.001$ or 1 µM single-dose treatment of the naringenin-type flavanone: ++ $p \leq 0.01$ and +++ $p \leq 0.001$.

4.5. Gene Expression Profiling Using Microarray Analysis

Following the evaluation of the transactivational activity of the flavonoids on the transgenic ERβ in RNDA cells using luciferase reporter gene assays (**Section 4.4**), it was of interest to evaluate the potential of flavonoids to regulate endogenous gene expression of estrogen responsive genes in RNDA cells as compared to regulation patterns in response to 17β-Estradiol. Accordingly, a closer view on the E2-dependent changes in the expression of the whole rat transcriptome in RNDA cells was initially mapped using a DNA microarray technique (**Section 3.2.6**). A total of 40,000 transcripts were identified in RNDA cells following DMSO and E2 treatments. From this data set, the list of transcripts that showed at least two-fold change of expression in response to DMSO and E2 treatment was selected. This list includes a total of 212 regulated transcripts; of which 64 are down-regulated (**Appendix 7-4**) and 148 are up-regulated (**Appendix 7-5**) in response to E2 treatment.

4.6. Gene Expression Validation Using Quantitative Real-Time PCR

From a total of 212 estrogen regulated transcripts with at least two-fold change of expression, six genes were selected according to specific features of estrogenic regulation of expression. Camello-like 5 (*Cml-5*), sex determining region Y-box 18 (*Sox-18*) and keratin type I cytoskeletal 19 (*Krt-19*) were selected for their highest fold-change in response to E2 treatment. Neurofilament medium polypeptide (*Nefm*) and zinc finger, DHHC-type containing 2 (*Zdhhc-2*) were chosen because of their high basal expression in response to E2 treatment. Solute carrier family 6 member 4 (*Slc6a4*) was selected for its functional relevance in this serotonergic cell line as it encodes the serotonin re-uptake transporter. The DNA microarray outcome of all six genes was validated using quantitative real-time PCR.

As depicted in **Figure 4-7 A**, *Cml-5* (73.92 ± 71.95 fold), *Sox-18* (16.04 ± 11.49 fold) and *Krt-19* (7.56 ± 7.87 fold) were significantly and highly up-regulated in RNDA cells following E2 treatment. *Nefm* (0.30 ± 0.09 fold) and *Zdhhc-2* (0.42 ± 0.14 fold) were significantly down-regulated in RNDA cells in response to E2 treatment (**Figure 4-7 B**). No significant regulation was observed for *Slc6a4* mRNA following E2 treatment (**Figure 4-7 B**).

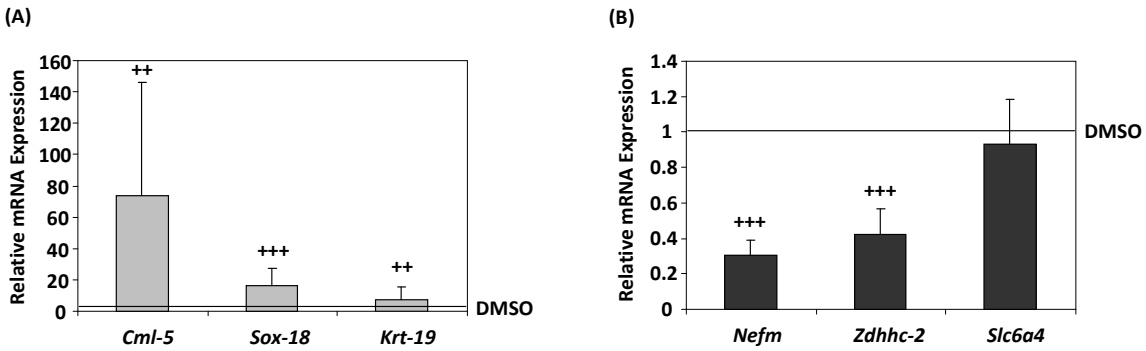

Figure 4-7: Validation of expression of six selected E2-regulated genes in RNDA cells using quantitative real-time PCR. Six genes were selected from the microarray according to specific features of estrogenic regulation of expression. Cells were treated with either 0.1 % DMSO (carrier control treatment) or 10 nM E2 (positive control treatment) for 24 hours prior to RNA isolation. **(A)** up-regulated genes in response to E2 treatment and **(B)** down-regulated genes in response to E2 treatment. Expression in response to DMSO treatment is represented by a black horizontal line set to 1. Data are normalized against the DMSO treatment. Plus signs indicate significance from DMSO treatment: ++ $p \leq 0.01$ and +++ $p \leq 0.001$.

4.7. Effect of Flavonoids on the Regulation of mRNA Expression of Estrogen-Responsive Genes in RNDA Cells

Following the identification and validation of expression of the six selected E2-regulated genes in RNDA cells (**Section 4.5 and Section 4.6**), the potential of flavonoids to regulate endogenous gene expression of the six selected estrogen responsive genes in RNDA cells was then investigated as compared to regulation patterns in response to 17β-Estradiol. Cells were treated for 24 hours prior to RNA isolation with 0.1 % DMSO, 10 nM E2 or 10 µM of each of the flavonoids (**Section 3.2.7.1**). It is important to note that out of all the tested seven flavonoids in the present study, 7-(O-prenyl)naringenin-4'-acetate was excluded from these set of experiments regarding gene expression analyses because it exhibited low activity on downstream transactivational pathways in RNDA cells (**Figure 4-6 C**) and due to the fact that it is not yet known to be present in medicinal plant extracts and food items including dietary supplements with respective health claims.

There was no basal *Cml-5* mRNA expression detectable in these sets of experiments, hence expression in response to DMSO treatment is represented by a red horizontal line set to 0 (**Figure 4-8 A**). *Cml-5* mRNA expression was clearly detectable following E2 treatment. Thus, values of *Cml-5* mRNA expression were normalized against the E2

treatment, yet significance of effects was calculated as compared to the DMSO treatment. Apart from the null regulation of *Cml-5* mRNA expression in response to either Naringenin or 6-(1,1-Dimethylallyl)naringenin treatment in RNDA cells, *Cml-5* mRNA was shown to be up-regulated in response to all the other tested substances, however significance of effects was only reached in response to E2, 8-Prenylnaringenin and Genistein as compared to the DMSO treatment (**Figure 4-8 A**).

In all remaining panels of **Figure 4-8** described hereafter, mRNA expression of the remaining genes was detectable in response to DMSO treatment. Thus, data were normalized against the DMSO treatment (black horizontal line set to 1). In **Figure 4-8 B**, a strong up-regulation of *Sox-18* mRNA was observed in response to E2 (35.16 ± 20.96 fold) as compared to the DMSO treatment (black horizontal line set to 1), although this was statistically not significant. However, significant effects were measured in response to 8-Prenylnaringenin (55.72 ± 12.04 fold), Genistein (48.21 ± 9.42 fold), Daidzein (29.11 ± 1.31 fold) and Equol (54.81 ± 18.50 fold) as compared to the DMSO treatment. Again, no change in regulation of *Sox-18* mRNA was observed in response to either Naringenin or 6-(1,1-Dimethylallyl)naringenin treatment in RNDA cells.

As represented in **Figure 4-8 C**, *Krt-19* mRNA was significantly and highly up-regulated in response to E2 (11.82 ± 0.53 fold), 8-Prenylnaringenin (9.11 ± 1.42 fold), Genistein (13.18 ± 0.72 fold), Daidzein (8.02 ± 0.33 fold) and Equol (8.55 ± 0.54 fold) as compared to the DMSO treatment (black horizontal line set to 1). Yet, no change in mRNA regulation was detected in response to either Naringenin or 6-(1,1-Dimethylallyl)naringenin as compared to the DMSO treatment.

As shown in **Figure 4-8 D**, *Nefm* mRNA was shown to be down-regulated in response to all tested substances, however significance of effects was only reached in response to E2 (0.42 ± 0.19 fold), 8-Prenylnaringenin (0.57 ± 0.06 fold), Genistein (0.36 ± 0.05 fold), Daidzein (0.38 ± 0.14 fold) and Equol (0.52 ± 0.02 fold) as compared to the DMSO treatment (black horizontal line set to 1).

Zdhhc-2 mRNA expression level (**Figure 4-8 E**) was significantly down-regulated in response to E2 (0.71 ± 0.09 fold), 8-Prenylnaringenin (0.68 ± 0.05 fold), Naringenin (0.74 ± 0.05 fold), Genistein (0.67 ± 0.03 fold), Daidzein (0.75 ± 0.01 fold) and Equol

(0.74 ± 0.02 fold) as compared to the DMSO treatment (black horizontal line set to 1). In contrast to the regulation of mRNA expression of the abovementioned genes in response to E2 or the flavonoids, **Figure 4-8 F** shows no significant regulation of *Slc6a4* mRNA expression in RNDA cells in response to either E2 or the flavonoids as compared to the DMSO control treatment (black horizontal line set to 1).

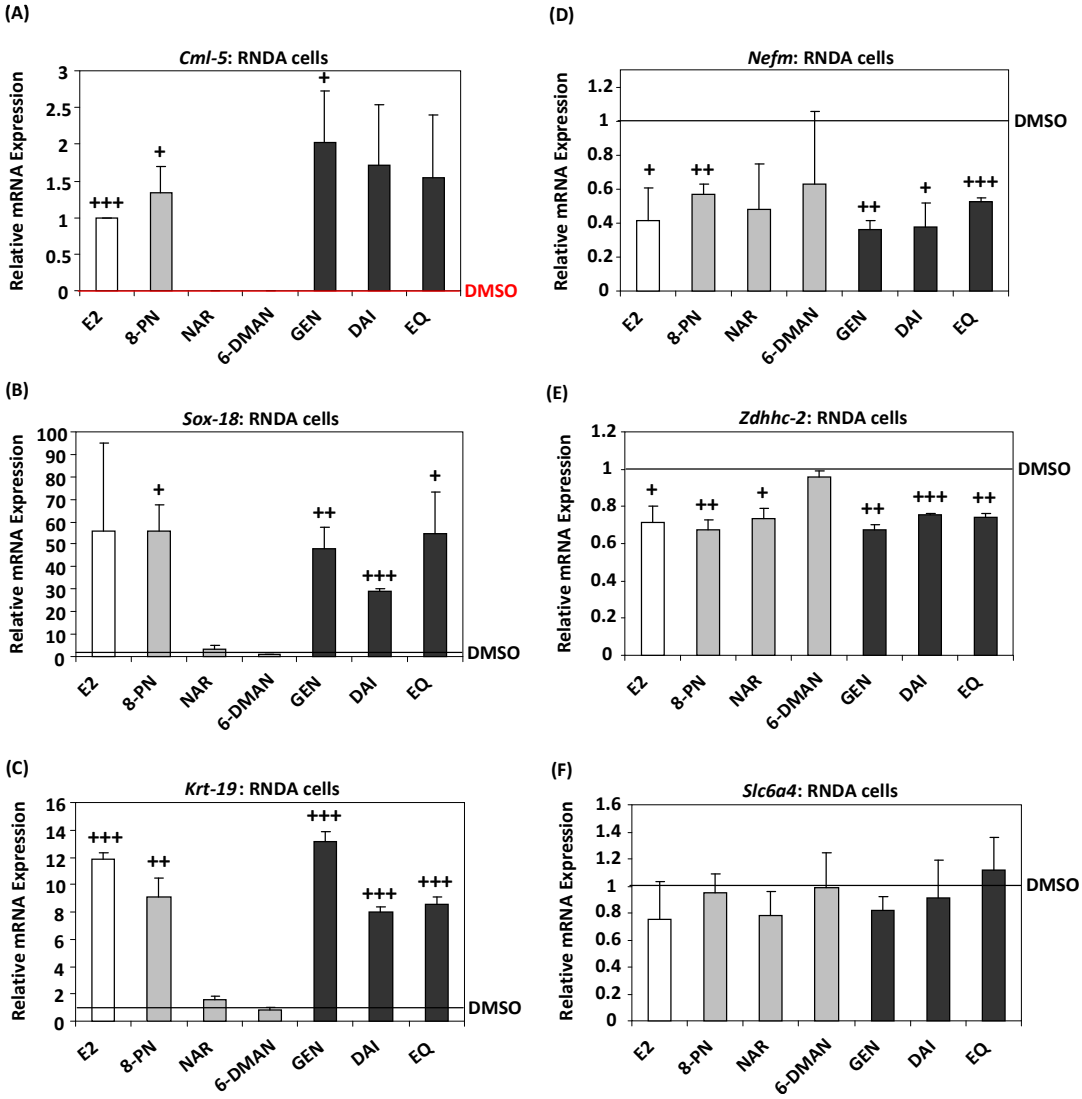

Figure 4-8: Effect of flavonoids on the regulation of mRNA expression of the six selected estrogen responsive genes in RNDA cells. Cells were treated with either 0.1 % DMSO, 10 nM E2, 10 µM of the naringenin-type flavanones (grey bars) or 10 µM of the isoflavones (black bars) for 24 hours prior to RNA isolation. **(A - C)** regulation of mRNA expression of *Cml-5*, *Sox-18* and *Krt-19* in response to E2 and flavonoids and **(D - F)** regulation of mRNA expression of *Nefm*, *Zdhhc-2* and *Slc6a4* in response to E2 and flavonoids. For panel A, data are normalized against the E2 treatment and expression in response to DMSO treatment is represented by a red horizontal line set to 0. For panels B – F, expression in response to DMSO treatment is represented by a black horizontal line set to 1 and data are normalized against the DMSO treatment. Plus signs indicate significance from DMSO treatment: + $p \leq 0.05$, ++ $p \leq 0.01$ and +++ $p \leq 0.001$.

4.8. Effect of Flavonoids on the Regulation of mRNA Expression of Estrogen-Responsive Genes in D-RNDA Cells

Since RNDA cells encode a temperature-sensitive mutant of the SV40 large T-antigen, neuronal differentiation is constitutive upon shifting them from permissive (proliferative conditions) to non-permissive temperature (differentiating conditions) (White and Whittemore, 1992; Whittemore and White, 1993; White *et al.*, 1994). Accordingly, it was not only of interest to evaluate the potential of flavonoids to regulate endogenous gene expression of the six selected estrogen responsive genes in RNDA cells grown under proliferative conditions (**Section 4.7**), but it was also of interest to look at their capacity to regulate endogenous gene expression in D-RNDA cells (i.e. RNDA cells grown under differentiation conditions); in which the cells are no longer under the mitotic drive of the temperature-sensitive mutant of SV40 large T-antigen.

However, confirming the switch of RNDA cellular status from proliferation to differentiation was a prerequisite to these gene expression studies. As a result, intracellular markers of neuronal differentiation, namely NF-L, NF-M, NF-H and NSE were visualized using immunocytochemistry (**Section 3.2.8.2**).

4.8.1. Cellular Differentiation of RNDA cells and Expression of Cell-Specific Antigens

At 33 °C (i.e. permissive temperature), RNDA cells divide and show fibroblast-like morphology (**Figure 4-9 A**). When RNDA cells are shifted to 39 °C (i.e. non-permissive temperature), the cells cease division and exhibit phenotypic properties of neurons (**Figure 4-9 B**). RNDA cells and D-RNDA cells were highly immunoreactive for NF-L (**Figure 4-9 C and D**, respectively) and NF-M (**Figure 4-9 E and F**, respectively). Very low levels of NF-H and NSE were detected in RNDA cells (**Figure 4-9 G and I**, respectively). Yet, increased levels of NF-H and NSE immunoreactivities were observed following RNDA cellular differentiation (**Figure 4-9 H and J**, respectively). All immunoreactivities were cytoplasmic. No staining was observed if cells were only incubated with either the primary or secondary antibody (**Appendix 7-6**).

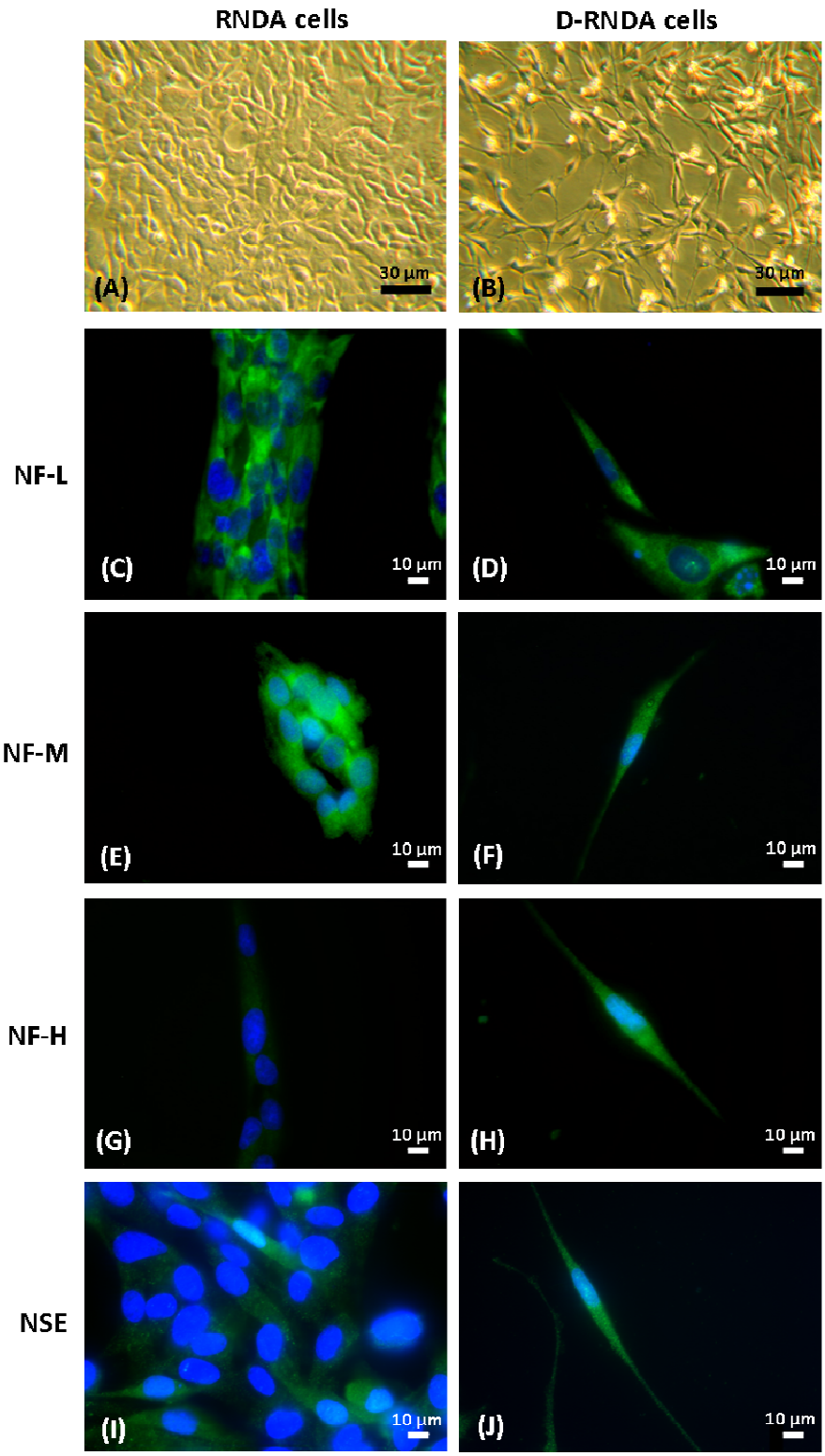

Figure 4-9: Phase contrast and fluorescence microscopy images of RNDA cells and D-RNDA cells. (A) a phase contrast microscopy image of RNDA cells at 33 °C, **(B)** a phase contrast microscopy image of RNDA cells at 39 °C (denoted as D-RNDA cells), **(C and D)** cells stained with NF-L monoclonal antibody (green channel), **(E and F)** cells stained with NF-M monoclonal antibody (green channel), **(G and H)** cells stained with NF-H monoclonal antibody (green channel) and **(I and J)** cells stained with NSE monoclonal antibody (green channel). Nuclei are stained with DAPI (blue channel).

4.8.2. Effect of Flavonoids on the Regulation of mRNA Expression Levels in D-RNDA Cells

As illustrated in **Figure 4-9**, RNDA cells differentiate along the neuronal lineage upon shifting them to a non-permissive temperature (i.e. differentiation conditions); where the temperature-sensitive mutant of the SV40 large T-antigen is inactivated. Since they possess the ability to undergo differentiation, it was of interest to evaluate the effects of the flavonoids on the regulation of mRNA expression of the six selected estrogen responsive genes in D-RNDA cells (i.e. RNDA cells grown under differentiation conditions). In this study, the analysis time points were chosen to be day 1 and day 4 following initiation of differentiation (refer to **Figure 3-6**). Cells were treated for 24 hours prior to RNA isolation with 0.1 % DMSO, 10 nM E2, 10 nM E2 plus 500 nM Fulvestrant or 10 µM of each of the flavonoids (**Section 3.2.7.2**).

Experiments described hereafter were evaluated based on two endpoints, namely (1) the impact of the process of cellular differentiation itself on the regulation of mRNA expression levels of the selected E2-regulated genes and (2) the responsiveness of the selected genes towards 17β-Estradiol or the flavonoids as RNDA cells undergo differentiation.

In **Figure 4-10 A**, *Cml-5* mRNA expression was not detectable in the day 0 sample treated with DMSO (green baseline set to 0) (also referred to as expression levels observed in the DMSO-treated RNDA cells grown under proliferative conditions). *Cml-5* mRNA became measurable during cellular differentiation. Hence, gene expression data of *Cml-5* were normalized in these set of experiments against the day 1 differentiated sample treated with DMSO. At day 1 following initiation of differentiation, *Cml-5* mRNA expression was found to be significantly up-regulated in response to E2 (1.74 ± 0.26 fold) and Genistein (10.54 ± 1.79 fold) as compared to the day 1 differentiated sample treated with DMSO. The effect of E2 on the regulation of *Cml-5* mRNA expression was completely antagonized by Fulvestrant (1.01 ± 0.21 fold); indicating the involvement of ERβ in this effect. There was a slight increase in *Cml-5* mRNA expression from day 1 up to day 4 following initiation of differentiation, implying that the process of RNDA cellular differentiation had an effect on the regulation of mRNA expression of *Cml-5*, yet no significant additional effects on

mRNA expression levels were observed in response to E2 or the flavonoids as compared to the day 4 differentiated sample treated with DMSO. Nevertheless, an observable increase (2.61-fold) in *Cml-5* mRNA expression was noticed in response to Genistein treatment only as compared to the day 4 differentiated sample treated with DMSO, although this was statistically not significant.

In **Figure 4-10 B**, mRNA expression of *Sox-18* was detectable in the day 0 sample treated with DMSO. Therefore, data were normalized against the day 0 sample treated with DMSO (black baseline set to 1). At day 1 following initiation of differentiation, an observable increase (8-fold) in *Sox-18* mRNA expression was noticed in response to Genistein treatment only as compared to the day 1 differentiated sample treated with DMSO, although this was statistically not significant. At day 4 following initiation of differentiation, expression of *Sox-18* mRNA remained at baseline levels with no significant additional effects on mRNA expression levels observed in response to E2 or the flavonoids as compared to the day 4 differentiated sample treated with DMSO.

In **Figure 4-10 C**, mRNA expression of *Krt-19* was also detectable in the day 0 sample treated with DMSO. Hence, data were normalized against the day 0 sample treated with DMSO (black baseline set to 1). At day 1 following initiation of differentiation, an up-regulation of *Krt-19* mRNA was noticed as compared to expression levels observed in the DMSO-treated RNDA cells grown under proliferative conditions (i.e. the set baseline). Additionally, a 1.32-fold significant increase in *Krt-19* mRNA expression was noticed in response to E2 treatment as compared to the day 1 differentiated sample treated with DMSO. This effect was shown to be completely antagonized by Fulvestrant. In addition, there was an observable increase in *Krt-19* mRNA in response to the isoflavones: Genistein (1.93-fold), Daidzein (1.62-fold) and Equol (1.46-fold) as compared to the day 1 differentiated sample treated with DMSO; however values did not reach statistical significance. At day 4 after initiation of differentiation, expression of *Krt-19* mRNA was dramatically reduced to baseline levels, implying that the process of RNDA cellular differentiation had an effect on the regulation of mRNA expression of *Krt-19*, yet no significant additional effects on mRNA expression levels were observed in response to E2 or the flavonoids as compared to the day 4 differentiated sample treated with DMSO.

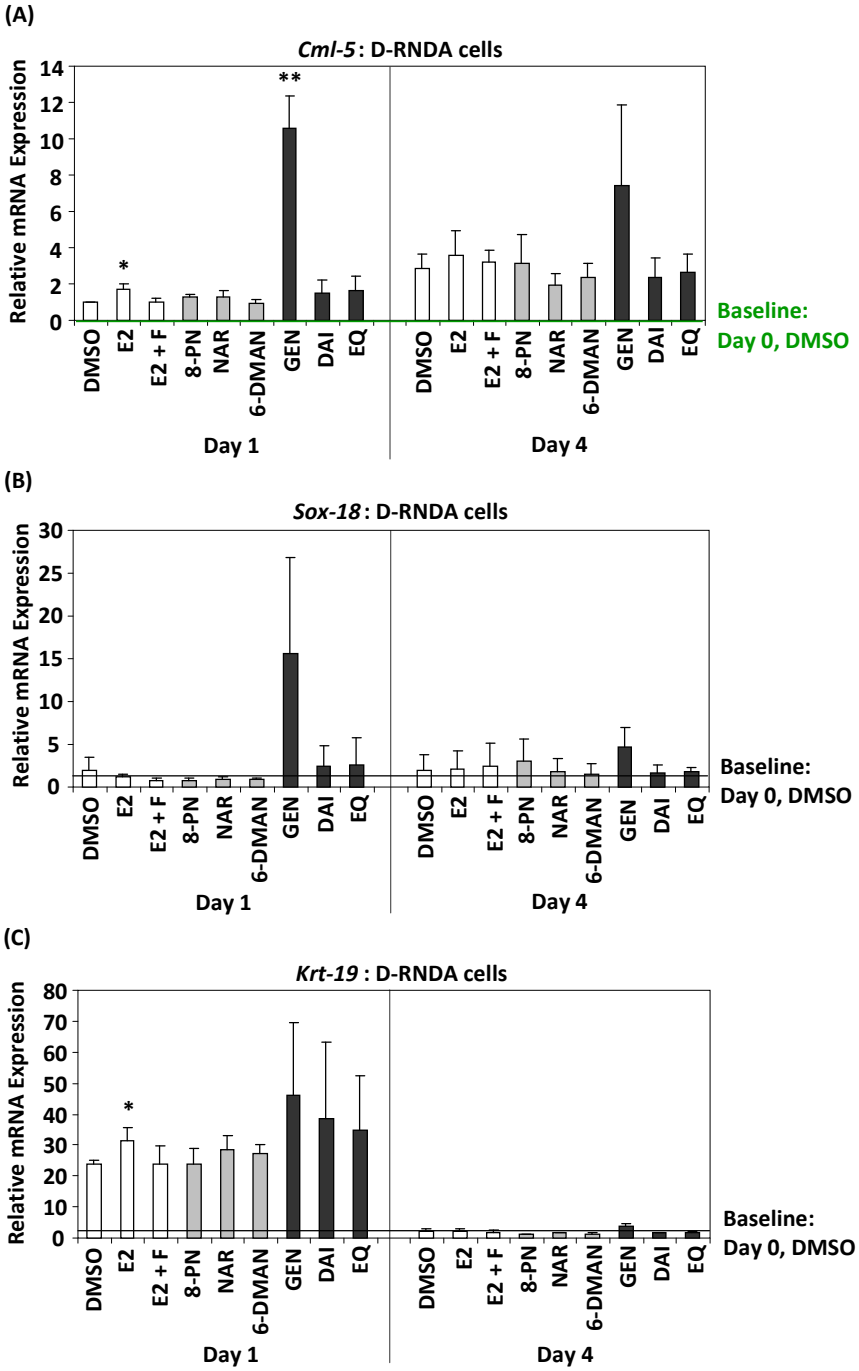

Figure 4-10: Effect of flavonoids on the regulation of mRNA expression of *Cml-5*, *Sox-18* and *Krt-19* in D-RNDA cells at day 1 and day 4 following initiation of differentiation. D-RNDA cells were treated with 0.1 % DMSO, 10 nM E2, 10 nM E2 plus 500 nM Fulvestrant, 10 µM of the naringenin-type flavanones (grey bars) or 10 µM of the isoflavones (black bars) for 24 hours prior to RNA isolation. In Panel A, data are normalized against the day 1 differentiated sample treated with DMSO and expression in response to DMSO treatment at the day 0 sample is represented by a green horizontal line set to 0. In Panels B and C, expression in response to DMSO treatment at the day 0 sample is represented by a black horizontal line set to 1. Data are normalized against the day 0 sample treated with DMSO. Asterisks indicate significance from the day 1 differentiated sample treated with DMSO: * $p \leq 0.05$ and ** $p \leq 0.01$.

In all panels of **Figure 4-11** described hereafter, mRNA expression of the genes was detectable in the day 0 sample treated with DMSO (also referred to as expression levels observed in the DMSO-treated RNDA cells grown under proliferative conditions). Thus, data were normalized against the day 0 sample treated with DMSO (black baseline set to 1). In contrast to the regulation of expression of *Krt-19* mRNA, regulation of expression of *Nefm* mRNA was at baseline levels at day 1 following initiation of differentiation with no significant additional effects on mRNA expression levels observed in response to E2 or the flavonoids as compared to the day 1 differentiated sample treated with DMSO (**Figure 4-11 A**). However, an up-regulation of *Nefm* mRNA was noticed at day 4 following initiation of differentiation as compared to the set baseline, yet no significant additional effects on mRNA expression levels were observed in response to E2 or the flavonoids as compared to the day 4 differentiated sample treated with DMSO.

In **Figure 4-11 B**, regulation of expression of *Zdhhc-2* mRNA was at baseline levels at day 1 following initiation of differentiation, however additional effects on mRNA expression levels were observed in response to E2 or the flavonoids as compared to the day 1 differentiated sample treated with DMSO. In particular, decreased expression of *Zdhhc-2* mRNA was observed in response to E2 treatment (0.75-fold) at day 1 following initiation of differentiation as compared to the day 1 differentiated sample treated with DMSO, although values did not reach statistical significance. This effect was completely antagonized by Fulvestrant. Similar to E2, decreased expression of *Zdhhc-2* mRNA was also observed in response to 8-Prenylnaringenin (0.75-fold), Naringenin (0.82-fold), Genistein (0.74-fold), Daidzein (0.83-fold) and Equol (0.80-fold) as compared to the day 1 differentiated sample treated with DMSO, even though statistical significance was also not reached. At day 4 following initiation of differentiation, there was an up-regulation of *Zdhhc-2* mRNA expression as compared to expression levels observed in the DMSO-treated RNDA cells grown under proliferative conditions (i.e. the set baseline), implying that the process of RNDA cellular differentiation had an effect on the regulation of mRNA expression of *Zdhhc-2.* A significant decrease in *Zdhhc-2* mRNA expression was noticed in response to E2 (0.65-fold) as compared to the day 4 differentiated sample treated with DMSO. Once again, this effect was completely antagonized by Fulvestrant. Similar to E2, decreased expression of *Zdhhc-2* mRNA was noticed in response to

8-Prenylnaringenin (0.73-fold), Naringenin (0.75-fold), 6-(1,1-Dimethylallyl)naringenin (0.76-fold) and Daidzein (0.67-fold), yet statistical significance was only reached in response to Genistein (0.66-fold) and Equol (0.65-fold) as compared to the day 4 differentiated sample treated with DMSO (**Figure 4-11 B**).

As shown in **Figure 4-11 C**, an up-regulation of *Slc6a4* mRNA expression was observed at day 1 following initiation of differentiation as compared to the set baseline. Decreased expression of *Slc6a4* mRNA was noticed in response to E2 treatment (0.70-fold) as compared to the day 1 differentiated sample treated with DMSO, even though values did not reach statistical significance. This effect was completely antagonized by Fulvestrant. Similar to E2, decreased expression of *Slc6a4* mRNA was observed in response to 8-Prenylnaringenin (0.71-fold), Naringenin (0.72-fold), Genistein (0.55-fold), Daidzein (0.80-fold) and Equol (0.80-fold) as compared to the day 1 differentiated sample treated with DMSO, nevertheless statistical significance was also not reached. At day 4 following initiation of differentiation, expression of *Slc6a4* mRNA was reduced to baseline levels implying that the process of RNDA cellular differentiation had an effect on the regulation of mRNA expression of *Slc6a4*, yet no significant additional effects on mRNA expression levels were observed in response to E2 or the flavonoids as compared to the day 4 differentiated sample treated with DMSO (**Figure 4-11 C**).

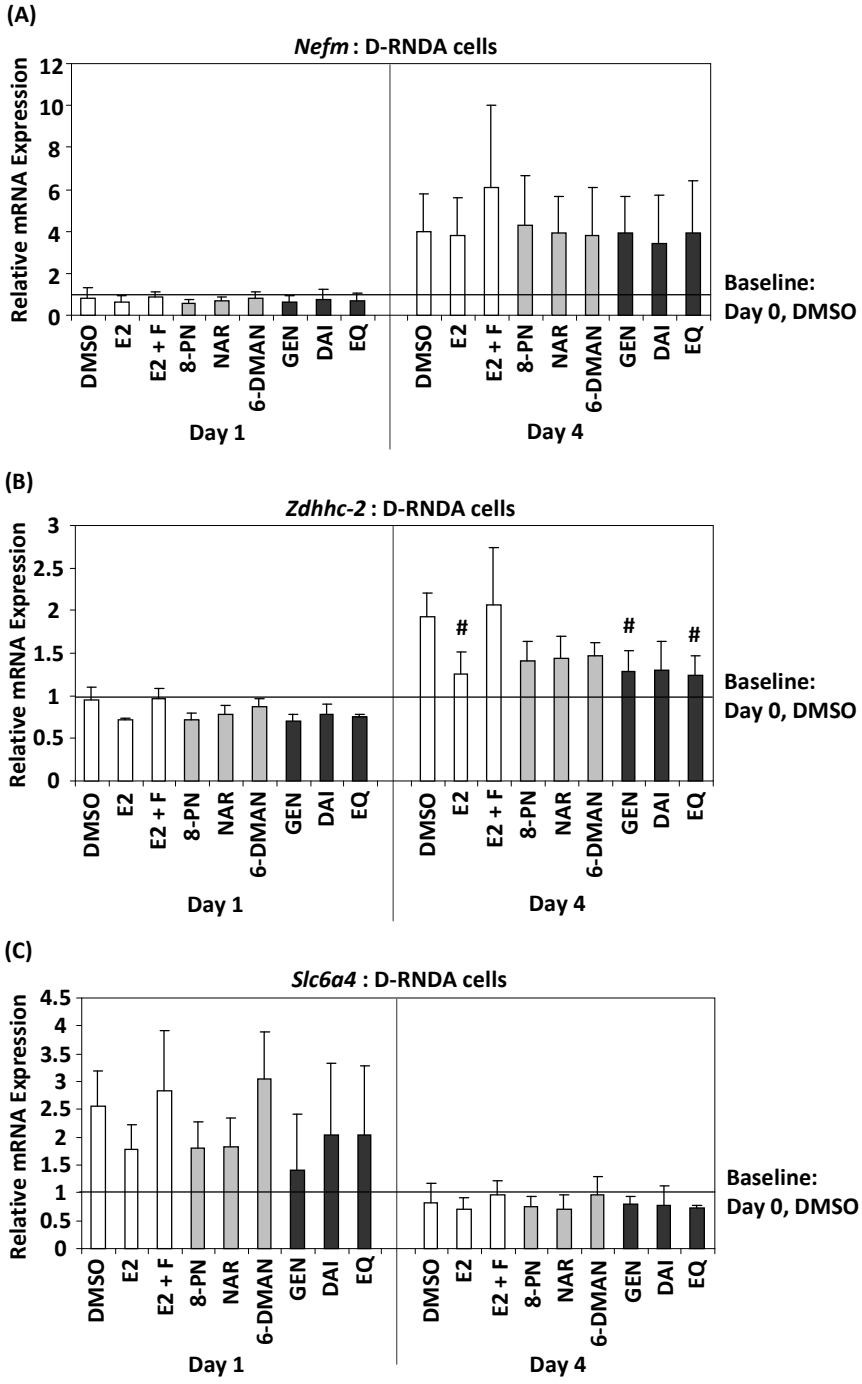

Figure 4-11: Effect of flavonoids on the regulation of mRNA expression of *Nefm*, *Zdhhc-2* and *Slc6a4* in D-RNDA cells at day 1 and day 4 following initiation of differentiation. D-RNDA cells were treated with 0.1 % DMSO, 10 nM E2, 10 nM E2 plus 500 nM Fulvestrant, 10 µM of the naringenin-type flavanones (grey bars) or 10 µM of the isoflavones (black bars) for 24 hours prior to RNA isolation. Expression in response to DMSO treatment in the day 0 sample is represented by a black horizontal line set to 1. Data are normalized against the day 0 sample treated with DMSO. Hash signs indicate significance from the day 4 differentiated sample treated with DMSO: # $p \leq 0.05$.

5. DISCUSSION

Estrogens are known to exert many actions on different brain regions; amongst them are the raphe nuclei, where ERβ is the most abundantly expressed estrogen receptor subtype. Accumulating evidence suggests that estrogenic effects on the raphe nuclei are primarily important for regulating significant neuropsychological behaviors, including depression, mood swings, anxiety and panic behaviors, by releasing serotonin (Bethea *et al.*, 2003; Nomura *et al.*, 2005; Donner and Handa, 2009). Because of this connection, phases of intense hormone fluctuations, for instance during menopause, are often associated with several mood disturbances that often reduce the quality of life of menopausal women. Accordingly, long-term use of HRT appeared to be the method of choice for many menopausal women to help alleviate vasomotor symptoms, which may include neuropsychological changes such as depression. Irrespective of the beneficial effects of HRT to alleviate mood disorders (Klaiber *et al.*, 1979; Schmidt *et al.*, 2000; Rasgon *et al.*, 2002), a number of health risks attributed to HRT, such as breast and endometrial cancers, were arising (Dupont and Page, 1991; Steinberg *et al.*, 1991; Beral *et al.*, 1999; Chlebowski *et al.*, 2003; Chlebowski *et al.*, 2009). Hence, a recurrence of consumer interest in phytoestrogens, i.e. plant-derived secondary metabolites possessing estrogen-like bioactivity, has been noticed due to their occurrence in medicinal plant extracts and a wide variety of food items including dietary supplements with respective health claims (Henderson *et al.*, 1994; Sullivan *et al.*, 1997; Torgerson and Bell-Syer, 2001). Even though these substances are sold as medicinal plant remedies or as dietary supplements and have reached quite remarkable market shares, sufficient data regarding their efficacy and safety remains to be unavailable.

Isoflavones and naringenin-type flavanones, collectively known as the flavonoids, belong to a group of polyphenolic plant-derived secondary metabolites known to possess estrogen-like bioactivities as they structurally or functionally mimic mammalian estrogens, partial or in total, and therefore may have significant impact on women's health (Cos *et al.*, 2003; Ososki and Kennelly, 2003). Nevertheless, conclusive data on their activity, measured in this study by their transactivational activity on ERβ, as well as

their effects on the regulation of mRNA expression of estrogen responsive genes in the raphe nuclei region of the brain remained to be elusive due to the lack of suitable raphe nuclei-derived cellular models expressing sufficient amounts of functional estrogen receptor β.

Hence, a raphe nuclei-derived cell line that expresses a functional ERβ was sought as a model to investigate effects of flavonoids in raphe nuclei *in vitro*. In this regard, RN46A-B14 cells derived from embryonic day 13 rat medullary raphe nuclei, were primarily used in this study as the main cellular source because previous reports indicate that those particular cells contain the same complement of nuclear estrogen receptors as the rat raphe serotonin neurons, hence providing a convenient *in vitro* cellular model for the study of estrogen action in raphe nuclei (Bethea *et al.*, 2003). Nonetheless, expression of endogenous ERβ in these cells was not sufficient to pursue downstream investigations of estrogen-dependent activities (**Appendix 7-1**). Therefore, a rat raphe nuclei-derived *in vitro* model that expresses sufficient amounts of functional estrogen receptor β was established (termed RNDA cells) by stably transducing its parent cell line, RN46A-B14 cells, with a suitable lentiviral expression vector encoding a human estrogen receptor β gene. The reason for stably integrating a human *ESR2* instead of a rat *Esr2* in the studied rat cell model was due to two reasons: (1) availability of human *ESR2* DNA fragment in the lab and (2) human ERβ shows approximately 89% identity in its translated region to the rat ERβ as compared to any other mammalian ERβ (Enmark and Gustafsson, 1999).

5.1. Stable Transduction, Expression and Functional Characterization of Transgenic ERβ in RNDA Cells

The use of simple retroviruses, such as oncoretroviral-based vectors, is becoming substituted by more sophisticated and efficient lentiviral expression vector systems that have superior transduction efficiency in modifying cells *in vitro* and *in vivo* (Bukrinsky *et al.*, 1993). Given that the provided RN46A-B14 cells in this study showed very low expression of endogenous ERβ, downstream *in vitro* investigations of effects of 17β-Estradiol and the flavonoids on the raphe nuclei could not be pursued. To overcome this deficit, lentiviral-based expression vectors, namely p6NST50 and p6NST50 + ERβ,

were the method of choice to successfully integrate human *ESR2* into the RN46A-B14 cellular genome. Two different viral stock dilutions (either UD or 1:10 diluted) were used to transduce RN46A-B14 cells. Percentage of RN46A-B14 cells transduced with the undiluted p6NST50 + ERβ viral particles (6.39 %) was lower than the percentage of RN46A-B14 cells transduced with the 1:10 diluted p6NST50 + ERβ viral particles (24.48 %). The reason for the low transduction efficiencies observed with the undiluted viral particles was due to the high toxic viral effects that eventually led to death of infected RN46A-B14 cells. Accordingly, RN46A-B14 cells transduced with the 1:10 diluted lentiviral vectors were chosen for the present study. Specifically, the RN46A-B14 cells transduced with the 1:10 diluted p6NST50 + ERβ were denoted as RNDA cells. The successful transduction of RNDA cells with *ESR2* was further verified in a two-step approach demonstrating first the expression of the transgenic human ERβ and subsequently its functional characterization.

Using quantitative real-time PCR, transgenic human *ESR2* mRNA expression was successfully confirmed in RNDA cells in contrast to the transduced RN46A-B14 cells with p6NST50 as well as the untransduced RN46A-B14 cells. Given that mRNA expression levels do not always directly correlate with protein expression levels (Hrabovszky *et al.*, 1998), Western blot analysis of RNDA whole-cell protein extracts confirmed the expression of the transgenic ERβ, as indicated at 55 kDa, as opposed to the transduced RN46A-B14 cells with p6NST50 and the untransduced RN46A-B14 cells. Functional activity of transgenic ERβ was later verified using luciferase reporter gene assays, where the newly generated RNDA cells were transiently transfected with the firefly luciferase reporter gene under the control of a double ERE-dependent promoter. Cell exposure to increasing concentrations of 17β-Estradiol resulted in a sigmoidal dose-response curve corresponding to an EC_{50} of 4.0×10^{-10} M. The EC_{50} for 17β-Estradiol in the present study demonstrates higher sensitivity than the established and highly sensitive luciferase assay in MVLN cells (a derivative of an ERα-positive breast cancer cell line, MCF-7, stably transfected with a vitellogenin-A2-promoter / luciferase reporter construct) as well as the ERα-dependent human bone-derived U2OS cells; measuring a 17β-Estradiol response with an EC_{50} of 5×10^{-12} M and 5×10^{-11} M, respectively (Zierau *et al.*, 2006). Nevertheless, this minor difference in EC_{50} does not really affect the degree of affinity of

E2 to both ER subtypes as it is most probably cell-specific. A final step for the characterization of the transgenic ERβ was the treatment with the selective ERβ agonist (Diarylpropionitril) and the selective ERα agonist (Propyl pyrazole triol). The study has shown a concentration-dependent increase in luciferase output in response to Diarylpropionitril as opposed to the null effects observed when cells were exposed to Propyl pyrazole triol, which clearly validates the generated system and indicates that any observed estrogenic activity in RNDA cells is specifically mediated through the transgenic ERβ and not ERα. Those findings are highly consistent with previous findings from Bethea and colleagues (2003) who illustrated, using immunocytochemistry and quantitative real-time PCR, that RN46A-B14 cells are completely devoid of the ERα subtype (Bethea *et al.*, 2003).

5.2. Transactivational Activity of Flavonoids in RNDA Cells

By establishing the functionality and sensitivity of the new cell model, the next aim of the present study was to evaluate the transactivational activity of three isoflavones and four naringenin-type flavanones on the transgenic ERβ in RNDA cells; as conclusive data on their transactivational activity and ultimately their estrogenic potency in the raphe nuclei region of the brain remain to be elusive.

Using the same aforementioned luciferase reporter gene assay, it has been shown in this study that treatment with all three isoflavones resulted in a high expression of the firefly luciferase starting at the lowest dose of 10 nM (**Figure 4-5**). All three isoflavones are known to bind both estrogen receptor subtypes, yet with a higher relative binding affinity for ERβ than for ERα (Kuiper *et al.*, 1998). Agonistic activities of the isoflavones via the estrogen receptors are particularly dependent on the position of the hydroxyl group at carbon-7 and carbon-4' in the core structure of the isoflavones (Joung *et al.*, 2003; Takeuchi *et al.*, 2009). As clearly depicted in **Figure 2-7**, the chemical structures of all three isoflavones fulfill the above specific structural requirements for agonistic activity of isoflavones via ERβ. Accordingly, clear agonistic activities were demonstrated in RNDA cells in response to increasing concentrations of all three isoflavones. The high activity of the isoflavones in the ERβ-raphe nuclei cell-based system is in accordance to their high

activity in another reporter gene assay using Chinese Hamster Ovarian cells transiently transfected with an expression plasmid for human ERα or human ERβ (Takeuchi *et al.*, 2009). Nevertheless, the induction of the luciferase reporter gene in response to the isoflavones was shown to be substantially higher in the ERβ-dependent RNDA cells in this study as compared to the study of Takeuchi and colleagues (2009). The variation in luciferase induction in response to the isoflavones between different cell-based models could possibly be due to the recruitment of cell-type specific co-regulators following the differential nuclear receptor conformational changes in response to the isoflavones (Routledge *et al.*, 2000). A slight additional effect was also observed in RNDA cells in response to a co-treatment of 10 nM 17β-Estradiol and 1 µM of either Genistein or Daidzein, but not Equol, if compared to the 17β-Estradiol single dose treatment (**Figure 4-5**). This slight additional effect is possibly due to the stabilization of the firefly luciferase reporter enzyme leading to an increase in the bioluminescent signal while conducting the experiment (Sotoca *et al.*, 2010). Nonetheless, by reflecting this observation in whole animal models, this may probably alter the estrogenic potency of the three isoflavones according to the circulating endogenous 17β-Estradiol and therefore may ultimately show significant impacts on human health (Cos *et al.*, 2003; Ososki and Kennelly, 2003).

In the ERβ-dependent RNDA cells, a high transactivational activity on the transgenic ERβ has also been observed in response to Naringenin in a concentration-dependent manner starting at the lowest dose of 100 nM, albeit to a lesser extent than its structurally related compound, Genistein. Relative binding affinities of Naringenin versus Genistein for ERβ is 0.11 versus 87, respectively (Kuiper *et al.*, 1998). Both dietary substances are structurally related by possessing hydroxyl groups at carbon-7 and carbon-4' (**Figure 2-8**). However, the difference in the binding affinities is due to the fact that the aromatic B-ring is not in conjugation with the aromatic A-ring in Naringenin as compared to Genistein. This is due to the absence of the double bond between carbon-2 and carbon-3 in Naringenin on its C-ring (Vaya and Tamir, 2004).

In this study, Naringenin showed high activity in the ERβ-raphe nuclei cell-based system as compared to its to weak activity in a different reporter gene assay using 293 human embryonal kidney cells transiently transfected with a luciferase reporter plasmid as well

as an expression plasmid for human ERβ, where Naringenin induced luciferase expression starting at the lowest dose of 1 µM (Kuiper *et al.*, 1998). Additionally, Ruh and colleagues (1995) reported the weak activity of Naringenin in their tested micromolar range in an ERα-dependent MCF-7 cells transiently transfected with a luciferase reporter plasmid (Ruh *et al.*, 1995). Furthermore, Kretzschmar and colleagues (2010) as well as Zierau and colleagues (2002) have also reported no transactivational activity for Naringenin in their ERα-dependent studied cell model, the MVLN breast cancer cells, at concentrations lower than 10 µM (Zierau *et al.*, 2002; Kretzschmar *et al.*, 2010). By comparing results from this study and results from the abovementioned studies, the present study clearly states that Naringenin is highly active in the ERβ-dependent raphe nuclei cell model as compared to other ER-dependent mammalian cell models.

It has previously been reported that the addition of a prenyl group (i.e. prenylation) at carbon-8 on the A-ring of the Naringenin backbone results in 8-Prenylnaringenin, a compound with stronger estrogenic characteristics (Milligan *et al.*, 2000; Zierau *et al.*, 2002; Kretzschmar *et al.*, 2010). Numerous studies have pointed out the strong estrogenic potency of 8-Prenylnaringenin in various cellular models and organs expressing either ERα or ERβ (Milligan *et al.*, 2000; Zierau *et al.*, 2002; Effenberger *et al.*, 2005; Overk *et al.*, 2008; Zierau *et al.*, 2008). In this study, a high transactivational activity was also observed on the transgenic ERβ in RNDA cells in response to 8-Prenylnaringenin in a concentration-dependent manner. Nevertheless, prenylation did not result in an obvious difference between the transactivational activity of 8-Prenylnaringenin and its parent compound Naringenin on the transgenic ERβ in RNDA cells. In fact, the study pointed out a significant antagonistic effect of 8-Prenylnaringenin when co-added with 17β-Estradiol in RNDA cells as opposed to a co-treatment of 17β-Estradiol and Naringenin. Hence, one could hypothesize that the process of prenylation could serve as a possible structural modification that could lead to antagonistic effects of prenylflavonoids. By reflecting this observation in whole animal models, this may possibly alter the estrogenic potency of 8-Prenylnaringenin according to the circulating endogenous 17β-Estradiol and therefore may ultimately show significant impacts on human health (Cos *et al.*, 2003; Ososki and Kennelly, 2003). The antagonistic effect in response to the process of naringenin prenylation has also been observed in RNDA cells following a co-treatment of

7-(O-prenyl)naringenin-4'-acetate and 17β-Estradiol, therefore, substantiating the aforementioned proposed hypothesis. Additionally, 7-(O-prenyl)naringenin-4'-acetate, showed weak transactivational activity on ERβ in RNDA cells starting at the lowest concentration of 1 µM. This was also noticed in the ERα-dependent MVLN cells at the same tested concentration range (Kretzschmar *et al.*, 2007). Hence, it may well be speculated that 7-(O-prenyl)naringenin-4'-acetate possesses considerable affinity for both estrogen receptor subtypes, yet may exhibit weak activity on downstream transactivational pathways.

Surprisingly and in contrast to the above tested compounds, the current study did not pick-up any transactivational activity in RNDA cells in response to 6-(1,1-Dimethylallyl)naringenin. These results are in contrast to studies reported by Zierau and colleagues, who reported a high measurable luciferase output in a concentration-dependent manner in other cell-based assays, such as the ERα-dependent MVLN cells, ERα-dependent human bone-derived U2OS cells and ERβ-dependent human bone-derived U2OS cells (Zierau *et al.*, 2002; Zierau *et al.*, 2008). Therefore, one could speculate that 6-(1,1-Dimethylallyl)naringenin could show selective estrogen receptor modulator-like properties (SERM) (Nilsson *et al.*, 2001; Gruber *et al.*, 2002; Shang and Brown, 2002). SERMs are defined as ligands that could mimic the action of E2 in some tissues, yet lack E2-like actions in others (Gruber *et al.*, 2002). SERMs and phytoestrogens, in addition to the endogenous estradiol, may induce different nuclear receptor conformational changes in its tertiary structure due to discrepancies in both steric and electrostatic properties (Paige *et al.*, 1999). Therefore, the assembly of the transcription machinery following the recruitment of cell-type specific co-regulators could vary (Routledge *et al.*, 2000). Accordingly, altering the ability of ERβ to recruit co-repressors or co-activators may possibly be different in the studied RNDA cell model as opposed to other cell models, hence affecting downstream transcriptional events.

Certainly, it is worth noting that identifying and pointing out the estrogenic potency (i.e. calculating the EC_{50}) of all test flavonoids would have provided a better image for proper comparison. However, based on the tested doses of all flavonoids in this study (i.e. 10 nM – 10 µM), calculation of the EC_{50} was not possible mathematically due to the

fact that the data do not fit in a sigmoidal dose-response relationship, where a plateau does not seem to be reached at 10 µM. Higher concentrations were not possible as the substances are most likely to show toxic effects on RNDA cells. Nevertheless, this study indicates that the high transactivational activity on ERβ and ultimately the strong estrogenicity of Genistein, Daidzein, Equol, Naringenin and 8-Prenylnaringenin in RNDA cells could possibly manifest itself in the raphe nuclei region of the brain, provided it can cross the blood brain barrier in significant amounts.

5.3. Identification of Estrogen Responsive Genes in RNDA Cells

Following the evaluation of the transactivational activity of the flavonoids on the transgenic ERβ in RNDA cells using luciferase reporter gene assays, it was of interest to assess the potential of flavonoids to regulate endogenous gene expression of estrogen responsive genes in RNDA cells. This approach was considered essential in order to investigate whether their activity on a reporter gene level can be mirrored on the level of regulation of expression of estrogen responsive genes as compared to regulation patterns in response to 17β-Estradiol. As a result, it was initially necessary to identify genes undergoing estrogenic regulation of expression via ERβ in RNDA cells using a DNA microarray, which was one of the main aims of the study presented here.

From a total of 40,000 transcripts, 212 regulated transcripts with at least two fold-change of expression were identified. This list is comparably big since it is approximately twice as large as compared to identified genes in other ER-based cell systems, such as the ERα- and ERβ-dependent human bone-derived U2OS cells, where only 80 and 76 transcripts with at least two fold-change of expression were E2 regulated, respectively (Monroe *et al.*, 2003). However, due to the different microarray approaches utilized between this study and the study of Monroe and colleagues (2003), a conclusive comparison would not be possible, as each system should be taken as a separate entity. From 212 E2-regulated transcripts in RNDA cells, the E2-dependent regulation of three serotonin-related genes, namely *Slc6a4*, serotonin receptor 3b (*Htr-3b*) and serotonin receptor 6 (*Htr-6*) was identified. This finding supports the hypothesis that estrogens influence serotonin signaling in raphe nuclei. Unfortunately, due to the low copy number of *Htr-3b* and *Htr-6*

in these cells, it was not possible to validate their E2-dependent regulation using quantitative real-time PCR. Instead, the attention was focused on *Slc6a4*, a gene encoding serotonin re-uptake transporter in relation to the special functional relevance in this serotonergic cell line, in addition to five other E2-responsive genes, namely *Cml-5*, *Sox-18*, *Krt-19*, *Nefm* and *Zdhhc-2*, which were selected according to specific features of estrogenic regulation of expression (**Section 4.6**). Interestingly, a number of olfactory receptors and voltage-gated ion channels as well as organic anion transporters where also regulated in response to E2 in RNDA cells (**Appendix 7-4 and Appendix 7-5**). Nonetheless, investigations on the role of these genes and others in raphe nuclei were postponed for further studies due to time limitations.

Microarray analysis has been well known to exhibit a lower dynamic range for detecting gene expression levels (Morey *et al.*, 2006). Thus, to verify the microarray results with a more sensitive analysis of gene expression, the six selected E2-regulated genes were analyzed using quantitative real-time PCR. On one hand, the expression of *Cml-5*, *Sox-18* and *Krt-19* was observed to be E2 up-regulated, whereas the expression of *Nefm* and *Zdhhc-2* was observed to be E2 down-regulated on the microarray and this was successfully and significantly confirmed using quantitative real-time PCR. On the other hand, the expression of *Slc6a4* was observed to be E2 down-regulated in RNDA cells using microarray analysis, unfortunately this could not be confirmed using quantitative real-time PCR. Nevertheless, the regulation of expression of *Slc6a4* in response to test substances was still considered throughout the course of this study; in relation to its special functional relevance in RNDA cells.

5.4. Effect of Flavonoids on the Regulation of mRNA Expression Levels in RNDA Cells

To study the effects of dietary estrogen-like compounds in RNDA cells, it is necessary to go through different levels of complexity where investigations start with reporter gene assays followed by analyses of their capacity to regulate endogenous gene expression in the studied cell model. From **Section 5.2**, the transactivational activity of the flavonoids descended in the order shown in **Table 5-1**.

Table 5-1: Transactivational activity of flavonoids in RNDA cells.

(+++) Very high Activity, +++ High Activity, + Low Activity

Substance	Transactivational activity deduced from the reporter gene assays in RNDA cells
GEN	(+++)
DAI	(+++)
EQ	(+++)
NAR	+++
8-PN	+++
7-O-PN	+
6-DMAN	No activity

Based on these results, it was vital to scrutinize whether the effects of flavonoids on luciferase expression can be mirrored on the basis of regulation of expression of the aforementioned six selected genes undergoing estrogenic regulation. However, out of all seven tested flavonoids in this study, 7-(O-prenyl)naringenin-4'-acetate was excluded from these set of experiments regarding gene expression analyses because it exhibited low activity on downstream transactivational pathways in RNDA cells and due to the fact that it is not yet known to be present in medicinal plant extracts and food items including dietary supplements with respective health claims. All flavonoids were used at a concentration of 10 µM, as deduced from results of the reporter gene assays, to achieve the maximum level of regulation of target gene expression.

Effects of flavonoids on the regulation of mRNA expression levels in RNDA cells (**Figure 4-8**) were in accordance with their transactivational activity. In particular, it was shown in the present study that gene regulation patterns in response to 8-Prenylnaringenin, Genistein, Daidzein and Equol on the mRNA up-regulation of *Cml-5*, *Sox-18* and *Krt-19* as well as the down-regulation of *Nefm* and *Zdhhc-2* are in line with regulation patterns in response to 17β-Estradiol, as summarized in **Table 5-2**. Surprisingly, there was no regulation of mRNA expression of *Cml-5*, *Sox-18* and *Krt-19* in response to Naringenin as opposed to its high transactivational activity in RNDA cells. Interestingly, mRNA down-regulation of *Nefm* and *Zdhhc-2* were noticed in response to Naringenin in line with regulation patterns in response to 17β-Estradiol (**Table 5-2**).

Table 5-2: Regulation of mRNA expression of estrogen responsive genes in response to the flavonoids in RNDA cells as compared to E2. ↔ No regulation, ↑ Up-regulation, ↓Down-regulation

Substance / Gene Symbol	DMSO	E2	8-PN	NAR	6-DMAN	GEN	DAI	EQ
Cml-5	↔	↑	↑	↔	↔	↑	↑	↑
Sox-18	↔	↑	↑	↔	↔	↑	↑	↑
Krt-19	↔	↑	↑	↔	↔	↑	↑	↑
Nefm	↔	↓	↓	↓	↔	↓	↓	↓
Zdhhc-2	↔	↓	↓	↓	↔	↓	↓	↓
Slc6a4	↔	↔	↔	↔	↔	↔	↔	↔

The classical pathway of estrogenic action is via ER dimerization followed by binding to estrogen responsive elements in the promoter region of target genes, hence leading to altered transcription and translation (**Section 2.4.1**). However, most of the target genes regulated by ERs lack ERE-like sequences (O'Lone *et al.*, 2004). Hence, their regulation is modulated via alternative "non-classical" pathways. These may include regulation of target genes by ERs without directly binding to DNA, but rather via the formation of the pre-initiation complex through protein-protein interactions with transcription factors, such as the Activator Protein-1, Specificity Protein-1 or the Nuclear Factor-kappa B (Nilsson *et al.*, 2001; Bjornstrom and Sjoberg, 2005; Cheskis *et al.*, 2007). Since Naringenin was able to induce high luciferase expression (mediated by ERE regulatory element) but not expression of *Cml-5*, *Sox-18* and *Krt-19* in RNDA cells, one could argue that regulation of *Cml-5*, *Sox-18* and *Krt-19* in RNDA cells is possibly modulated via a "non-classical" pathway. In line with this thought, it can also be argued that the down-regulation of *Nefm* and *Zdhhc-2* is possibly mediated either by an ERE regulatory element or by a different mechanism than the one employed for the regulation of *Cml-5*, *Sox-18* and *Krt-19* in RNDA cells due to the fact that the regulation of *Nefm* and *Zdhhc-2* in response to Naringenin were in line with 17β-Estradiol. In addition, the results clearly indicate that 8-Prenylnaringenin, Genistein, Daidzein and Equol act via the same mechanism as 17β-Estradiol in RNDA cells in the regulation of expression of the selected estrogen responsive genes, irrespective of the employed regulatory element.

Furthermore, 6-(1,1-Dimethylallyl)naringenin did not regulate the mRNA expression level of *Cml-5*, *Sox-18*, *Krt-19*, *Nefm* and *Zdhhc-2* in the present study (**Table 5-2**), in accordance to its missing transactivational activity on reporter gene expression through ERβ (**Table 5-1**). In contrast to the present study, Zierau and colleagues have previously reported that 6-(1,1-Dimethylallyl)naringenin seems to exert estrogenic activity *in vivo* predominantly by influencing uterine mRNA expression of estrogen responsive genes containing ERE (Zierau *et al.*, 2004; Zierau *et al.*, 2008). It has also been reported that 6-(1,1-Dimethylallyl)naringenin lacked any proliferative effect on the uterus due to the fact that uterine proliferation appears to be mediated by mechanisms other than ERE-mediated mechanisms (O'Brien *et al.*, 2006). Taking these studies into consideration, 6-(1,1-Dimethylallyl)naringenin still seems to show SERM-like properties, as it can influence mRNA expression of estrogen responsive genes in the uterus (Zierau *et al.*, 2004; Zierau *et al.*, 2008), yet lacks the ability to regulate the expression of the six selected estrogen responsive genes in RNDA cells in the present study. Moreover, this study clearly reveals that 6-(1,1-Dimethylallyl)naringenin does not have any effects on the regulation of expression of estrogen responsive genes in the raphe nuclei-derived cell model neither via the classical ERE-dependent pathway nor via any other “non-classical” pathway. Nevertheless, further experimentations are required to support this assumption.

Unfortunately, the study pointed out no regulation of mRNA expression of *Slc6a4* in response to 17β-Estradiol and all flavonoids (**Table 5-2**). This is surprising because this contradicts results reported by Pecins-Thompson and colleagues (1998), where they clearly showed a down-regulation of *Slc6a4* mRNA in rhesus macaques in response to 17β-Estradiol, which is consistent with the therapeutic efficacy of 17β-Estradiol on mood in post-menopausal women (Pecins-Thompson *et al.*, 1998). Nonetheless, the regulation of expression of *Slc6a4* mRNA was still considered for further experimentations in this study; in relation to the final aim of the present study that is evaluating the effects of the flavonoids on the regulation of mRNA expression of the six selected E2-regulated genes in RNDA cells undergoing neuronal differentiation (denoted as D-RNDA cells).

5.5. Effect of Flavonoids on the Regulation of mRNA Expression Levels in D-RNDA Cells

RNDA cells, a rat serotonergic neuronal cell line, encode a temperature-sensitive mutant of the SV40 large T-antigen just as their parent cell line RN46A-B14 cells. Accordingly, differentiation of this cell line along the neuronal lineage is initiated in response to shifting cells from their proliferative conditions (i.e. permissive temperatures) to differentiation conditions (i.e. non-permissive temperatures); in which the cells are no longer under the mitotic drive of the temperature-sensitive mutant of the SV40 large T-antigen (White and Whittemore, 1992; Whittemore and White, 1993; White *et al.*, 1994). The expression of intracellular neuronal differentiation markers was investigated in this study to primarily evaluate the switch of RNDA cells from their proliferative to differentiation cellular status using immunocytochemistry (**Section 3.2.8.2**). In this study, potential markers were represented by neurofilament proteins which are class IV intermediate 10 nm filamentous proteins composed of three subunits (low, medium and high). The names were designated according to their distinct molecular weights; where NF-L is 68-70 kDa, NF-M is 145-160 kDa and finally NF-H is 200-220 kDa. Neurofilaments are found in neurons of vertebrates and are known to be formed in high concentrations during the development of neuronal axons (Cleverley *et al.*, 1998; Lalonde and Strazielle, 2003). NSE, an acid soluble protein of the glycolytic isoenzyme enolase that is composed of two gamma subunits, was additionally selected for this study. It is exclusively confined to neurons of the central and peripheral nervous systems as well as cells of neuroendocrine origin and is thought to serve as a growth factor in neurons (Schmechel *et al.*, 1978; Schmechel *et al.*, 1980; Kirino *et al.*, 1983).

Immunocytochemistry results presented in this study complement earlier work by White and colleagues (1994) (White *et al.*, 1994), where RNDA cells expressed high levels of NF-L and NF-M in addition to low levels of NF-H and NSE. As cells differentiated (i.e. designated as D-RNDA cells), an enhanced NSE and neurofilament expression was noticed, indicating successful initiation of RNDA cellular differentiation. Unfortunately, RNDA cells do not proliferate as monolayer cultures. As a result, quantitation and comparative analysis of the presented immunostainings in this study could not be reported.

Following the proof of cellular differentiation, two main questions were addressed: (1) would the process of cellular differentiation itself regulate mRNA expression levels of the six selected E2-regulated genes? and (2) would the genes retain their responsiveness towards 17β-Estradiol or the flavonoids as RNDA cells differentiate? A prerequisite to the abovementioned questions was the proof of the stable expression of the ERβ as RNDA cells undergo differentiation. This is not considered trivial as retroviruses may in some cases possess an important drawback that is the inability to sustain expression of transgenes due to transcriptional silencing or self-inactivation (Swindle and Klug, 2002). In view of that, the present study pointed out sufficient mRNA expression of the transgenic ERβ in D-RNDA cells, which was highly maintained throughout the experimental period, as compared to expression levels in RNDA cells (**Appendix 7-7**).

Initially, the impact of cellular differentiation on the regulation of mRNA expression levels of the six selected E2-regulated genes was evaluated. Apart from *Sox-18*, it was clearly shown that the process of cellular differentiation had either increased or decreased regulation of mRNA expression levels of the remaining genes as compared to levels during cellular proliferation (The set baseline in **Figure 4-10** and **Figure 4-11**). In particular, an increase in mRNA expression levels of *Nefm* and *Zdhhc-2* was observed throughout the process of cellular differentiation from day 1 up to day 4. The former gene encodes the NF-M protein. Thus, the up-regulation of *Nefm* in D-RNDA cells at day 4 following initiation of differentiation substantiates the immunocytochemistry results presented in this study. In addition, *Zdhhc-2* encodes a palmitolyation-related enzyme required for neuronal protein palmitolyation that are essential for neuronal development and cellular differentiation (Fukata and Fukata, 2010). Accordingly, increased regulation of *Zdhhc-2* during cellular differentiation was to be expected. Based on these observations, one could argue that an up-regulation of *Zdhhc-2* mRNA expression in RNDA cells undergoing differentiation may serve as an additional marker for neuronal differentiation in the raphe nuclei. Additionally, keratin-19 is a member of the keratin family, which are major protein components of the intermediate filaments responsible for the cell's cytoarchitecture (Choi *et al.*, 2000). Hence, a down-regulation of *Krt-19* mRNA expression in RNDA cells undergoing differentiation could also serve as a further marker for neuronal differentiation in the raphe nuclei. Nonetheless, quantification of the respective gene products must be pursued to confirm the above observations.

Surprisingly, the regulation of *Slc6a4* mRNA expression was reduced to baseline levels from day 1 up to day 4 following initiation of differentiation (**Figure 4-11**). As previously mentioned, *Slc6a4* encodes a serotonin re-uptake transporter in this serotonergic cell line, a monoamine transporter protein which functions in all serotonergic neurons by means of transporting serotonin from synaptic spaces into presynaptic neurons (Murphy *et al.*, 2008). The reason why a down-regulation, instead of the expected up-regulation, was noticed at day 4 following initiation of differentiation is not yet clear. Furthermore, serotonin production was found to be extremely low in D-RNDA cells (Personal Communication; Annekathrin Schwabe, 2007). Thus, cell function analysis in relation to a serotonergic context was difficult to pursue during the time frame of the present study.

Besides the change in regulation of mRNA expression levels in response to the process of cellular differentiation, a change in the responsiveness towards 17β-Estradiol and the test substances was also noticed in D-RNDA cells. For example, a down-regulation of *Slc6a4* mRNA expression in response to 17β-Estradiol and the flavonoids was observed in D-RNDA cells as opposed to no regulation in RNDA cells, which indicates that the process of RNDA cellular differentiation enhances the regulatory mechanism required for the suppression of *Slc6a4* mRNA expression by 17β-Estradiol and the flavonoids. This clearly associates with the ongoing research stating that 17β-Estradiol treatment down-regulates *Slc6a4* mRNA, which is consistent with the therapeutic efficacy of E2 on mood in post-menopausal women (Pecins-Thompson *et al.*, 1998). In addition, regulation of mRNA expression of *Cml-5* and *Sox-18* was highly sensitive to Genistein treatment only in D-RNDA cells in a time point-dependent manner. The mechanism underlying this obvious sensitivity of *Cml-5* and *Sox-18* regulation in response to Genistein treatment and ultimately its biological relevance is not yet clear. Nonetheless, the present study clearly shows that the impact of the process of cellular differentiation itself on the regulation of expression of the six selected target genes seemed to be highly dominant over the effects caused in response to either 17β-Estradiol or any of the tested flavonoids at the studied time points. Results from D-RNDA cells are yet to be highly interpreted based on additional experiments. However, this is considered challenging given that insufficient cell quantities for larger experiments are currently obtainable; in other words, optimization of the differentiation protocol is a prerequisite to be able to perform further investigations on D-RNDA cells.

6. CONCLUSIONS AND FUTURE DIRECTIONS

In the present study, the stable transduction of RN46A-B14 cells with the human *ESR2* following a lentiviral expression system was successfully achieved; thereby generating the new rat raphe nuclei-derived cell line, RNDA cells. The success of this transduction has been demonstrated biochemically by determining the ERβ expression on the mRNA as well as protein level and by characterizing its function using the firefly luciferase reporter gene under the control of a double ERE-dependent promoter. The reporter gene assay has also been used to demonstrate that target gene transcription in this cell line is solely and specifically mediated via the transgenic ERβ. Hence, this study clearly presents the establishment of an *in vitro* raphe nuclei-derived model that overexpresses a functional ERβ to investigate downstream effects of dietary substances in the raphe nuclei.

Accordingly, the transactivational activity of three isoflavones and four naringenin-type flavanones were clearly demonstrated in RNDA cells using the same aforementioned reporter gene assay. The study clearly illustrates the high transactivational activity of Genistein, Daidzein, Equol, Naringenin and 8-Prenylnaringenin in RNDA cells by stimulating luciferase expression in a concentration-dependent manner. However, no transactivational activity was noticed in response to 6-(1,1-Dimethylallyl)naringenin in the studied cell model. Results from the reporter gene assays were validated on the basis of regulation of mRNA expression of six estrogen responsive genes that were selected according to specific features of estrogenic regulation of expression from a DNA microarray.

Apart from *Slc6a4*, the E2-dependent regulation of *Cml-5*, *Sox-18*, *Krt-19*, *Nefm* and *Zdhhc-2* was successfully confirmed in RNDA cells using quantitative real-time PCR. The study reported that 17β-Estradiol up-regulated mRNA expression of *Cml-5*, *Sox-18* and *Krt-19*. Similar effects were observed in response to 8-Prenylnaringenin, Genistein, Daidzein and Equol. This was consistent with earlier findings obtained with an ERE-driven reporter gene assay in the same cell line. In addition, 17β-Estradiol down-regulated mRNA expression of *Nefm* and *Zdhhc-2*. Similar effects were observed in response to

8-Prenylnaringenin, Naringenin, Genistein, Daidzein and Equol. This clearly demonstrates that 17β-Estradiol and Naringenin induce different estrogen receptor β-mediated responses in RNDA cells. In addition, the study clearly indicates that 8-Prenylnaringenin, Genistein, Daidzein and Equol act via the same mechanism as 17β-Estradiol in the regulation of expression of those estrogen responsive genes in RNDA cells, irrespective of the employed regulatory element. Nevertheless, further experimentations such as co-immunoprecipitation experiments should be pursued to further identify which transcription factors are being involved.

It was additionally proven that RNDA cells could differentiate under non-permissive conditions (denoted as D-RNDA cells) by expressing potential markers for cellular differentiation of neuronal cells. It was clearly shown from the present study that under these differentiation conditions, changes in cell morphology, in mRNA expression levels and in responsiveness towards 17β-Estradiol or the flavonoids were observed. Most importantly, the study pointed out that the down-regulation of *Krt-19* as well as the up-regulation of *Nefm* and *Zdhhc-2* serve as indicators for RNDA cellular differentiation and that the responsiveness of the six selected genes towards 17β-Estradiol treatment as well as treatment with all tested flavonoids is almost lost in D-RNDA cells.

Despite all these findings, it is crucial to further investigate the regulation of expression of these newly identified E2-regulated genes in rat brain tissue sections using, for instance, *in situ* hybridization to investigate whether the observed *in vitro* regulation of gene expression is also present *in vivo*. It would also be of interest to track whether the regulation of these genes is only restricted to the raphe nuclei region or to other brain regions. Nevertheless, this *in vitro*-based study provides the basis to shed light on the complex molecular and cellular events following the interplay of phytoestrogens, particularly the flavonoids, with neural cell populations in the raphe nuclei.

At this point of the study, RNDA cells are still not conclusively proven useful as a good model to study effects of estrogen on serotonin production and signaling, because these processes do not seem to take place yet in the cellular phenotype of RNDA cells established so far. Therefore, future studies may include: (1) clustering the DNA

microarray data to help infer the functional role of other genes, besides the main serotonergic-related genes, that may be involved in the serotonergic pathway; hence enhancing the neuronal serotonergic phenotype of RNDA cells and (2) investigating whether 17β-Estradiol in addition to 8-Prenylnaringenin, Naringenin, Genistein, Daidzein and Equol could possibly regulate the process of serotonin production and signaling in RNDA cells. Such findings may possibly provide new avenues for the pharmacotherapeutic intervention in mood disorders related to periods of intense hormone fluctuations during menopause.

7. APPENDICES

Appendix 7-1: Proof of insufficient endogenous expression of ERβ in RN46A-B14 cells in response to 10 nM 17β-Estradiol treatment as compared to the carrier control treatment DMSO (set to 100 %).

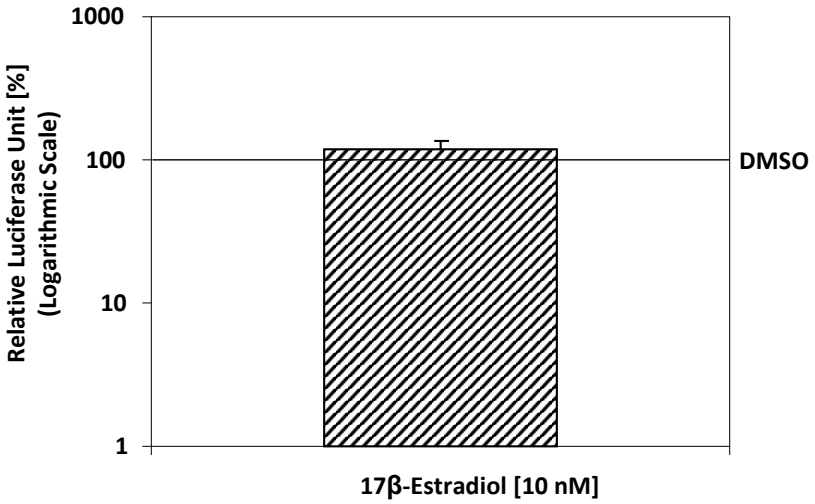

Appendix 7-2: Human *ESR2* isoform 1 genomic sequence

```
atggatataa aaaactcacc atctagcctt aattctcctt cctcctacaa ctgcagtcaa
tccatcttac ccctggagca cggctccata tacatacctt cctcctatgt agacagccac
catgaatatc cagccatgac attctatagc cctgctgtga tgaattacag cattcccagc
aatgtcacta acttggaagg tgggcctggt cggcagacca caagcccaaa tgtgttgtgg
ccaacacctg ggcacctttc tcctttagtg gtccatcgcc agttatcaca tctgtatgcg
gaacctcaaa agagtccctg gtgtgaagca agatcgctag aacacacctt acctgtaaac
agagagacac tgaaaaggaa ggttagtggg aaccgttgcg ccagccctgt tactggtcca
ggttcaaaga gggatgctca cttctgcgct gtctgcagcg attacgcatc gggatatcac
tatggagtct ggtcgtgtga aggatgtaag gccttttta aaagaagcat tcaaggacat
aatgattata tttgtccagc tacaaatcag tgtacaatcg ataaaaaccg gcgcaagagc
tgccaggcct gccgacttcg gaagtgttac gaagtgggaa tggtgaagtg tggctcccgg
agagagagat gtgggtaccg ccttgtgcgg agacagagaa gtgccgacga gcagctgcac
tgtgccggca aggccaagag aagtggcggc cacgcgcccc gagtgcggga gctgctgctg
gacgccctga gccccgagca gctagtgctc accctcctgg aggctgagcc gccccatgtg
ctgatcagcc gccccagtgc gcccttcacc gaggcctcca tgatgatgtc cctgaccaag
ttggccgaca aggagttggt acacatgatc agctgggcca agaagattcc cggctttgtg
gagctcagcc tgttcgacca agtgcggctc ttggagagct gttggatgga ggtgttaatg
atggggctga tgtggcgctc aattgaccac cccggcaagc tcatctttgc tccagatctt
gttctggaca gggatgaggg gaaatgcgta gaaggaattc tggaaatctt tgacatgctc
ctggcaacta cttcaaggtt tcgagagtta aaactccaac acaaagaata tctctgtgtc
aaggccatga tcctgctcaa ttccagtatg taccctctgg tcacagcgac ccaggatgct
gacagcagcc ggaagctggc tcacttgctg aacgccgtga ccgatgcttt ggtttgggtg
attgccaaga gcggcatctc ctcccagcag caatccatgc gcctggctaa cctcctgatg
ctcctgtccc acgtcaggca tgcgagtaac aagggcatgg aacatctgct caacatgaag
tgcaaaaatg tggtcccagt gtatgacctg ctgctggaga tgctgaatgc ccacgtgctt
cgcgggtgca agtcctccat cacggggtcc gagtgcagcc cggcagagga cagtaaaagc
aaagagggct cccagaaccc acagtctcag tga
```

Appendix 7-3: Lentiviral transfer vector map

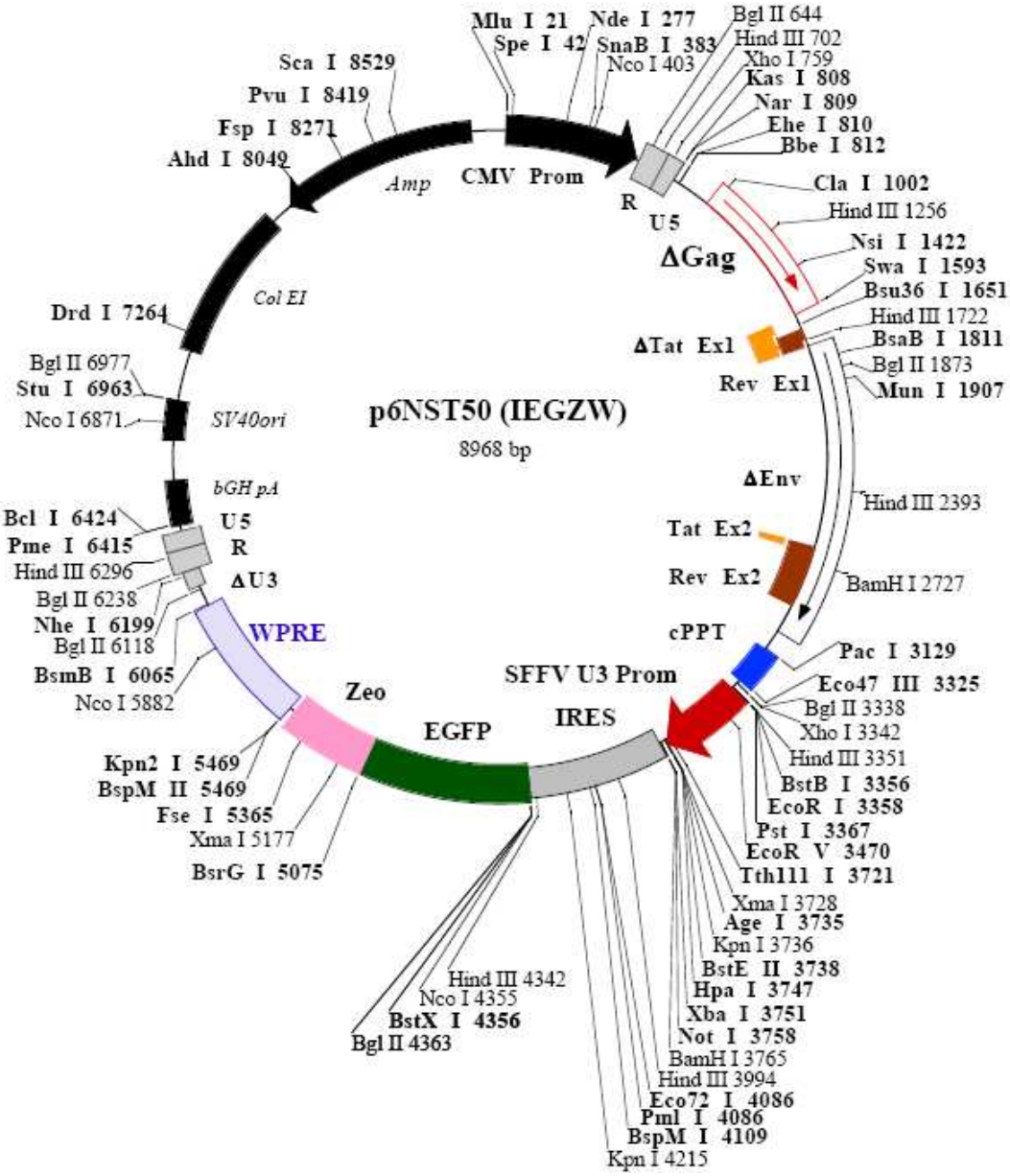

Single cutter in bold
The following enzymes do not cut in p6NST50 (IEGZW):

aax	Blp I	BsiW I	Bst XI	Bst1107 I
Esp I	Nru I	Rsr II	Sal I	Sfi I
Sph I	Spl I	Srf I	Xca I	Xcm I

Appendix 7-4: List of down-regulated transcripts in response to E2 treatment in RNDA cells (Total: 64)

Genes		
Symbol	**Description (*Rattus norvegicus* …)**	**Accession ID**
Ednrb	Endothelin Receptor type B	NM_017333
Mgc-114464	Similar to expressed sequence AI836003	NM_001024909
Tcte-3	T-complex-associated testis expressed 3	XM_344846
Enpp-1	Ectonucleotide pyrophosphatase / phosphodiesterase 1	NM_053535
Fam161a	Family with sequence similarity 161, member A	NM_001013876
Akap-11	A kinase (PRKA) anchor protein 11	AW533317
Glod-5	Glyoxalase domain containing 5	NM_001106957
Sema-3e	Sema domain, immunoglobulin domain (Ig), short basic domain, secreted, (semaphorin) 3E	NM_001106579
Olfml-2A	Olfactomedin-like 2A	NM_001106572
Hopx	HOP homeobox	NM_133621
Tgfbi	Transforming growth factor, beta induced	NM_053802
Rxrg	Retinoid X receptor gamma	NM_031765
Fmo-4	Flavin containing monooxygenase 4, transcript variant 1	NM_144562
Mgat4a	Mannosyl (alpha-1,3-)-glycoprotein beta-1,4-N-acetylglucosaminyltransferase, isozyme A, transcript variant 2	NM_001012225
Atp8a1	ATPase, aminophospholipid transporter (APLT), class I, type 8A, member 1	XM_223390
Slc6a4	**Solute carrier family 6 member 4**	**NM_013034**
Loc-363337	Similar to RIKEN cDNA 1700081O22	NM_001014221
Olr-631	olfactory receptor 631	NM_001000339
Hook-1	Hook homolog 1 (Drosophila)	NM_001107946
Rgd-1563978	Similar to mKIAA1387 protein	XM_228611
Trim-71	Tripartite motif-containing 71	XM_236676
Scn-1a	Sodium channel, voltage-gated, type I, alpha	NM_030875
Mpz	Myelin protein zero	NM_017027
Gpr-132	G protein-coupled receptor 132	NM_001170595

Ppp2r2b	Protein phosphatase 2 (formerly 2A), regulatory subunit B (PR 52), beta isoform (Ppp2r2b)	NM_022209
Loc-365528	Similar to tripartite motif-containing 40; ring finger RNF35	XM_345077
Olr-303	Olfactory receptor 303	NM_001000239
Mbl-1	Mannose-binding lectin (protein A) 1	NM_012599
Rgd-1311103	Similar to RIKEN cDNA 2410146L05	XR_007793
Htra-3	HtrA serine peptidase 3	XM_341237
Aytl-1b	Acyltransferase like 1B (Aytl1b)	NM_001025631
Cdx-2	Caudal type homeo box 2	NM_023963
Rgd-1564894	Similar to glycine-N-acyltransferase isoform a	NM_001126278
Zdhhc-2	**Zinc finger, DHHC-type containing 2**	**NM_145096**
Cpa-6	Carboxypeptidase A6	NM_001107900
Loc-296723	Similar to Fatty acid-binding protein, epidermal (E-FABP) (Cutaneous fatty acid-binding protein) (C-FABP) (DA11)	XR_005499
Bche	Butyrylcholinesterase	NM_022942
Nefm	**Neurofilament, medium polypeptide**	**NM_017029**
Slc7a11	Solute carrier family 7 (cationic amino acid transporter, y+ system), member 11	NM_001107673
G0s2	G0/G1switch 2	NM_001009632
Aldh1a3	Aldehyde dehydrogenase 1 family, member A3	NM_153300
Reln	Reelin	NM_080394
Tlr-2	Toll-like receptor 2	NM_198769
Fam101a	Family with sequence similarity 101, member A	NM_001109547
Mat-1a	Methionine adenosyltransferase I, alpha	NM_012860
Epb4.1l3	Erythrocyte protein band 4.1-like 3	NM_053927

Expressed Sequence Tags	
Description (*Rattus norvegicus* …)	**Accession ID**
UI-R-CN0 cDNA clone UI-R-CN0-bky-b-03-0-UI 3' end	BF417274
NIH_MGC_255 cDNA clone IMAGE:7318127 5' end	CO394414
Normalised rat muscle, Bento Soares cDNA clone RMUCN59 3' end	AI175447
Wackym-Soares normalised rat vestibular cDNA library	DV716578
UI-R-E1 cDNA clone UI-R-E1-fi-e-08-0-UI 3'end	AA956109
UI-R-CN1 cDNA clone UI-R-CN1-cmn-b-09-0-UI 3' end	BQ196019

UI-R-A0 cDNA clone UI-R-A0-ax-e-11-0-UI 3' similar to gb	AA818298
UI-R-AE1 cDNA clone UI-R-AE1-zj-h-05-0-UI 3' end	CK839132
UI-R-C4 cDNA clone UI-R-C4-ald-b-11-0-UI 5' end	BF564082
Wackym-Soares normalised rat vestibular cDNA library	DV713600
UI-R-EP0 cDNA clone UI-R-EP0-cnx-o-18-0-UI 3' end	BQ209143
UI-R-C3 cDNA clone UI-R-C3-sz-d-06-0-UI 3' end	AI547622
UI-R-EP0 cDNA clone UI-R-EP0-cnx-l-14-0-UI 3' end	BQ209488
Normalised rat embryo, Bento Soares cDNA clone RGICV38 5' end	AW915435
Normalised rat heart, Bento Soares cDNA clone RHEAB83 3' end	AA799505
UI-R-E1 cDNA clone UI-R-E1-gc-d-03-0-UI 5’ end	BF557223
UI-R-CA0 cDNA clone UI-R-CA0-bgm-c-12-0-UI 3' end	BF401583
Normalised rat lung, Bento Soares cDNA clone RLUCS36 3' end	AI233887

Appendix 7-5: List of up-regulated transcripts in response to E2 treatment in RNDA cells (Total: 148)

Genes		
Symbol	**Description (*Rattus norvegicus* …)**	**Accession ID**
Ckb	Creatine kinase, brain	NM_012529
Prl6a1	Prolactin family 6, subfamily a, member 1	NM_022176
Sox-9	SRY-box containing gene 9	XM_343981
Agt	Angiotensinogen (serpin peptidase inhibitor, clade A, member 8)	NM_134432
Tas2r143	Taste receptor, type 2, member 143	NM_001025061
Slco2b1	Solute carrier organic anion transporter family, member 2b1	NM_080786
Prkcz	Protein kinase C, zeta	NM_022507
Olr-264	Olfactory receptor 264	NM_001000999
Idi-2	Isopentenyl-diphosphate delta isomerase 2	XM_577595
Rgd-1306091	Similar to mixed lineage kinase 4	XM_226572
Inmt	Indolethylamine N-methyltransferase	NM_001109022
Esrrb	Estrogen-related receptor beta	NM_001008516

Tnfrsf-14	Tumor necrosis factor receptor superfamily, member 14 (herpesvirus entry mediator)	NM_001015034
Cybb	Cytochrome b-245, beta polypeptide	NM_023965
Cldn-22	Claudin 22	NM_001110143
Olr-185	Olfactory receptor 185	NM_001000183
Pnpla-5	Patatin-like phospholipase domain containing 5	NM_001130497
Tusc-5	Tumour suppressor candidate 5	NM_001039163
Loc-307938	Similar to tripartite motif-containing 9 (*TRIM9*)-like protein	XM_226563
Loc-363326	Hypothetical LOC363326	NM_001126289
Olr-1633	Olfactory receptor 1633	NM_001000835
Loc-292493	Similar to necdin	XM_218132
Cbln-1	Cerebellin 1 precursor	NM_001109127
Mfsd6l	Major facilitator superfamily domain containing 6-like	NM_001105787
Cfl	Complement factor I	NM_024157
Ocln	Occludin	NM_031329
Rgd-1310773	Similar to hypothetical protein FLJ31810	NM_001107926
Rgd-1310495	Similar to KIAA1919 protein	XM_228270
Rgd-1563150	Similar to B-cell translocation gene 1	XM_233323
Krt-19	**Keratin, type I cytoskeletal 19**	**NM_199498**
Loc-301128	Similar to jumonji domain containing 2B	BC098860
Vgll-1	Vestigial like 1 (Drosophila)	XM_343832
Otp	Orthopedia homeobox	AY169319
Gpcr-12	G protein-coupled receptor 12	NM_030831
Olr-307	Olfactory receptor 307	NM_001000241
Rgd-1303271	similar to chromosome 1 open reading frame 172	NM_001004268
Loc-367313	Similar to alpha 3 type VI collagen isoform 1 precursor; collagen VI, alpha-3 polypeptide	XM_346073
Dchs-2	Dachsous 2 (Drosophila)	XR_008777
Htr-3b	**5-hydroxytryptamine (serotonin) receptor 3b**	**NM_022189**
Rbm-4b	RNA binding motif protein 4B	AA901213
Dppa-1	Developmental pluripotency associated 1	NM_001105905
Dmp-1	Dentin matrix acidic phosphoprotein 1	NM_203493

Gas-6	Growth arrest specific 6	NM_057100
Ermap	Erythroblast membrane-associated protein	XM_233453
Olr-1733	Olfactory receptor 1733	NM_001000510
Olr-736	Olfactory receptor 736	NM_001001384
Prss-34	Protease, serine, 34	NM_001105772
Loc-246267	Resection-induced TPI (rs11)	NM_144751
Pla2g5	Phospholipase A2, group V	NM_017174
Rgd-1562546	Similar to trophinin isoform 1	XM_344729
Sstr-3	Somatostatin receptor 3	NM_133522
Pkd2l1	Polycystic kidney disease 2-like 1	NM_001106352
Olr-482	Olfactory receptor 482	NM_001000561
Slc34a1	Solute carrier family 34 (sodium phosphate), member 1	NM_013030
Tmigd-1	Transmembrane and immunoglobulin domain containing 1	NM_001135029
Mbp	Myelin basic protein, transcript variant 3	NM_001025293
Nr5a2	Nuclear receptor subfamily 5, group A, member 2	NM_021742
Havcr-2	Hepatitis A virus cellular receptor 2	NM_001100762
Gpr-35	G protein-coupled receptor 35	NM_001037359
Ckmt-2	Creatine kinase, mitochondrial 2, sarcomeric, nuclear gene encoding mitochondrial protein	NM_001127652
Sstr-2	Somatostatin receptor 2	NM_019348
Tex-19.2	Testis expressed gene 19.2	NM_001109622
Olr-851	Olfactory receptor 851	NM_001000400
Klk-10	Kallikrein related-peptidase 10	NM_001004100
Olr-1346	Olfactory receptor 1346	NM_001000520
Olr-1639	Olfactory receptor 1639	NM_001000833
Stac-2	SH3 and cysteine rich domain 2	NM_001108834
Loc-301133	Similar to tumour necrosis factor ligand superfamily member 14 (CD258 antigen)	XM_236794
Rgd-1560565	Similar to tumour protein p53 inducible protein 5	XM_574586
Olr-837	Olfactory receptor 837	NM_001000897
Loc-291014	Similar to serine/threonine kinase	XM_225194
Olr-441	Olfactory receptor 441	NM_001000283

Loc-307974	Similar to pecanex-like 2 isoform 1	XM_226603
Cacna2d2	Calcium channel, voltage-dependent, alpha 2/delta subunit 2	NM_175592
Olr-461	Olfactory receptor 461	NM_001000294
Sox-18	**Sex determining region Y-box 18**	**NM_001024781**
Rnase1l2	Ribonuclease, RNase A family, 1-like 2 (pancreatic)	NM_001025116
Wfdc-5	WAP four-disulfide core domain 5	NM_001106538
Nos1ap	Nitric oxide synthase 1 (neuronal) adaptor protein	NM_138922
Ptprt	Protein tyrosine phosphatase, receptor type, T	NM_001108603
Taar7e	Trace-amine-associated receptor 7e	NM_175590
Olr-841	Olfactory receptor 841	NM_001000405
Masp-1	Mannan-binding lectin serine peptidase 1	NM_022257
Trim-58	Tripartite motif-containing 58	XM_001075898
Il13ra1	Interleukin 13 receptor, alpha 1	NM_145789
Olr-1538	Olfactory receptor 1538	NM_001000530
Cpxm-2	Carboxypeptidase X (M14 family), member 2	NM_001106306
Cadps	Ca^{++}-dependent secretion activator	NM_013219
Olr-91	Olfactory receptor 91	NM_001000139
Bai-3	Brain-specific angiogenesis inhibitor 3	NM_001106898
Lrfn-2	Leucine rich repeat and fibronectin type III domain containing 2	NM_001039699
Igsf-1	Immunoglobulin superfamily, member 1	NM_175763
Olr-1016	Olfactory receptor 1016	NM_001000070
Cnrip-1	Cannabinoid receptor interacting protein 1	NM_001014232
Olr-252	Olfactory receptor 252	NM_001000219
Haao	3-hydroxyanthranilate 3,4-dioxygenase	NM_020076
Loc-691700	Similar to heparan sulfate D-glucosaminyl 3-O-sulfotransferase 4	XM_001079317
Olr-141	Olfactory receptor 141	NM_001001274
Olr-1428	Olfactory receptor 1428	NM_001000011
Loc-307084	Similar to heat shock protein 8	XR_006798
Olr-1598	Olfactory receptor 1598	NM_001000910
Ccdc-114	Coiled-coil domain containing 114	NM_001126277

Tcfap2d	Transcription factor AP-2, delta	NM_001106895
Htr-6	**5-hydroxytryptamine (serotonin) receptor 6**	**NM_024365**
Srebf-1	Sterol regulatory element binding factor 1	XM_213329
Loc-295811	Similar to Transcription factor DP-1 (E2F dimerization partner 1) (DRTF1-polypeptide-1)	XM_230157
Kcna-5	Potassium voltage-gated channel, shaker-related subfamily, member 5	NM_012972
Mgat5b	Mannosyl (alpha-1,6-)-glycoprotein beta-1,6-N-acetyl-glucosaminyltransferase, isozyme B	NM_001107068
Lrp-2	Low density lipoprotein-related protein 2	NM_030827
Olr-35	Olfactory receptor 35	NM_001000121
Loc-362932	Similar to cytochrome P-450-11beta	XM_343261
Alx-3	Aristaless-like homeobox 3	NM_001007012
Hhatl	Hedgehog acyltransferase-like	NM_001106868
Loc-302508	Similar to Putative deoxyribonuclease KIAA0218	XM_228696
Cora2a	Coronin, actin binding protein 2A	NM_001012101
Loc-689103	Similar to vitelliform macular dystrophy 2-like 2, transcript variant 2	XM_001066317
Gpbar-1	G protein-coupled bile acid receptor 1	NM_177936
Rgd-1565213	Similar to channel, sperm associated 4	XM_342941
Pcdhb-6	Protocadherin beta 6	NM_001014780
Cml-5	**Camello-like 5**	**NM_080884**
Olr-1309	Olfactory receptor 1309	NM_001000466
Clec11a	C-type lectin domain family 11, member a	NM_001012459
Olr-826	Olfactory receptor 826	NM_001000903

Expressed Sequence Tags	
Description (*Rattus norvegicus* …)	**Accession ID**
UI-R-E1 cDNA clone UI-R-E1-fe-h-04-0-UI 3' end	AA956265
UI-R-E0 cDNA clone UI-R-E0-dd-h-10-0-UI 3' end	AA900238
UI-R-CX0 cDNA clone UI-R-CX0-bxl-b-12-0-UI 3' end	BI276762
UI-R-C1 cDNA clone UI-R-C1-ks-e-10-0-UI 3' end	AI059063
NCI_CGAP_DZ1 cDNA clone IMAGE:7348303 3' end	BQ209739
UI-R-A0 cDNA clone UI-R-A0-am-e-04-0-UI 3' end	AA818093
Normalised rat lung, Bento Soares Rattus sp. cDNA clone RLUCS03 3' end	AI233855

UI-R-CA1 cDNA clone UI-R-CA1-biy-e-22-0-UI 3' end	BF403327
Normalised rat heart, Bento Soares Rattus sp. cDNA clone RHEAD03 3' end	AA799601
UI-R-BJ0 Rattus norvegicus cDNA clone UI-R-BJ0-aee-d-04-0-UI 3' end	AW252115
UI-R-E1 cDNA clone UI-R-E1-fv-c-11-0-UI 3' end	AA963043
UI-R-A1 cDNA clone UI-R-A1-eq-f-07-0-UI 5' end	BF556330
UI-R-CA1 cDNA clone UI-R-CA1-bip-a-10-0-UI 3' end	BF405054
UI-R-BS1 cDNA clone UI-R-BS1-ayx-a-08-0-UI 3' end	BE108243
UI-R-BT1 cDNA clone UI-R-BT1-bmy-b-09-0-UI 3' end	BF412064
UI-R-DQ0 cDNA clone UI-R-DQ0-cja-a-09-0-UI 3' end	BI303371
UI-R-E0 cDNA clone UI-R-E0-cl-a-08-0-UI 3' end	AA859335
UI-R-C2p cDNA clone UI-R-C2p-ro-c-01-0-UI 3' end	AI556829
UI-R-DK0 cDNA clone UI-R-DK0-cgk-g-07-0-UI 3' end	BI297059
UI-R-A1 cDNA clone UI-R-A1-ex-e-09-0-UI 3' end	AA955473
UI-R-C0 cDNA clone UI-R-C0-he-b-07-0-UI 3' end	AA996504
UI-R-CA0 cDNA clone UI-R-CA0-bfe-e-06-0-UI 3' end	BF392124
UI-R-C0 cDNA clone UI-R-C0-jn-c-07-0-UI 3' end	AI030133
UI-R-BJ1 cDNA clone UI-R-BJ1-awd-g-11-0-UI 3' end	BE113335
UI-R-Y0 cDNA clone UI-R-Y0-mk-b-12-0-UI 3' end	AI111559

Appendix 7-6: Proof of specificity of antibodies utilized in immunocytochemistry

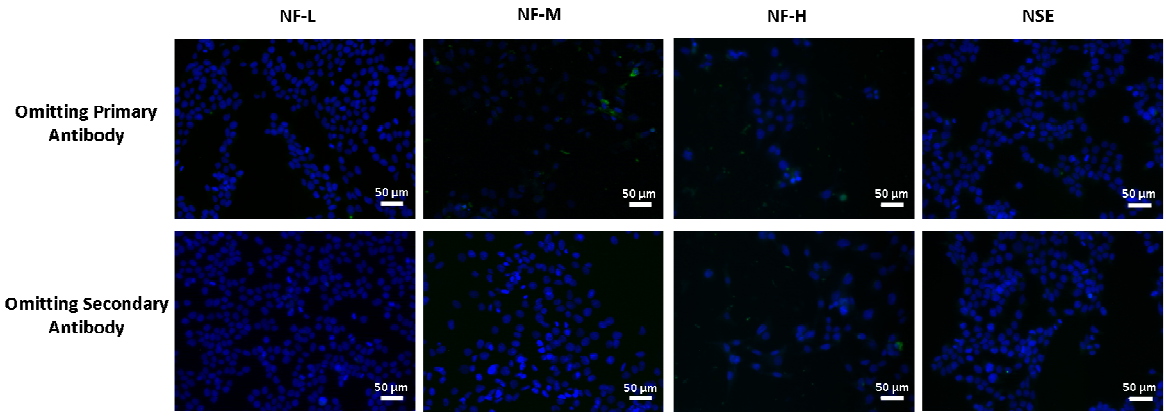

Appendix 7-7: Human ERβ mRNA expression in RNDA cells under conditions promoting proliferation (set to 1) and differentiation at either day 1 or day 4 following initiation of differentiation. Cells are treated with 0.1 % DMSO.

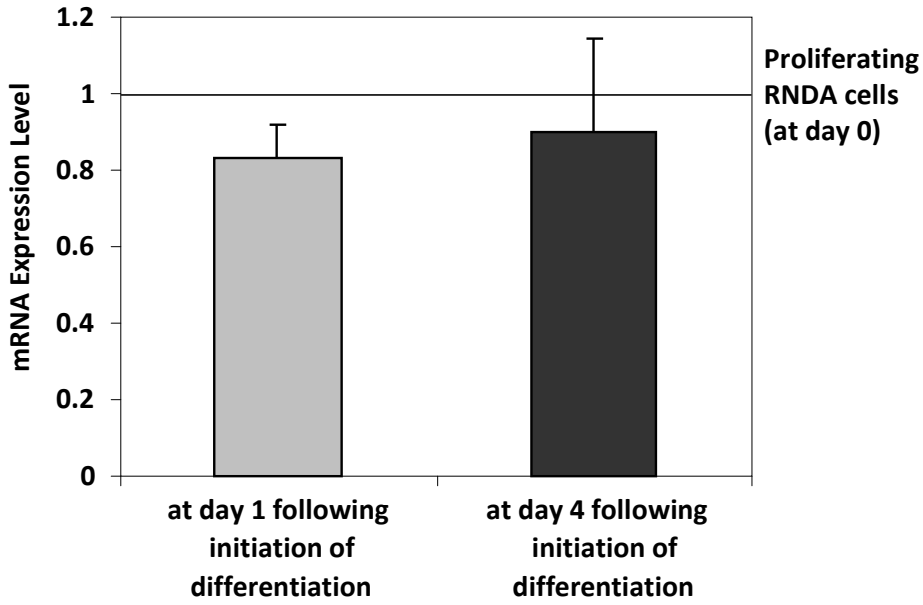

8. BIBLIOGRAPHY

Abe T. (1999). Infantile leukemia and soybeans--a hypothesis. *Leukemia* **13**(3): 317-320.

Adlercreutz H, Mazur W. (1997). Phyto-oestrogens and Western diseases. *Ann Med* **29**(2): 95-120.

Akinc A, Thomas M, Klibanov AM, Langer R. (2005). Exploring polyethylenimine-mediated DNA transfection and the proton sponge hypothesis. *J Gene Med* **7**(5): 657-663.

Amin Z, Canli T, Epperson CN. (2005). Effect of estrogen-serotonin interactions on mood and cognition. *Behav Cogn Neurosci Rev* **4**(1): 43-58.

Andreadis ST, Brott D, Fuller AO, Palsson BO. (1997). Moloney murine leukemia virus-derived retroviral vectors decay intracellularly with a half-life in the range of 5.5 to 7.5 hours. *J Virol* **71**(10): 7541-7548.

Angold A, Costello EJ, Erkanli A, Worthman CM. (1999). Pubertal changes in hormone levels and depression in girls. *Psychol Med* **29**(5): 1043-1053.

Axelson M, Sjovall J, Gustafsson BE, Setchell KD. (1984). Soya--a dietary source of the non-steroidal oestrogen equol in man and animals. *J Endocrinol* **102**(1): 49-56.

Basu S, Campbell HM, Dittel BN, Ray A. (2010). Purification of specific cell population by fluorescence activated cell sorting (FACS). *J Vis Exp*(41).

Beato M. (1989). Gene regulation by steroid hormones. *Cell* **56**(3): 335-344.

Beral V, Banks E, Reeves G, Appleby P. (1999). Use of HRT and the subsequent risk of cancer. *J Epidemiol Biostat* **4**(3): 191-210; discussion 210-195.

Berry M, Metzger D, Chambon P. (1990). Role of the two activating domains of the oestrogen receptor in the cell-type and promoter-context dependent agonistic activity of the anti-oestrogen 4-hydroxytamoxifen. *Embo J* **9**(9): 2811-2818.

Bethea CL. (1994). Regulation of progestin receptors in raphe neurons of steroid-treated monkeys. *Neuroendocrinology* **60**(1): 50-61.

Bethea CL, Lu NZ, Reddy A, Shlaes T, Streicher JM, Whittemore SR. (2003). Characterization of reproductive steroid receptors and response to estrogen in a rat serotonergic cell line. *J Neurosci Methods* **127**(1): 31-41.

Beyer C. (1999). Estrogen and the developing mammalian brain. *Anat Embryol (Berl)* **199**(5): 379-390.

Bjornstrom L, Sjoberg M. (2005). Mechanisms of estrogen receptor signaling: convergence of genomic and nongenomic actions on target genes. *Mol Endocrinol* **19**(4): 833-842.

Bocchinfuso WP, Korach KS. (1997). Mammary gland development and tumorigenesis in estrogen receptor knockout mice. *J Mammary Gland Biol Neoplasia* **2**(4): 323-334.

Bortolato M, Chen K, Shih JC. (2008). Monoamine oxidase inactivation: from pathophysiology to therapeutics. *Adv Drug Deliv Rev* **60**(13-14): 1527-1533.

Boussif O, Lezoualc'h F, Zanta MA, Mergny MD, Scherman D, Demeneix B *et al.* (1995). A versatile vector for gene and oligonucleotide transfer into cells in culture and in vivo: polyethylenimine. *Proc Natl Acad Sci U S A* **92**(16): 7297-7301.

Bowler J, Lilley TJ, Pittam JD, Wakeling AE. (1989). Novel steroidal pure antiestrogens. *Steroids* **54**(1): 71-99.

Brandenberger AW, Tee MK, Lee JY, Chao V, Jaffe RB. (1997). Tissue distribution of estrogen receptors alpha (ER-alpha) and beta (ER-beta) mRNA in the midgestational human fetus. *J Clin Endocrinol Metab* **82**(10): 3509-3512.

Breckpot K, Corthals J, Heirman C, Bonehill A, Michiels A, Tuyaerts S *et al.* (2004). Activation of monocytes via the CD14 receptor leads to the enhanced lentiviral transduction of immature dendritic cells. *Hum Gene Ther* **15**(6): 562-573.

Brown NM, Setchell KD. (2001). Animal models impacted by phytoestrogens in commercial chow: implications for pathways influenced by hormones. *Lab Invest* **81**(5): 735-747.

Brzozowski AM, Pike AC, Dauter Z, Hubbard RE, Bonn T, Engstrom O *et al.* (1997). Molecular basis of agonism and antagonism in the oestrogen receptor. *Nature* **389**(6652): 753-758.

Bukrinsky MI, Haggerty S, Dempsey MP, Sharova N, Adzhubel A, Spitz L *et al.* (1993). A nuclear localization signal within HIV-1 matrix protein that governs infection of non-dividing cells. *Nature* **365**(6447): 666-669.

Bulayeva NN, Gametchu B, Watson CS. (2004). Quantitative measurement of estrogen-induced ERK 1 and 2 activation via multiple membrane-initiated signaling pathways. *Steroids* **69**(3): 181-192.

Byers M, Kuiper GG, Gustafsson JA, Park-Sarge OK. (1997). Estrogen receptor-beta mRNA expression in rat ovary: down-regulation by gonadotropins. *Mol Endocrinol* **11**(2): 172-182.

Campbell-Thompson M, Lynch IJ, Bhardwaj B. (2001). Expression of estrogen receptor (ER) subtypes and ERbeta isoforms in colon cancer. *Cancer Res* **61**(2): 632-640.

Cassidy A, Albertazzi P, Lise Nielsen I, Hall W, Williamson G, Tetens I *et al.* (2006). Critical review of health effects of soyabean phyto-oestrogens in post-menopausal women. *Proc Nutr Soc* **65**(1): 76-92.

Chan HM, La Thangue NB. (2001). p300/CBP proteins: HATs for transcriptional bridges and scaffolds. *J Cell Sci* **114**(Pt 13): 2363-2373.

Chan YL, Paz V, Wool IG. (1991). The primary structure of rat ribosomal protein S18. *Biochem Biophys Res Commun* **178**(3): 1212-1218.

Chen FP. (2009). Postmenopausal hormone therapy and risk of breast cancer. *Chang Gung Med J* **32**(2): 140-147.

Cheskis BJ, Greger JG, Nagpal S, Freedman LP. (2007). Signaling by estrogens. *J Cell Physiol* **213**(3): 610-617.

Chlebowski RT, Hendrix SL, Langer RD, Stefanick ML, Gass M, Lane D *et al.* (2003). Influence of estrogen plus progestin on breast cancer and mammography in healthy postmenopausal women: the Women's Health Initiative Randomized Trial. *Jama* **289**(24): 3243-3253.

Chlebowski RT, Kuller LH, Prentice RL, Stefanick ML, Manson JE, Gass M *et al.* (2009). Breast cancer after use of estrogen plus progestin in postmenopausal women. *N Engl J Med* **360**(6): 573-587.

Choi I, Gudas LJ, Katzenellenbogen BS. (2000). Regulation of keratin 19 gene expression by estrogen in human breast cancer cells and identification of the estrogen responsive gene region. *Mol Cell Endocrinol* **164**(1-2): 225-237.

Christoffel J, Rimoldi G, Wuttke W. (2006). Effects of 8-prenylnaringenin on the hypothalamo-pituitary-uterine axis in rats after 3-month treatment. *J Endocrinol* **188**(3): 397-405.

Chung BC, Picado-Leonard J, Haniu M, Bienkowski M, Hall PF, Shively JE *et al.* (1987). Cytochrome P450c17 (steroid 17 alpha-hydroxylase/17,20 lyase): cloning of human adrenal and testis cDNAs indicates the same gene is expressed in both tissues. *Proc Natl Acad Sci U S A* **84**(2): 407-411.

Cleverley KE, Betts JC, Blackstock WP, Gallo JM, Anderton BH. (1998). Identification of novel in vitro PKA phosphorylation sites on the low and middle molecular mass neurofilament subunits by mass spectrometry. *Biochemistry* **37**(11): 3917-3930.

Cos P, De Bruyne T, Apers S, Vanden Berghe D, Pieters L, Vlietinck AJ. (2003). Phytoestrogens: recent developments. *Planta Med* **69**(7): 589-599.

Couse JF, Curtis SW, Washburn TF, Lindzey J, Golding TS, Lubahn DB *et al.* (1995). Analysis of transcription and estrogen insensitivity in the female mouse after

targeted disruption of the estrogen receptor gene. *Mol Endocrinol* **9**(11): 1441-1454.

Couse JF, Korach KS. (1999). Estrogen receptor null mice: what have we learned and where will they lead us? *Endocr Rev* **20**(3): 358-417.

Crain DA, Janssen SJ, Edwards TM, Heindel J, Ho SM, Hunt P *et al.* (2008). Female reproductive disorders: the roles of endocrine-disrupting compounds and developmental timing. *Fertil Steril* **90**(4): 911-940.

Danielian PS, White R, Lees JA, Parker MG. (1992). Identification of a conserved region required for hormone dependent transcriptional activation by steroid hormone receptors. *Embo J* **11**(3): 1025-1033.

Darimont BD, Wagner RL, Apriletti JW, Stallcup MR, Kushner PJ, Baxter JD *et al.* (1998). Structure and specificity of nuclear receptor-coactivator interactions. *Genes Dev* **12**(21): 3343-3356.

Dauvois S, White R, Parker MG. (1993). The antiestrogen ICI 182780 disrupts estrogen receptor nucleocytoplasmic shuttling. *J Cell Sci* **106 (Pt 4)**: 1377-1388.

Davis SR, Dalais FS, Simpson ER, Murkies AL. (1999). Phytoestrogens in health and disease. *Recent Prog Horm Res* **54**: 185-210; discussion 210-181.

Day M, Sung A, Logue S, Bowlby M, Arias R. (2005). Beta estrogen receptor knockout (BERKO) mice present attenuated hippocampal CA1 long-term potentiation and related memory deficits in contextual fear conditioning. *Behav Brain Res* **164**(1): 128-131.

Dilworth FJ, Chambon P. (2001). Nuclear receptors coordinate the activities of chromatin remodeling complexes and coactivators to facilitate initiation of transcription. *Oncogene* **20**(24): 3047-3054.

Dilworth FJ, Fromental-Ramain C, Yamamoto K, Chambon P. (2000). ATP-driven chromatin remodeling activity and histone acetyltransferases act sequentially during transactivation by RAR/RXR In vitro. *Mol Cell* **6**(5): 1049-1058.

Donner N, Handa RJ. (2009). Estrogen receptor beta regulates the expression of tryptophan-hydroxylase 2 mRNA within serotonergic neurons of the rat dorsal raphe nuclei. *Neuroscience* **163**(2): 705-718.

Dötsch J, Dörr HG, Wildt L. (2001). *The Handbook of Environmental Chemistry: Exposure to Endogenous Estrogens During Lifetime.* Berlin Heidelberg: Springer-Verlag.

Douma SL, Husband C, O'Donnell ME, Barwin BN, Woodend AK. (2005). Estrogen-related mood disorders: reproductive life cycle factors. *ANS Adv Nurs Sci* **28**(4): 364-375.

Driscoll MD, Sathya G, Muyan M, Klinge CM, Hilf R, Bambara RA. (1998). Sequence requirements for estrogen receptor binding to estrogen response elements. *J Biol Chem* **273**(45): 29321-29330.

DuBridge RB, Tang P, Hsia HC, Leong PM, Miller JH, Calos MP. (1987). Analysis of mutation in human cells by using an Epstein-Barr virus shuttle system. *Mol Cell Biol* **7**(1): 379-387.

Dupont S, Krust A, Gansmuller A, Dierich A, Chambon P, Mark M. (2000). Effect of single and compound knockouts of estrogen receptors alpha (ERalpha) and beta (ERbeta) on mouse reproductive phenotypes. *Development* **127**(19): 4277-4291.

Dupont WD, Page DL. (1991). Menopausal estrogen replacement therapy and breast cancer. *Arch Intern Med* **151**(1): 67-72.

Effenberger KE, Johnsen SA, Monroe DG, Spelsberg TC, Westendorf JJ. (2005). Regulation of osteoblastic phenotype and gene expression by hop-derived phytoestrogens. *J Steroid Biochem Mol Biol* **96**(5): 387-399.

Eisenberg E, Levanon EY. (2003). Human housekeeping genes are compact. *Trends Genet* **19**(7): 362-365.

Ellis RJ, van der Vies SM, Hemmingsen SM. (1989). The molecular chaperone concept. *Biochem Soc Symp* **55**: 145-153.

Enmark E, Gustafsson JA. (1999). Oestrogen receptors - an overview. *J Intern Med* **246**(2): 133-138.

Enmark E, Pelto-Huikko M, Grandien K, Lagercrantz S, Lagercrantz J, Fried G *et al.* (1997). Human estrogen receptor beta-gene structure, chromosomal localization, and expression pattern. *J Clin Endocrinol Metab* **82**(12): 4258-4265.

Enna SJ. (2010). A legacy of discovery: From monoamines to GABA. *Neuropharmacology* **Epub ahead of print**: 1-8.

Evans RM. (1988). The steroid and thyroid hormone receptor superfamily. *Science* **240**(4854): 889-895.

Fare TL, Coffey EM, Dai H, He YD, Kessler DA, Kilian KA *et al.* (2003). Effects of atmospheric ozone on microarray data quality. *Anal Chem* **75**(17): 4672-4675.

Fisher JS. (2004). Environmental anti-androgens and male reproductive health: focus on phthalates and testicular dysgenesis syndrome. *Reproduction* **127**(3): 305-315.

Foley EF, Jazaeri AA, Shupnik MA, Jazaeri O, Rice LW. (2000). Selective loss of estrogen receptor beta in malignant human colon. *Cancer Res* **60**(2): 245-248.

Forman BM, Samuels HH. (1990). Interactions among a subfamily of nuclear hormone receptors: the regulatory zipper model. *Mol Endocrinol* **4**(9): 1293-1301.

Freeman WM, Robertson DJ, Vrana KE. (2000). Fundamentals of DNA hybridization arrays for gene expression analysis. *Biotechniques* **29**(5): 1042-1046, 1048-1055.

Friso A, Tomanin R, Salvalaio M, Scarpa M. (2010). Genistein reduces glycosaminoglycan levels in a mouse model of mucopolysaccharidosis type II. *Br J Pharmacol* **159**(5): 1082-1091.

Fukata Y, Fukata M. (2010). Protein palmitoylation in neuronal development and synaptic plasticity. *Nat Rev Neurosci* **11**(3): 161-175.

Furukawa A, Miyatake A, Ohnishi T, Ichikawa Y. (1998). Steroidogenic acute regulatory protein (StAR) transcripts constitutively expressed in the adult rat central nervous system: colocalization of StAR, cytochrome P-450SCC (CYP XIA1), and 3beta-hydroxysteroid dehydrogenase in the rat brain. *J Neurochem* **71**(6): 2231-2238.

Geisler JG, Zawalich W, Zawalich K, Lakey JR, Stukenbrok H, Milici AJ *et al.* (2002). Estrogen can prevent or reverse obesity and diabetes in mice expressing human islet amyloid polypeptide. *Diabetes* **51**(7): 2158-2169.

George FW, Wilson JD. (1988). *The Physiology of Reproduction.* New York: Raven Press.

Gester S, Metz P, Zierau O, Vollmer G. (2001). An Efficient Synthesis of the Potent Phytoestrogens 8-Prenylnaringenin and 6-(1,1-Dimethylallyl)naringenin by Europium(III)-Catalyzed Claisen Rearrangement. *Tetrahedron* **57**: 1015-1018.

Giguere V, Yang N, Segui P, Evans RM. (1988). Identification of a new class of steroid hormone receptors. *Nature* **331**(6151): 91-94.

Givan AL. (2004). Flow cytometry: an introduction. *Methods Mol Biol* **263**: 1-32.

Green S, Chambon P. (1986). A superfamily of potentially oncogenic hormone receptors. *Nature* **324**(6098): 615-617.

Green S, Walter P, Kumar V, Krust A, Bornert JM, Argos P *et al.* (1986). Human oestrogen receptor cDNA: sequence, expression and homology to v-erb-A. *Nature* **320**(6058): 134-139.

Grigoriadis S, Kennedy SH. (2002). Role of estrogen in the treatment of depression. *Am J Ther* **9**(6): 503-509.

Grodstein F, Stampfer MJ, Colditz GA, Willett WC, Manson JE, Joffe M *et al.* (1997). Postmenopausal hormone therapy and mortality. *N Engl J Med* **336**(25): 1769-1775.

Gruber CJ, Tschugguel W, Schneeberger C, Huber JC. (2002). Production and actions of estrogens. *N Engl J Med* **346**(5): 340-352.

Gu Q, Moss RL. (1996). 17 beta-Estradiol potentiates kainate-induced currents via activation of the cAMP cascade. *J Neurosci* **16**(11): 3620-3629.

Gundlah C, Lu NZ, Bethea CL. (2002). Ovarian steroid regulation of monoamine oxidase-A and -B mRNAs in the macaque dorsal raphe and hypothalamic nuclei. *Psychopharmacology (Berl)* **160**(3): 271-282.

Gundlah C, Lu NZ, Mirkes SJ, Bethea CL. (2001). Estrogen receptor beta (ERbeta) mRNA and protein in serotonin neurons of macaques. *Brain Res Mol Brain Res* **91**(1-2): 14-22.

Hasbi A, O'Dowd BF, George SR. (2005). A G protein-coupled receptor for estrogen: the end of the search? *Mol Interv* **5**(3): 158-161.

Henderson VW, Paganini-Hill A, Emanuel CK, Dunn ME, Buckwalter JG. (1994). Estrogen replacement therapy in older women. Comparisons between Alzheimer's disease cases and nondemented control subjects. *Arch Neurol* **51**(9): 896-900.

Hilakivi-Clarke L, Onojafe I, Raygada M, Cho E, Skaar T, Russo I *et al.* (1999). Prepubertal exposure to zearalenone or genistein reduces mammary tumorigenesis. *Br J Cancer* **80**(11): 1682-1688.

Hiller-Sturmhofel S, Bartke A. (1998). The endocrine system: an overview. *Alcohol Health Res World* **22**(3): 153-164.

Hornung JP. (2003). The human raphe nuclei and the serotonergic system. *J Chem Neuroanat* **26**(4): 331-343.

Hoyer D, Hannon JP, Martin GR. (2002). Molecular, pharmacological and functional diversity of 5-HT receptors. *Pharmacol Biochem Behav* **71**(4): 533-554.

Hrabovszky E, Kallo I, Hajszan T, Shughrue PJ, Merchenthaler I, Liposits Z. (1998). Expression of estrogen receptor-beta messenger ribonucleic acid in oxytocin and vasopressin neurons of the rat supraoptic and paraventricular nuclei. *Endocrinology* **139**(5): 2600-2604.

Ise R, Han D, Takahashi Y, Terasaka S, Inoue A, Tanji M *et al.* (2005). Expression profiling of the estrogen responsive genes in response to phytoestrogens using a customized DNA microarray. *FEBS Lett* **579**(7): 1732-1740.

Jensen EV, Jacobson HI. (1962). Basic guides to the mechanism of estrogen action. *Recent Prog Horm Res* **18**: 387-414.

Jenuwein T, Allis CD. (2001). Translating the histone code. *Science* **293**(5532): 1074-1080.

Jin Y, Wu H, Cohen EM, Wei J, Jin H, Prentice H *et al.* (2007). Genistein and daidzein induce neurotoxicity at high concentrations in primary rat neuronal cultures. *J Biomed Sci* **14**(2): 275-284.

Johnston SJ, Cheung KL. (2010). Fulvestrant - a novel endocrine therapy for breast cancer. *Curr Med Chem* **17**(10): 902-914.

Joung KE, Kim YW, Sheen YY. (2003). Assessment of the estrogenicity of isoflavonoids, using MCF-7-ERE-Luc cells. *Arch Pharm Res* **26**(9): 756-762.

Julius D. (1991). Molecular biology of serotonin receptors. *Annu Rev Neurosci* **14**: 335-360.

Kalbe C, Mau M, Wollenhaupt K, Rehfeldt C. (2007). Evidence for estrogen receptor alpha and beta expression in skeletal muscle of pigs. *Histochem Cell Biol* **127**(1): 95-107.

Kalra SP, Kalra PS. (2010). Neuroendocrine control of energy homeostasis: update on new insights. *Prog Brain Res* **181**: 17-33.

Karlsson JO, Ostwald K, Kabjorn C, Andersson M. (1994). A method for protein assay in Laemmli buffer. *Anal Biochem* **219**(1): 144-146.

Kato S, Endoh H, Masuhiro Y, Kitamoto T, Uchiyama S, Sasaki H *et al.* (1995). Activation of the estrogen receptor through phosphorylation by mitogen-activated protein kinase. *Science* **270**(5241): 1491-1494.

Katzenellenbogen JA, O'Malley BW, Katzenellenbogen BS. (1996). Tripartite steroid hormone receptor pharmacology: interaction with multiple effector sites as a basis for the cell- and promoter-specific action of these hormones. *Mol Endocrinol* **10**(2): 119-131.

Kelly MJ, Lagrange AH, Wagner EJ, Ronnekleiv OK. (1999). Rapid effects of estrogen to modulate G protein-coupled receptors via activation of protein kinase A and protein kinase C pathways. *Steroids* **64**(1-2): 64-75.

Kent WJ, Sugnet CW, Furey TS, Roskin KM, Pringle TH, Zahler AM *et al.* (2002). The human genome browser at UCSC. *Genome Res* **12**(6): 996-1006.

Kessler RC, McGonagle KA, Zhao S, Nelson CB, Hughes M, Eshleman S *et al.* (1994). Lifetime and 12-month prevalence of DSM-III-R psychiatric disorders in the United States. Results from the National Comorbidity Survey. *Arch Gen Psychiatry* **51**(1): 8-19.

Kim J. (2008). Protective effects of Asian dietary items on cancers - soy and ginseng. *Asian Pac J Cancer Prev* **9**(4): 543-548.

Kirino T, Brightman MW, Oertel WH, Schmechel DE, Marangos PJ. (1983). Neuron-specific enolase as an index of neuronal regeneration and reinnervation. *J Neurosci* **3**(5): 915-923.

Klaiber EL, Broverman DM, Vogel W, Kobayashi Y. (1979). Estrogen therapy for severe persistent depressions in women. *Arch Gen Psychiatry* **36**(5): 550-554.

Klinge CM. (2001). Estrogen receptor interaction with estrogen response elements. *Nucleic Acids Res* **29**(14): 2905-2919.

Knapen D, Vergauwen L, Laukens K, Blust R. (2009). Best practices for hybridization design in two-colour microarray analysis. *Trends Biotechnol* **27**(7): 406-414.

Knight DC, Eden JA. (1996). A review of the clinical effects of phytoestrogens. *Obstet Gynecol* **87**(5 Pt 2): 897-904.

Kobayashi Y, Kitamoto T, Masuhiro Y, Watanabe M, Kase T, Metzger D *et al.* (2000). p300 mediates functional synergism between AF-1 and AF-2 of estrogen receptor alpha and beta by interacting directly with the N-terminal A/B domains. *J Biol Chem* **275**(21): 15645-15651.

Koh SS, Chen D, Lee YH, Stallcup MR. (2001). Synergistic enhancement of nuclear receptor function by p160 coactivators and two coactivators with protein methyltransferase activities. *J Biol Chem* **276**(2): 1089-1098.

Koike S, Sakai M, Muramatsu M. (1987). Molecular cloning and characterization of rat estrogen receptor cDNA. *Nucleic Acids Res* **15**(6): 2499-2513.

Kousteni S, Bellido T, Plotkin LI, O'Brien CA, Bodenner DL, Han L *et al.* (2001). Nongenotropic, sex-nonspecific signaling through the estrogen or androgen receptors: dissociation from transcriptional activity. *Cell* **104**(5): 719-730.

Krege JH, Hodgin JB, Couse JF, Enmark E, Warner M, Mahler JF *et al.* (1998). Generation and reproductive phenotypes of mice lacking estrogen receptor beta. *Proc Natl Acad Sci U S A* **95**(26): 15677-15682.

Kretzschmar G, Vollmer G, Schwab P, Tischer S, Metz P, Zierau O. (2007). Effects of the chemically synthesized flavanone 7-(O-prenyl)naringenin-4'-acetate on the estrogen signaling pathway in vivo and in vitro. *J Steroid Biochem Mol Biol* **107**(1-2): 114-119.

Kretzschmar G, Zierau O, Wober J, Tischer S, Metz P, Vollmer G. (2010). Prenylation has a compound specific effect on the estrogenicity of naringenin and genistein. *J Steroid Biochem Mol Biol* **118**(1-2): 1-6.

Kroeze WK, Kristiansen K, Roth BL. (2002). Molecular biology of serotonin receptors structure and function at the molecular level. *Curr Top Med Chem* **2**(6): 507-528.

Kuiper GG, Carlsson B, Grandien K, Enmark E, Haggblad J, Nilsson S *et al.* (1997). Comparison of the ligand binding specificity and transcript tissue distribution of estrogen receptors alpha and beta. *Endocrinology* **138**(3): 863-870.

Kuiper GG, Enmark E, Pelto-Huikko M, Nilsson S, Gustafsson JA. (1996). Cloning of a novel receptor expressed in rat prostate and ovary. *Proc Natl Acad Sci U S A* **93**(12): 5925-5930.

Kuiper GG, Lemmen JG, Carlsson B, Corton JC, Safe SH, van der Saag PT *et al.* (1998). Interaction of estrogenic chemicals and phytoestrogens with estrogen receptor beta. *Endocrinology* **139**(10): 4252-4263.

Kumar V, Green S, Stack G, Berry M, Jin JR, Chambon P. (1987). Functional domains of the human estrogen receptor. *Cell* **51**(6): 941-951.

Kurata K, Takebayashi M, Kagaya A, Morinobu S, Yamawaki S. (2001). Effect of beta-estradiol on voltage-gated Ca(2+) channels in rat hippocampal neurons: a comparison with dehydroepiandrosterone. *Eur J Pharmacol* **416**(3): 203-212.

Lalonde R, Strazielle C. (2003). Neurobehavioral characteristics of mice with modified intermediate filament genes. *Rev Neurosci* **14**(4): 369-385.

Langer G, Bader B, Meoli L, Isensee J, Delbeck M, Noppinger PR *et al.* (2010). A critical review of fundamental controversies in the field of GPR30 research. *Steroids* **75**(8-9): 603-610.

Le Doux JM, Davis HE, Morgan JR, Yarmush ML. (1999). Kinetics of retrovirus production and decay. *Biotechnol Bioeng* **63**(6): 654-662.

Lee HJ, Macbeth AH, Pagani JH, Young WS, 3rd. (2009). Oxytocin: the great facilitator of life. *Prog Neurobiol* **88**(2): 127-151.

Lewis PF, Emerman M. (1994). Passage through mitosis is required for oncoretroviruses but not for the human immunodeficiency virus. *J Virol* **68**(1): 510-516.

Li J, Wang J, Wang J, Nawaz Z, Liu JM, Qin J *et al.* (2000). Both corepressor proteins SMRT and N-CoR exist in large protein complexes containing HDAC3. *Embo J* **19**(16): 4342-4350.

Losel R, Wehling M. (2003). Nongenomic actions of steroid hormones. *Nat Rev Mol Cell Biol* **4**(1): 46-56.

Lu H, Ozawa H, Nishi M, Ito T, Kawata M. (2001). Serotonergic neurones in the dorsal raphe nucleus that project into the medial preoptic area contain oestrogen receptor beta. *J Neuroendocrinol* **13**(10): 839-845.

Lubahn DB, Moyer JS, Golding TS, Couse JF, Korach KS, Smithies O. (1993). Alteration of reproductive function but not prenatal sexual development after insertional

disruption of the mouse estrogen receptor gene. *Proc Natl Acad Sci U S A* **90**(23): 11162-11166.

Lucki NC, Sewer MB. (2010). The interplay between bioactive sphingolipids and steroid hormones. *Steroids* **75**(6): 390-399.

Lundholm L, Moverare S, Steffensen KR, Nilsson M, Otsuki M, Ohlsson C *et al.* (2004). Gene expression profiling identifies liver X receptor alpha as an estrogen-regulated gene in mouse adipose tissue. *J Mol Endocrinol* **32**(3): 879-892.

Maggiolini M, Picard D. (2010). The unfolding stories of GPR30, a new membrane-bound estrogen receptor. *J Endocrinol* **204**(2): 105-114.

Malik S, Roeder RG. (2005). Dynamic regulation of pol II transcription by the mammalian Mediator complex. *Trends Biochem Sci* **30**(5): 256-263.

Mangelsdorf DJ, Thummel C, Beato M, Herrlich P, Schutz G, Umesono K *et al.* (1995). The nuclear receptor superfamily: the second decade. *Cell* **83**(6): 835-839.

Margolis RN, Christakos S. (2010). The nuclear receptor superfamily of steroid hormones and vitamin D gene regulation. An update. *Ann N Y Acad Sci* **1192**: 208-214.

Margueron R, Trojer P, Reinberg D. (2005). The key to development: interpreting the histone code? *Curr Opin Genet Dev* **15**(2): 163-176.

Markiewicz L, Garey J, Adlercreutz H, Gurpide E. (1993). In vitro bioassays of non-steroidal phytoestrogens. *J Steroid Biochem Mol Biol* **45**(5): 399-405.

Martin PM, Horwitz KB, Ryan DS, McGuire WL. (1978). Phytoestrogen interaction with estrogen receptors in human breast cancer cells. *Endocrinology* **103**(5): 1860-1867.

Maxwell BL, McDonnell DP, Conneely OM, Schulz TZ, Greene GL, O'Malley BW. (1987). Structural organization and regulation of the chicken estrogen receptor. *Mol Endocrinol* **1**(1): 25-35.

McEwen BS. (2001). Invited review: Estrogens effects on the brain: multiple sites and molecular mechanisms. *J Appl Physiol* **91**(6): 2785-2801.

McEwen BS, Alves SE. (1999). Estrogen actions in the central nervous system. *Endocr Rev* **20**(3): 279-307.

McInerney EM, Rose DW, Flynn SE, Westin S, Mullen TM, Krones A *et al.* (1998). Determinants of coactivator LXXLL motif specificity in nuclear receptor transcriptional activation. *Genes Dev* **12**(21): 3357-3368.

Meethal SV, Liu T, Chan HW, Ginsburg E, Wilson AC, Gray DN *et al.* (2009). Identification of a regulatory loop for the synthesis of neurosteroids: a steroidogenic acute

regulatory protein-dependent mechanism involving hypothalamic-pituitary-gonadal axis receptors. *J Neurochem* **110**(3): 1014-1027.

Meltzer-Brody S. (2010). Puberty to perimenopause: Understanding and treating mood disorders across the reproductive years. *Sexuality, Reproduction & Menopause* **8**(4): 12-18.

Meyers MJ, Sun J, Carlson KE, Marriner GA, Katzenellenbogen BS, Katzenellenbogen JA. (2001). Estrogen receptor-beta potency-selective ligands: structure-activity relationship studies of diarylpropionitriles and their acetylene and polar analogues. *J Med Chem* **44**(24): 4230-4251.

Miller WL. (1988). Molecular biology of steroid hormone synthesis. *Endocr Rev* **9**(3): 295-318.

Milligan S, Kalita J, Pocock V, Heyerick A, De Cooman L, Rong H *et al.* (2002). Oestrogenic activity of the hop phyto-oestrogen, 8-prenylnaringenin. *Reproduction* **123**(2): 235-242.

Milligan SR, Kalita JC, Pocock V, Van De Kauter V, Stevens JF, Deinzer ML *et al.* (2000). The endocrine activities of 8-prenylnaringenin and related hop (Humulus lupulus L.) flavonoids. *J Clin Endocrinol Metab* **85**(12): 4912-4915.

Miyamoto T, Kakizawa T, Ichikawa K, Nishio S, Takeda T, Suzuki S *et al.* (2001). The role of hinge domain in heterodimerization and specific DNA recognition by nuclear receptors. *Mol Cell Endocrinol* **181**(1-2): 229-238.

Moggs JG, Ashby J, Tinwell H, Lim FL, Moore DJ, Kimber I *et al.* (2004). The need to decide if all estrogens are intrinsically similar. *Environ Health Perspect* **112**(11): 1137-1142.

Monroe DG, Getz BJ, Johnsen SA, Riggs BL, Khosla S, Spelsberg TC. (2003). Estrogen receptor isoform-specific regulation of endogenous gene expression in human osteoblastic cell lines expressing either ERalpha or ERbeta. *J Cell Biochem* **90**(2): 315-326.

Moras D, Gronemeyer H. (1998). The nuclear receptor ligand-binding domain: structure and function. *Curr Opin Cell Biol* **10**(3): 384-391.

Morey JS, Ryan JC, Van Dolah FM. (2006). Microarray validation: factors influencing correlation between oligonucleotide microarrays and real-time PCR. *Biol Proced Online* **8**: 175-193.

Moss GP. (1989). IUPAC-IUB Joint Commission on Biochemical Nomenclature (JCBN). The nomenclature of steroids. Recommendations 1989. *Eur J Biochem* **186**(3): 429-458.

Mosselman S, Polman J, Dijkema R. (1996). ER beta: identification and characterization of a novel human estrogen receptor. *FEBS Lett* **392**(1): 49-53.

Munro IC, Harwood M, Hlywka JJ, Stephen AM, Doull J, Flamm WG *et al.* (2003). Soy isoflavones: a safety review. *Nutr Rev* **61**(1): 1-33.

Murphy DL, Fox MA, Timpano KR, Moya PR, Ren-Patterson R, Andrews AM *et al.* (2008). How the serotonin story is being rewritten by new gene-based discoveries principally related to SLC6A4, the serotonin transporter gene, which functions to influence all cellular serotonin systems. *Neuropharmacology* **55**(6): 932-960.

Muthyala RS, Ju YH, Sheng S, Williams LD, Doerge DR, Katzenellenbogen BS *et al.* (2004). Equol, a natural estrogenic metabolite from soy isoflavones: convenient preparation and resolution of R- and S-equols and their differing binding and biological activity through estrogen receptors alpha and beta. *Bioorg Med Chem* **12**(6): 1559-1567.

Naldini L, Blomer U, Gallay P, Ory D, Mulligan R, Gage FH *et al.* (1996). In vivo gene delivery and stable transduction of nondividing cells by a lentiviral vector. *Science* **272**(5259): 263-267.

Nelson HD. (2008). Menopause. *Lancet* **371**(9614): 760-770.

Nilsson S, Makela S, Treuter E, Tujague M, Thomsen J, Andersson G *et al.* (2001). Mechanisms of estrogen action. *Physiol Rev* **81**(4): 1535-1565.

Nolan T, Hands RE, Bustin SA. (2006). Quantification of mRNA using real-time RT-PCR. *Nat Protoc* **1**(3): 1559-1582.

Nomura M, Akama KT, Alves SE, Korach KS, Gustafsson JA, Pfaff DW *et al.* (2005). Differential distribution of estrogen receptor (ER)-alpha and ER-beta in the midbrain raphe nuclei and periaqueductal gray in male mouse: Predominant role of ER-beta in midbrain serotonergic systems. *Neuroscience* **130**(2): 445-456.

Norris JD, Paige LA, Christensen DJ, Chang CY, Huacani MR, Fan D *et al.* (1999). Peptide antagonists of the human estrogen receptor. *Science* **285**(5428): 744-746.

Noteboom WD, Gorski J. (1965). Stereospecific binding of estrogens in the rat uterus. *Arch Biochem Biophys* **111**(3): 559-568.

O'Brien JE, Peterson TJ, Tong MH, Lee EJ, Pfaff LE, Hewitt SC *et al.* (2006). Estrogen-induced proliferation of uterine epithelial cells is independent of estrogen receptor alpha binding to classical estrogen response elements. *J Biol Chem* **281**(36): 26683-26692.

O'Lone R, Frith MC, Karlsson EK, Hansen U. (2004). Genomic targets of nuclear estrogen receptors. *Mol Endocrinol* **18**(8): 1859-1875.

Ogawa S, Lubahn DB, Korach KS, Pfaff DW. (1997). Behavioral effects of estrogen receptor gene disruption in male mice. *Proc Natl Acad Sci U S A* **94**(4): 1476-1481.

Ogawa S, Taylor JA, Lubahn DB, Korach KS, Pfaff DW. (1996). Reversal of sex roles in genetic female mice by disruption of estrogen receptor gene. *Neuroendocrinology* **64**(6): 467-470.

Olsen JC, Sechelski J. (1995). Use of sodium butyrate to enhance production of retroviral vectors expressing CFTR cDNA. *Hum Gene Ther* **6**(9): 1195-1202.

Oreffo RO, Kusec V, Virdi AS, Flanagan AM, Grano M, Zambonin-Zallone A *et al.* (1999). Expression of estrogen receptor-alpha in cells of the osteoclastic lineage. *Histochem Cell Biol* **111**(2): 125-133.

Ososki AL, Kennelly EJ. (2003). Phytoestrogens: a review of the present state of research. *Phytother Res* **17**(8): 845-869.

Overk CR, Guo J, Chadwick LR, Lantvit DD, Minassi A, Appendino G *et al.* (2008). In vivo estrogenic comparisons of Trifolium pratense (red clover) Humulus lupulus (hops), and the pure compounds isoxanthohumol and 8-prenylnaringenin. *Chem Biol Interact* **176**(1): 30-39.

Paige LA, Christensen DJ, Gron H, Norris JD, Gottlin EB, Padilla KM *et al.* (1999). Estrogen receptor (ER) modulators each induce distinct conformational changes in ER alpha and ER beta. *Proc Natl Acad Sci U S A* **96**(7): 3999-4004.

Parent A, Descarries L, Beaudet A. (1981). Organization of ascending serotonin systems in the adult rat brain. A radioautographic study after intraventricular administration of [3H]5-hydroxytryptamine. *Neuroscience* **6**(2): 115-138.

Park F. (2007). Lentiviral vectors: are they the future of animal transgenesis? *Physiol Genomics* **31**(2): 159-173.

Parker KL, Schimmer BP. (1995). Transcriptional regulation of the genes encoding the cytochrome P-450 steroid hydroxylases. *Vitam Horm* **51**: 339-370.

Patisaul HB, Jefferson W. (2010). The pros and cons of phytoestrogens. *Front Neuroendocrinol* **31**(4): 400-419.

Patterson TA, Lobenhofer EK, Fulmer-Smentek SB, Collins PJ, Chu TM, Bao W *et al.* (2006). Performance comparison of one-color and two-color platforms within the MicroArray Quality Control (MAQC) project. *Nat Biotechnol* **24**(9): 1140-1150.

Pecins-Thompson M, Bethea CL. (1999). Ovarian steroid regulation of serotonin-1A autoreceptor messenger RNA expression in the dorsal raphe of rhesus macaques. *Neuroscience* **89**(1): 267-277.

Pecins-Thompson M, Brown NA, Bethea CL. (1998). Regulation of serotonin re-uptake transporter mRNA expression by ovarian steroids in rhesus macaques. *Brain Res Mol Brain Res* **53**(1-2): 120-129.

Pecins-Thompson M, Brown NA, Kohama SG, Bethea CL. (1996). Ovarian steroid regulation of tryptophan hydroxylase mRNA expression in rhesus macaques. *J Neurosci* **16**(21): 7021-7029.

Peixoto BR, Vencio RZ, Egidio CM, Mota-Vieira L, Verjovski-Almeida S, Reis EM. (2006). Evaluation of reference-based two-color methods for measurement of gene expression ratios using spotted cDNA microarrays. *BMC Genomics* **7**: 35.

Perez SE, Chen EY, Mufson EJ. (2003). Distribution of estrogen receptor alpha and beta immunoreactive profiles in the postnatal rat brain. *Brain Res Dev Brain Res* **145**(1): 117-139.

Perissi V, Rosenfeld MG. (2005). Controlling nuclear receptors: the circular logic of cofactor cycles. *Nat Rev Mol Cell Biol* **6**(7): 542-554.

Permutt A, Chirgwin J, Giddings S, Kakita K, Rotwein P. (1981). Insulin biosynthesis and diabetes mellitus. *Clin Biochem* **14**(5): 230-236.

Petersen DN, Tkalcevic GT, Koza-Taylor PH, Turi TG, Brown TA. (1998). Identification of estrogen receptor beta2, a functional variant of estrogen receptor beta expressed in normal rat tissues. *Endocrinology* **139**(3): 1082-1092.

Pettersson K, Grandien K, Kuiper GG, Gustafsson JA. (1997). Mouse estrogen receptor beta forms estrogen response element-binding heterodimers with estrogen receptor alpha. *Mol Endocrinol* **11**(10): 1486-1496.

Pfaffl MW. (2001). A new mathematical model for relative quantification in real-time RT-PCR. *Nucleic Acids Res* **29**(9): e45.

Pierce JG, Parsons TF. (1981). Glycoprotein hormones: structure and function. *Annu Rev Biochem* **50**: 465-495.

Pratt WB, Toft DO. (1997). Steroid receptor interactions with heat shock protein and immunophilin chaperones. *Endocr Rev* **18**(3): 306-360.

Prossnitz ER, Arterburn JB, Smith HO, Oprea TI, Sklar LA, Hathaway HJ. (2008). Estrogen signaling through the transmembrane G protein-coupled receptor GPR30. *Annu Rev Physiol* **70**: 165-190.

Rachez C, Lemon BD, Suldan Z, Bromleigh V, Gamble M, Naar AM *et al.* (1999). Ligand-dependent transcription activation by nuclear receptors requires the DRIP complex. *Nature* **398**(6730): 824-828.

Rampp T, Tan L, Zhang L, Sun ZJ, Klose P, Musial F *et al.* (2008). Menopause in German and Chinese women--an analysis of symptoms, TCM-diagnosis and hormone status. *Chin J Integr Med* **14**(3): 194-196.

Rasgon NL, Altshuler LL, Fairbanks LA, Dunkin JJ, Davtyan C, Elman S *et al.* (2002). Estrogen replacement therapy in the treatment of major depressive disorder in perimenopausal women. *J Clin Psychiatry* **63 Suppl 7**: 45-48.

Rasheed S, Nelson-Rees WA, Toth EM, Arnstein P, Gardner MB. (1974). Characterization of a newly derived human sarcoma cell line (HT-1080). *Cancer* **33**(4): 1027-1033.

Razandi M, Oh P, Pedram A, Schnitzer J, Levin ER. (2002). ERs associate with and regulate the production of caveolin: implications for signaling and cellular actions. *Mol Endocrinol* **16**(1): 100-115.

Rhead B, Karolchik D, Kuhn RM, Hinrichs AS, Zweig AS, Fujita PA *et al.* (2010). The UCSC Genome Browser database: update 2010. *Nucleic Acids Res* **38**(Database issue): D613-619.

Richter SN, Frasson I, Palu G. (2009). Strategies for inhibiting function of HIV-1 accessory proteins: a necessary route to AIDS therapy? *Curr Med Chem* **16**(3): 267-286.

Robinson-Rechavi M, Escriva Garcia H, Laudet V. (2003). The nuclear receptor superfamily. *J Cell Sci* **116**(Pt 4): 585-586.

Routledge EJ, White R, Parker MG, Sumpter JP. (2000). Differential effects of xenoestrogens on coactivator recruitment by estrogen receptor (ER) alpha and ERbeta. *J Biol Chem* **275**(46): 35986-35993.

Rozen S, Skaletsky H. (2000). Primer3 on the WWW for general users and for biologist programmers. *Methods Mol Biol* **132**: 365-386.

Ruh MF, Zacharewski T, Connor K, Howell J, Chen I, Safe S. (1995). Naringenin: a weakly estrogenic bioflavonoid that exhibits antiestrogenic activity. *Biochem Pharmacol* **50**(9): 1485-1493.

Ryan KJ. (1982). Biochemistry of aromatase: significance to female reproductive physiology. *Cancer Res* **42**(8 Suppl): 3342s-3344s.

Ryser MF, Roesler J, Gentsch M, Brenner S. (2007). Gene therapy for chronic granulomatous disease. *Expert Opin Biol Ther* **7**(12): 1799-1809.

Sambrook J, Fritsch EF, Maniatis T. (1989). *Molecular Cloning: A Laboratory Manual.* New York, USA: Cold Spring Harbor Laboratory Press.

Sanderson JT. (2006). The steroid hormone biosynthesis pathway as a target for endocrine-disrupting chemicals. *Toxicol Sci* **94**(1): 3-21.

Saunders PT, Maguire SM, Gaughan J, Millar MR. (1997). Expression of oestrogen receptor beta (ER beta) in multiple rat tissues visualised by immunohistochemistry. *J Endocrinol* **154**(3): R13-16.

Schlegel A, Wang C, Katzenellenbogen BS, Pestell RG, Lisanti MP. (1999). Caveolin-1 potentiates estrogen receptor alpha (ERalpha) signaling. caveolin-1 drives ligand-independent nuclear translocation and activation of ERalpha. *J Biol Chem* **274**(47): 33551-33556.

Schmechel D, Marangos PJ, Zis AP, Brightman M, Goodwin FK. (1978). Brain endolases as specific markers of neuronal and glial cells. *Science* **199**(4326): 313-315.

Schmechel DE, Brightman MW, Marangos PJ. (1980). Neurons switch from non-neuronal enolase to neuron-specific enolase during differentiation. *Brain Res* **190**(1): 195-214.

Schmidt PJ, Nieman L, Danaceau MA, Tobin MB, Roca CA, Murphy JH *et al.* (2000). Estrogen replacement in perimenopause-related depression: a preliminary report. *Am J Obstet Gynecol* **183**(2): 414-420.

Seo EK, Silva GL, Chai HB, Chagwedera TE, Farnsworth NR, Cordell GA *et al.* (1997). Cytotoxic prenylated flavanones from Monotes engleri. *Phytochemistry* **45**(3): 509-515.

Shang Y, Brown M. (2002). Molecular determinants for the tissue specificity of SERMs. *Science* **295**(5564): 2465-2468.

Shao W, Brown M. (2004). Advances in estrogen receptor biology: prospects for improvements in targeted breast cancer therapy. *Breast Cancer Res* **6**(1): 39-52.

Shiau AK, Barstad D, Loria PM, Cheng L, Kushner PJ, Agard DA *et al.* (1998). The structural basis of estrogen receptor/coactivator recognition and the antagonism of this interaction by tamoxifen. *Cell* **95**(7): 927-937.

Shughrue PJ, Komm B, Merchenthaler I. (1996). The distribution of estrogen receptor-beta mRNA in the rat hypothalamus. *Steroids* **61**(12): 678-681.

Shughrue PJ, Lane MV, Merchenthaler I. (1997). Comparative distribution of estrogen receptor-alpha and -beta mRNA in the rat central nervous system. *J Comp Neurol* **388**(4): 507-525.

Simons SS, Jr. (2008). What goes on behind closed doors: physiological versus pharmacological steroid hormone actions. *Bioessays* **30**(8): 744-756.

Singleton DW, Khan SA. (2003). Xenoestrogen exposure and mechanisms of endocrine disruption. *Front Biosci* **8**: s110-118.

Smith DF, Toft DO. (1993). Steroid receptors and their associated proteins. *Mol Endocrinol* **7**(1): 4-11.

Sotoca AM, Bovee TF, Brand W, Velikova N, Boeren S, Murk AJ *et al.* (2010). Superinduction of estrogen receptor mediated gene expression in luciferase based reporter gene assays is mediated by a post-transcriptional mechanism. *J Steroid Biochem Mol Biol* **122**(4): 204-211.

Stauffer SR, Coletta CJ, Tedesco R, Nishiguchi G, Carlson K, Sun J *et al.* (2000). Pyrazole ligands: structure-affinity/activity relationships and estrogen receptor-alpha-selective agonists. *J Med Chem* **43**(26): 4934-4947.

Steinberg KK, Thacker SB, Smith SJ, Stroup DF, Zack MM, Flanders WD *et al.* (1991). A meta-analysis of the effect of estrogen replacement therapy on the risk of breast cancer. *Jama* **265**(15): 1985-1990.

Suen CS, Berrodin TJ, Mastroeni R, Cheskis BJ, Lyttle CR, Frail DE. (1998). A transcriptional coactivator, steroid receptor coactivator-3, selectively augments steroid receptor transcriptional activity. *J Biol Chem* **273**(42): 27645-27653.

Sugawara T, Holt JA, Kiriakidou M, Strauss JF, 3rd. (1996). Steroidogenic factor 1-dependent promoter activity of the human steroidogenic acute regulatory protein (StAR) gene. *Biochemistry* **35**(28): 9052-9059.

Sullivan JM, El-Zeky F, Vander Zwaag R, Ramanathan KB. (1997). Effect on survival of estrogen replacement therapy after coronary artery bypass grafting. *Am J Cardiol* **79**(7): 847-850.

Sun J, Baudry J, Katzenellenbogen JA, Katzenellenbogen BS. (2003). Molecular basis for the subtype discrimination of the estrogen receptor-beta-selective ligand, diarylpropionitrile. *Mol Endocrinol* **17**(2): 247-258.

Swindle CS, Klug CA. (2002). Mechanisms that regulate silencing of gene expression from retroviral vectors. *J Hematother Stem Cell Res* **11**(3): 449-456.

Takeuchi S, Takahashi T, Sawada Y, Iida M, Matsuda T, Kojima H. (2009). Comparative study on the nuclear hormone receptor activity of various phytochemicals and their metabolites by reporter gene assays using Chinese hamster ovary cells. *Biol Pharm Bull* **32**(2): 195-202.

Tokalov SV, Henker Y, Schwab P, Metz P, Gutzeit HO. (2004). Toxicity and cell cycle effects of synthetic 8-prenylnaringenin and derivatives in human cells. *Pharmacology* **71**(1): 46-56.

Torgerson DJ, Bell-Syer SE. (2001). Hormone replacement therapy and prevention of nonvertebral fractures: a meta-analysis of randomized trials. *Jama* **285**(22): 2891-2897.

Tremblay GB, Tremblay A, Copeland NG, Gilbert DJ, Jenkins NA, Labrie F *et al.* (1997). Cloning, chromosomal localization, and functional analysis of the murine estrogen receptor beta. *Mol Endocrinol* **11**(3): 353-365.

Tuppurainen M, Harma K, Komulainen M, Kiviniemi V, Kroger H, Honkanen R *et al.* (2010). Effects of continuous combined hormone replacement therapy and clodronate on bone mineral density in osteoporotic postmenopausal women: a 5-year follow-up. *Maturitas* **66**(4): 423-430.

Vadakkadath Meethal S, Atwood CS. (2005). The role of hypothalamic-pituitary-gonadal hormones in the normal structure and functioning of the brain. *Cell Mol Life Sci* **62**(3): 257-270.

Vanacker JM, Pettersson K, Gustafsson JA, Laudet V. (1999). Transcriptional targets shared by estrogen receptor- related receptors (ERRs) and estrogen receptor (ER) alpha, but not by ERbeta. *Embo J* **18**(15): 4270-4279.

VanGuilder HD, Vrana KE, Freeman WM. (2008). Twenty-five years of quantitative PCR for gene expression analysis. *Biotechniques* **44**(5): 619-626.

Vaya J, Tamir S. (2004). The relation between the chemical structure of flavonoids and their estrogen-like activities. *Curr Med Chem* **11**(10): 1333-1343.

Wakeling AE, Bowler J. (1987). Steroidal pure antioestrogens. *J Endocrinol* **112**(3): R7-10.

Wakeling AE, Bowler J. (1992). ICI 182,780, a new antioestrogen with clinical potential. *J Steroid Biochem Mol Biol* **43**(1-3): 173-177.

Wakeling AE, Dukes M, Bowler J. (1991). A potent specific pure antiestrogen with clinical potential. *Cancer Res* **51**(15): 3867-3873.

Waliszewski P, Blaszczyk M, Wolinska-Witort E, Drews M, Snochowski M, Hurst RE. (1997). Molecular study of sex steroid receptor gene expression in human colon and in colorectal carcinomas. *J Surg Oncol* **64**(1): 3-11.

Walker P, Germond JE, Brown-Luedi M, Givel F, Wahli W. (1984). Sequence homologies in the region preceding the transcription initiation site of the liver estrogen-responsive vitellogenin and apo-VLDLII genes. *Nucleic Acids Res* **12**(22): 8611-8626.

Walther DJ, Peter JU, Bashammakh S, Hortnagl H, Voits M, Fink H *et al.* (2003). Synthesis of serotonin by a second tryptophan hydroxylase isoform. *Science* **299**(5603): 76.

Wang L, Andersson S, Warner M, Gustafsson JA. (2001). Morphological abnormalities in the brains of estrogen receptor beta knockout mice. *Proc Natl Acad Sci U S A* **98**(5): 2792-2796.

Wang L, Andersson S, Warner M, Gustafsson JA. (2003). Estrogen receptor (ER)beta knockout mice reveal a role for ERbeta in migration of cortical neurons in the developing brain. *Proc Natl Acad Sci U S A* **100**(2): 703-708.

Weber K, Osborn M. (1969). The reliability of molecular weight determinations by dodecyl sulfate-polyacrylamide gel electrophoresis. *J Biol Chem* **244**(16): 4406-4412.

Wehrenberg U, Prange-Kiel J, Rune GM. (2001). Steroidogenic factor-1 expression in marmoset and rat hippocampus: co-localization with StAR and aromatase. *J Neurochem* **76**(6): 1879-1886.

Weigt C. (2008). Etablierung und Charakterisierung einer Raphe-Kern-Zelllinie zur Untersuchung Östrogenrezeptor ß vermittelter Effekte auf das serotonerge System. [Diploma]. Dresden, Technische Universität Dresden: 1-87.

Welch BL. (1938). The Significance of the Difference Between Two Means when the Population Variances are Unequal. *Biometrika* **29**: 350-362.

Wells KB, Stewart A, Hays RD, Burnam MA, Rogers W, Daniels M *et al.* (1989). The functioning and well-being of depressed patients. Results from the Medical Outcomes Study. *Jama* **262**(7): 914-919.

White JH, Fernandes I, Mader S, Yang XJ. (2004). Corepressor recruitment by agonist-bound nuclear receptors. *Vitam Horm* **68**: 123-143.

White LA, Eaton MJ, Castro MC, Klose KJ, Globus MY, Shaw G *et al.* (1994). Distinct regulatory pathways control neurofilament expression and neurotransmitter synthesis in immortalized serotonergic neurons. *J Neurosci* **14**(11 Pt 1): 6744-6753.

White LA, Whittemore SR. (1992). Immortalization of raphe neurons: an approach to neuronal function in vitro and in vivo. *J Chem Neuroanat* **5**(4): 327-330.

White R, Lees JA, Needham M, Ham J, Parker M. (1987). Structural organization and expression of the mouse estrogen receptor. *Mol Endocrinol* **1**(10): 735-744.

Whittemore SR, White LA. (1993). Target regulation of neuronal differentiation in a temperature-sensitive cell line derived from medullary raphe. *Brain Res* **615**(1): 27-40.

Windahl SH, Norgard M, Kuiper GG, Gustafsson JA, Andersson G. (2000). Cellular distribution of estrogen receptor beta in neonatal rat bone. *Bone* **26**(2): 117-121.

Winer J, Jung CK, Shackel I, Williams PM. (1999). Development and validation of real-time quantitative reverse transcriptase-polymerase chain reaction for monitoring gene expression in cardiac myocytes in vitro. *Anal Biochem* **270**(1): 41-49.

Wittchen HU, Hoyer J. (2001). Generalized anxiety disorder: nature and course. *J Clin Psychiatry* **62 Suppl 11**: 15-19; discussion 20-11.

Witte D, Chirala M, Younes A, Li Y, Younes M. (2001). Estrogen receptor beta is expressed in human colorectal adenocarcinoma. *Hum Pathol* **32**(9): 940-944.

Wyckoff MH, Chambliss KL, Mineo C, Yuhanna IS, Mendelsohn ME, Mumby SM *et al.* (2001). Plasma membrane estrogen receptors are coupled to endothelial nitric-oxide synthase through Galpha(i). *J Biol Chem* **276**(29): 27071-27076.

Yang J, Singleton DW, Shaughnessy EA, Khan SA. (2008). The F-domain of estrogen receptor-alpha inhibits ligand induced receptor dimerization. *Mol Cell Endocrinol* **295**(1-2): 94-100.

Zand RS, Jenkins DJ, Diamandis EP. (2000). Steroid hormone activity of flavonoids and related compounds. *Breast Cancer Res Treat* **62**(1): 35-49.

Zhao L, Chen Q, Diaz Brinton R. (2002). Neuroprotective and neurotrophic efficacy of phytoestrogens in cultured hippocampal neurons. *Exp Biol Med (Maywood)* **227**(7): 509-519.

Zierau O, Geis RB, Tischer S, Schwab P, Metz P, Vollmer G. (2004). Uterine effects of the phytoestrogen 6-(1,1-dimethylallyl)naringenin in rats. *Planta Med* **70**(7): 590-593.

Zierau O, Gester S, Schwab P, Metz P, Kolba S, Wulf M *et al.* (2002). Estrogenic activity of the phytoestrogens naringenin, 6-(1,1-dimethylallyl)naringenin and 8-prenylnaringenin. *Planta Med* **68**(5): 449-451.

Zierau O, Hamann J, Tischer S, Schwab P, Metz P, Vollmer G *et al.* (2005). Naringenin-type flavonoids show different estrogenic effects in mammalian and teleost test systems. *Biochem Biophys Res Commun* **326**(4): 909-916.

Zierau O, Kolba S, Olff S, Vollmer G, Diel P. (2006). Analysis of the promoter-specific estrogenic potency of the phytoestrogens genistein, daidzein and coumestrol. *Planta Med* **72**(2): 184-186.

Zierau O, Kretzschmar G, Moller F, Weigt C, Vollmer G. (2008). Time dependency of uterine effects of naringenin type phytoestrogens in vivo. *Mol Cell Endocrinol* **294**(1-2): 92-99.

- **Websites:**

Agilent Feature Extraction Software Version 9.5 User Manual
(http://www.chem.agilent.com/Library/usermanuals/Public/UserGuide_050415.pdf)

Agilent One-Colour Microarray-Based Gene Expression Analysis Manual Version 5.7
(http://www.chem.agilent.com/Library/usermanuals/Public/G4140-90041_One-Color_Tecan.pdf)

Agilent Technologies GeneSpring GX 9 Software User Manual
(http://www.chem.agilent.com/cag/bsp/products/gsgx/manuals/GeneSpringGX9_QuickStartGuide.pdf)

GraphPad Guide to Non-Linear Regression
(http://www.graphpad.com/curvefit/introduction89.htm)

peqGOLD TriFast™ Standard Protocol
(http://www.peqlab.com/wcms/en/pdf/30-2010_m.pdf)

Primer3 Version 2.2.3
(http://frodo.wi.mit.edu/primer3/)

RNA Quality Control using the Agilent 2100 Bioanalyzer Manual
(http://www.chem.agilent.com/Library/applications/5989-1086EN.pdf)

UCSC Genome Browser Database
(http://genome.ucsc.edu/)